KAMILA ANNA MEISSNER

Análise do estado redox e seu efeito sobre a proliferação de *Plasmodium falciparum* em eritrócitos geneticamente diferentes

Tese apresentada ao programa de Pós-Graduação em Biologia da Relação Patógeno-Hospedeiro do Departamento de Parasitologia do Instituto de Ciências Biomédicas da Universidade de São Paulo para obtenção do Título de Doutor em Ciências.

São Paulo
2017

KAMILA ANNA MEISSNER

Analysis of the Redox Status and its Effect on the Proliferation of *Plasmodium falciparum* in Genetically Different Erythrocytes

Ph. D. Thesis presented to the Post-graduation program Biology of Host-Pathogen Interactions at the Institute of Biomedical Sciences of the University of São Paulo, in order to obtain the degree of Doctor in Sciences

São Paulo
2017

KAMILA ANNA MEISSNER

Análise do estado redox e seu efeito sobre a proliferação de *Plasmodium falciparum* em eritrócitos geneticamente diferentes

Tese apresentada ao programa de Pós-Graduação em Biologia da Relação Patógeno-Hospedeiro do Departamento de Parasitologia do Instituto de Ciências Biomédicas da Universidade de São Paulo para obtenção do Título de Doutor em Ciências.

Área de concentração: Biologia da Relação Patógeno-Hospedeiro

Orientador: Prof. Dr. Carsten Wrenger

Versão original

São Paulo
2017

KAMILA ANNA MEISSNER

Analysis of the Redox Status and its Effect on the Proliferation of *Plasmodium falciparum* in Genetically Different Erythrocytes

Ph. D. Thesis presented to the Post-graduation program Biology of Host-Pathogen Interactions at the Institute of Biomedical Sciences of the University of São Paulo, in order to obtain the degree of Doctor in Sciences

Area: Biology of Host-Pathogen Interactions

Supervisor: Prof. Dr. Carsten Wrenger

Original Version

São Paulo
2017

CATALOGAÇÃO NA PUBLICAÇÃO (CIP)
Serviço de Biblioteca e informação Biomédica
do Instituto de Ciências Biomédicas da Universidade de São Paulo

Ficha Catalográfica elaborada pelo(a) autor(a)

Meissner, Kamila Anna
Análise do estado redox e seu efeito sobre a proliferação de Plasmodium falciparum em eritrócitos geneticamente diferentes / Kamila Anna Meissner; orientador Carsten Wrenger. -- São Paulo, 2017.
112 p.

Tese (Doutorado)) -- Universidade de São Paulo, Instituto de Ciências Biomédicas.

1. Malária. 2. Glutathiona. 3. Deficiência em G6PD. 4. Estresse oxidativo. 5. Glutationa-S-Transferase. I. Wrenger, Carsten, orientador. II. Título.

UNIVERSIDADE DE SÃO PAULO
INSTITUTO DE CIÊNCIAS BIOMÉDICAS

Candidato(a): Kamila Anna Meissner

Título da Tese: Análise do estado redox e seu efeito sobre a proliferação de Plasmodium falciparum em eritrócitos geneticamente diferentes

Orientador(a): Prof. Dr. Carsten Wrenger

A Comissão Julgadora dos trabalhos de Defesa da Tese de Doutorado, em sessão pública realizada a ...../...../....., considerou

( ) Aprovado(a) **( ) Reprovado(a)**

Examinador(a): Assinatura: .....
Nome: .....
Instituição: .....

Examinador(a): Assinatura: .....
Nome: .....
Instituição: .....

Examinador(a): Assinatura: .....
Nome: .....
Instituição: .....

Presidente: Assinatura: .....
Nome: .....
Instituição: .....

UNIVERSIDADE DE SÃO PAULO
INSTITUTO DE CIÊNCIAS BIOMÉDICAS

Cidade Universitária "Armando de Salles Oliveira"
Av. Prof. Lineu Prestes, 2415 – CEP. 05508-000 São Paulo, SP – Brasil
Telefone :(55) (11) 3091-7733 - telefax : (55) (11) 3091-8405
e-mail: cep@icb.usp.br

Comissão de Ética em Pesquisa

CERTIFICADO DE ISENÇÃO

Certificamos que o Protocolo CEP-ICB Nº **580/13** referente ao projeto intitulado: "*Analysis of the redox status of plasmodium falciparum proliferation in genetically modified erythocytes* " sob a responsabilidade de **Kamila Anna Meissner,** foi analisado na presente data pela CEUA - COMISSÃO DE ÉTICA NO USO DE ANIMAIS e pela CEPSH- COMISSÃO DE ÉTICA EM PESQUISA COM SERES HUMANOS, tendo sido deliberado que o referido projeto não utilizará animais que estejam sob a égide da lei 11.794 de 8 de outubro de 2008, nem envolverá procedimentos regulados pela Resolução CONEP nº196 de 1996.

São Paulo, 19 de junho de 2013.

PROF. DR. WOTHAN TAVARES DE LIMA
Coordenador da CEUA - ICB/USP

PROF. DR. PAOLO M.A ZANOTTO
Coordenador da CEPsh - ICB/USP

This work was supported by the São Paulo state funding agency FAPESP (grant 2012/12807-3)

ACKNOWLEDGMENT

Firstly, I would like to express my sincere gratitude to my advisor and mentor Prof. Carsten Wrenger who showed me the entrance into the world of science. I am grateful for his patience, motivation and the continuous support but above all for his steady believe and trust in me. I learned much more than what is written in this thesis. Thank you for all this years together in which you allowed me to grow as a scientist!

Besides my advisor, I would like to thank Prof. Eva Liebau who even in the distance was a great support in many ways. I also would like to thank the rest of my committee members, Prof. Jose E. Krieger, Prof. Claudio R. Farias Marinho, for serving as my committee members even at hardship and for letting my defence be an enjoyable moment with a lot of brilliant comments and suggestions.

My sincere thanks also go to Prof. Dr Prof. Alan H. Fairlamb, who provided me with an opportunity to join his team as an intern at The Wellcome Trust Biocentre (Dundee, Scotland), and who gave access to the laboratory and research facilities.

I want to thank Dr. Isolmar T.Schettert for helping with the blood supply, without him this project would have been impossible to realize.

I want to thank present and past members of the UDD laboratory, first of all, Prof. Gerhard Wunderlich, who is an important enrichment in the daily lab life. Thank you for joining us! Thanks to all my fellow labmates for all the time together if in the lab working or at one of our various *churrascos* and *festinhas*. A special thank go to all my *filhotes* for showing me that I am on the right way in my life.

Then thanks to my ex-roommate, still lab mate and forever friend for all the help and discussions and fun we had and hopefully will have together. Furthermore, I am not forgetting all my friends, if in Brazil or aboard, thanks for not giving up on me even when I am someone who is always occupied and never responds to emails. And of course I have to mention my breakfast, ice-cream and garlic bread crew, thanks for lightening up this last month, it would not have been the same without you.

Last but not the least; I would like to thank my family, my mother Joanna and my father Darius Meissner. Thank you for supporting me in every right and wrong decision I took during this thesis and furthermore. I am sorry for all of the sacrifices that you've made on my behalf thank you for your patience and understanding. Kocham was!

Dla moich rodziców
Mimo odległości były zawsze przy mnie!

FIGURE LIST

TABLE LIST

LIST OF ABBREVIATIONS

$^1O_2$	SINGLET OXYGEN
Ac	ACETATE
AHT	ANHYDROTETRACYCLINE
AS	ANTISENSE
BC	BEFORE CHRIST
CAT	CATALASE
CDNB	2,4-DINITROCHLOROBENZENE
CM-H2DCFDA	5-(AND-6)-CHLOROMETHYL-2',7'-DICHLORODIHYDROFLUORESCEIN DIACETATE
CQ	CHLOROQUINE
CRT	CHLOROQUINE RESISTANCE TRANSPORTER
CYP	CYTOCHROME P450
DARC	DUFFY ANTIGEN CHEMOKINE RECEPTOR
DCF	HIGHLY FLUORESCENT 2',7'-DICHLOROFLUORESCEIN
DLS	DYNAMIC LIGHT SCATTERING
DV	DIGESTIVE VACUOLE
EDTA	ETHYLENEDIAMINETETRAACETIC ACID
EMP	INFECTED ERYTHROCYTE MEMBRANE PROTEIN
ER	ENDOPLASMIC RETICULAR
ETC	ELECTRON TRANSPORT CHAIN
ETOH	ETHANOL
FPLC	FAST PROTEIN LIQUID CHROMATOGRAPHY (FPLC)
G6PD	GLUCOSE 6-PHOSPHATE DEHYDROGENASE
gDNA	GENOMIC DEOXYRIBONUCLEIC ACID
GFP	GREEN FLUORESCENT PROTEIN
gGCS	GAMMA-GLUTAMYLCYSTEINE SYNTHETASE
GLUPHO	GLUCOSE-6-PHOSPHATE DEHYDROGENASE-6-PHOSPHOGLUCONOLACTONASE
gMFI	GEOMETRIC MEAN OF FLUORESCENCE INTENSITY
GR	GLUTATHIONE REDUCTASE
GS	GLUTATHIONE SYNTHETASE
GSH	REDUCED GLUTATHIONE
GSSG	OXIDIZED GLUTATHIONE
GST	GLUTATHIONE S-TRANSFERASE
H_2O_2	HYDROGEN PEROXIDE
Hb	HAEMOGLOBIN
hDHFR	HUMAN DIHYDROFOLATE REDUCTASE CASSETTE
HEPES	4-(2-HYDROXYETHYL)-1-PIPERAZINEETHANESULFONIC ACID
HO	HEME OXYGENASE
HO•	HYDROXYL RADICAL
HOCl	HYPOCHLOROUS ACID

HRP	HORSERADISH PEROXIDASE
IDH	ISOCITRATE DEHYDROGENASE
iRBC	INFECTED RED BLOOD CELLS
IRS	INDOOR RESIDUAL SPRAYING
ISA	INSUFISIENT ACTIVITY
ITN	TREATED MOSQUITO NET
LB	LURIA BROTH
LC-ESI-MS/MS	LIQUID CHROMATOGRAPHY ELECTROSPRAY IONIZATION TANDEM MASS SPECTROMETRY
LLIN	LONG-LASTING INSECTICIDAL NET
mRNA	MESSENGER RIBONUCLEIC ACID
MRP	MULTIDRUG RESISTANCE-ASSOCIATED PROTEIN
NADPH	NICOTINAMIDE ADENINE DINUCLEOTIDE PHOSPHATE
NEM	N-ETHYLMALEIMIDE
$O_2^{\bullet-}$	SUPEROXIDE ANION
O_3	OZONE
ORF	OPEN READING FRAMES
P	PLASMODIUM
PCR	POLYMERASE CHAIN REACTION
PEP	PHOSPHOENOLPYRUVATE
PK	PYRUVATE KINASE
PKLR	PK, LIVER AND RBC
PPP	PENTOSE PHOSPHATE PATHWAY
PRDX	PEROXIREDOXIN
qRT-PCR	QUANTITATIVE REAL TIME PCR
RBC	RED BLOOD CELLS
RNS	REACTIVE NITROGEN SPECIES
RO•	ALKOXYL RADICAL
RO_2•	PEROXYL RADICAL
ROS	REACTIVE OXYGEN SPECIES
RT-PCR	REVERSE TRANSCRIPTASE-PCR
S	SENSE
SDS-PAGE	SODIUM DODECYL SULPHATE POLYACRYLAMIDE GEL ELECTROPHORESIS
SNIP	SINGLE NUCLEOTIDE SUBSTITUTION POLYMORPHISM
SOD	SUPEROXIDE DISMUTASE
TAE	TRIS-ACETATE-EDTA BUFFER
TE	TRIS-EDTA
TRXPX	THIOREDOXIN PEROXIDASE
TRXR	THIOREDOXIN REDUCTASE
TXN	THIOREDOXIN
UPR	UNFOLDED PROTEIN RESPONSE
WT	WILD TYPE

TABLE OF CONTENTS

RESUMO

Meissner, KA. Análise do estado redox e seu efeito sobre a proliferação de Plasmodium falciparum em eritrócitos geneticamente diferentes. Tese (Doutorado em Parasitologia).

Malária, causada por parasitas *Plasmodium spp*., ainda contribui com cerca de 400 mil mortes anuais sendo uma das mais vastas doenças de nosso tempo. *Plasmodium falciparum*, que causa a malária tropical, leva a forma mais severa da doença. Não obstante, há alguns grupos com resistência nativa conhecidas como, por exemplo, a siclemia ou enzimopatias como no caso da deficiência da glicose 6-fosfato desidrogenase. Apesar dos anos de pesquisa, até hoje os exatos mecanismos que conferem proteção, permanecem desconhecidos. Contudo, várias hipóteses, como o aumento da resposta imune inata ou a resposta melhorada contra os danos oxidativos dentro dos eritrócitos são discutidos. Este trabalho foca nos sistemas de defesa contra danos oxidativos em *Plasmodium falciparum* usando parasitas geneticamente modificados em células sanguíneas vermelhas anormais. O aumento de diferentes sistemas antioxidantes deveria fornecer um olhar aprofundado dos mecanismos de proteção destes eritrócitos modificados. Neste trabalho demonstramos a importância da Glutationa-S-Transferase para a sobrevivência do parasita em eritrócitos com a deficiência da glicose 6-fosfato desidrogenase. Isso leva a hipótese de que níveis aumentados de ROS nas células vermelhas geram uma alta quantidade de xenobióticos no parasita, resultando na morte da célula.

Palavras-chave: Malária. Glutathiona. Deficiência em G6PD. Estresse oxidativo.

ABSTRACT

Meissner, KA. Analysis of the Redox Status and its Effect on the Proliferation of *Plasmodium falciparum* in Genetically Different Erythrocytes. Ph.D (Parasitology).

Malaria, caused by *Plasmodium* spp., remains with more than 400.000 deaths annually one of the vastest diseases of our time. *Plasmodium falciparum*, is the most dangerous species leading to severe malaria. Nevertheless, there are some native resistances known like sickle cell trait or enzymopathies such as glucose-6-phosphate dehydrogenase deficiency. However, the protection mechanism is still unknown. Hypotheses like a better innate immune response or the increased oxidative stress inside the altered erythrocytes are discussed. This work is focusing on the oxidative defence system of *P. falciparum* using transgenically modified parasites cultured in wild-type and abnormal red blood cells. Elevated expression levels of different anti-oxidative systems in *P. falciparum* should give a deeper insight of the protection mechanism of the altered erythrocytes. In this work, we show the importance of the plasmodial Glutathione-S-Transferase (*Pf*GST) for the proliferation of the malaria pathogen in erythrocytes with glucose-6-phosphate dehydrogenase deficiency. This leads to the hypothesis that the increased ROS level in these red blood cells generating a high amount of xenobiotics within the parasite which results in cell death.

Keywords: Malaria. Glutathione. G6PD deficiency. Oxidative stress.

1 INTRODUCTION

1.1 History and Distribution of Malaria

Malaria is a life-threatening disease with nearly a quarter of the world's population living in areas of high risks. In 2015, 212 million malaria cases, leading to about half a million deaths, were recorded, most of them African children under the age of five years. With over 90% of all malaria cases and 92% of malaria deaths shows the Sub-Saharan Africa harbouring the highest global malaria burden. On the American continent, 18 countries are endemic for malaria and the majority of cases occur in one of the nine amazonic countries, which includes Brazil (1).

Figure 1 – World distribution and cases of death through malaria.

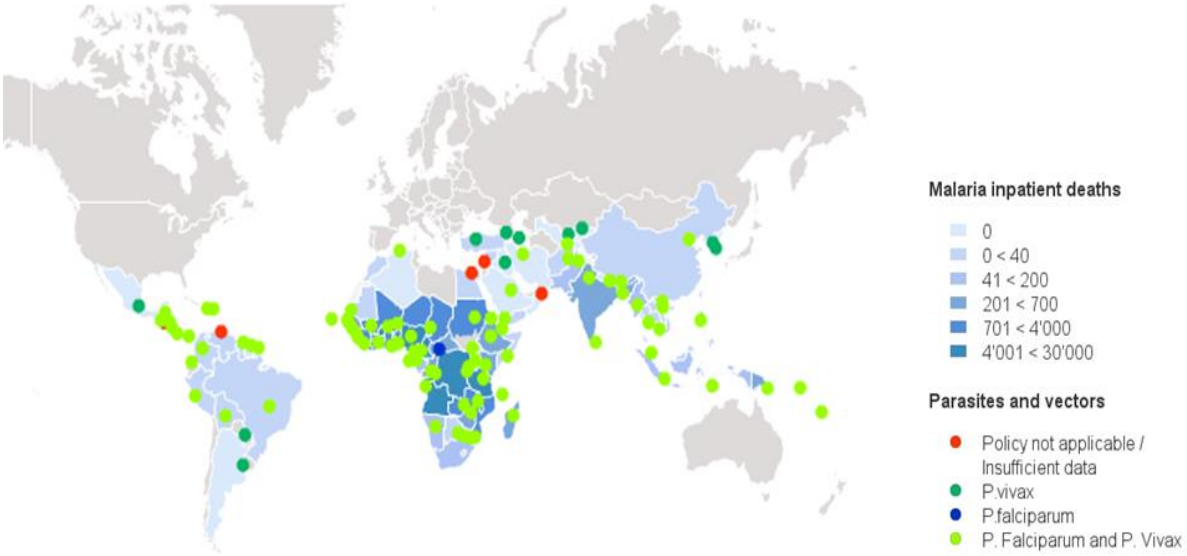

Spots are demonstrating the global distribution of *P. falciparum* and *P. vivax* infections correlating with the number of death in blue caused by malaria in 2016. Data were available at http://www.who.int/en/ 31.01.2017.

The history of malaria extends into antiquity with records from China in 2700 before Christ (BC), Greece and the Roman Empire. Already Hippocrates mentioned in the 5th century BC the correlation between marshes and the characteristic periodic fevers of disease (2). Suspecting that the reason for the disease was the miasmas rising from the swamps, the name malaria occurred, which is driven from the Italian mal'aria, bad air. However, the disease continued spreading around the Mediterranean Sea up to the 19th century including central Europe. Through the

systematic draining of swamps and the use of insecticide, malaria has been finally eradicated in the 1960s in Europe (3).

In 1880 Alphonse Laveran, a French army surgeon was the first to find the parasite in the blood of a patient suffering from malaria (2). Almost 20 years later Ronald Ross, a British medical doctor, introduced the anopheles mosquito as a possible vector for transmission of the malaria parasite (4). Additional 50 years were needed to find the missing link between after the infection of the parasite and its occurrence in the human blood. When in 1947, Henry Shortt and Cyril Garnham, were finally able to show a primary division of the parasite in liver cells (5). Subsequently, Krotoski and colleagues discovered that some *P. vivax* strains could remain in this liver stage for several months (6).

Up today there are more than 200 known species of the genus *Plasmodium (P.)*, but just five of them are causing human malaria, including *P. vivax*, *P. ovale*, *P. malariae*, *P. knowlesi* and the most virulent, *P. falciparum* (7). The genus *Plasmodium* belongs to the phylum Apicomplexa, which consist of a large group of unicellular eukaryotes sharing the same invasion machinery, the apical complex. Together with dinoflagellates and ciliates, they are forming the higher group of Alveolata (8).

All *Plasmodium* spp share a complex life cycle happening within an insect and a vertebrate host. The human malaria is transmitted via the female Anopheles mosquito, which injects sporozoites during the blood meal. After invading liver cells each sporozoite can mature into up to 40,000 merozoites, which will then be released into the blood stream via merosomes (9). However, *P. vivax* and *P. ovale* are able to form hypnozoites, a special form of sporozoites, which can remain in the liver for several months before proceeding to the blood stage. The released merozoites can infect red blood cells (RBCs), which start to remodel these cells in order to facilitate their proliferation and differentiation from ring to trophozoite and then into schizont. One of the reasons of the high virulence of *P. falciparum* is the export of *Pf*EMP1 (*P. falciparum* infected erythrocyte membrane protein 1) to the infected RBC (iRBC) surface. *Pf*EMP allows the iRBC to bind to the endothelium avoiding the clearance by the spleen and are leading to a disrupted blood flow which can cause cerebral or placental malaria when occurring in the brain or placenta (10). The asexual blood cycle ends with the haemolysis and release of new merozoite forms into the

bloodstream, resulting in both anaemia and periodic fevers characteristic of the disease. While most of the merozoites will reinfect other erythrocytes, some follow a different path differentiating into male and female gametocytes. These gametocytes will differentiate into gametes within the mid-gut of a female *Anopheles* mosquito after the next blood meal and the sexual proliferation can take place. After formation of the diploid zygote, the zygote differentiates to the ookinete and later oocysts and subsequently, new sporozoites are formed. The released sporozoites migrate to the mosquito's salivary gland, where they will be transmitted during the next blood meal of the mosquito (11).

Figure 2 – Life cycle of *Plasmodium* spp.

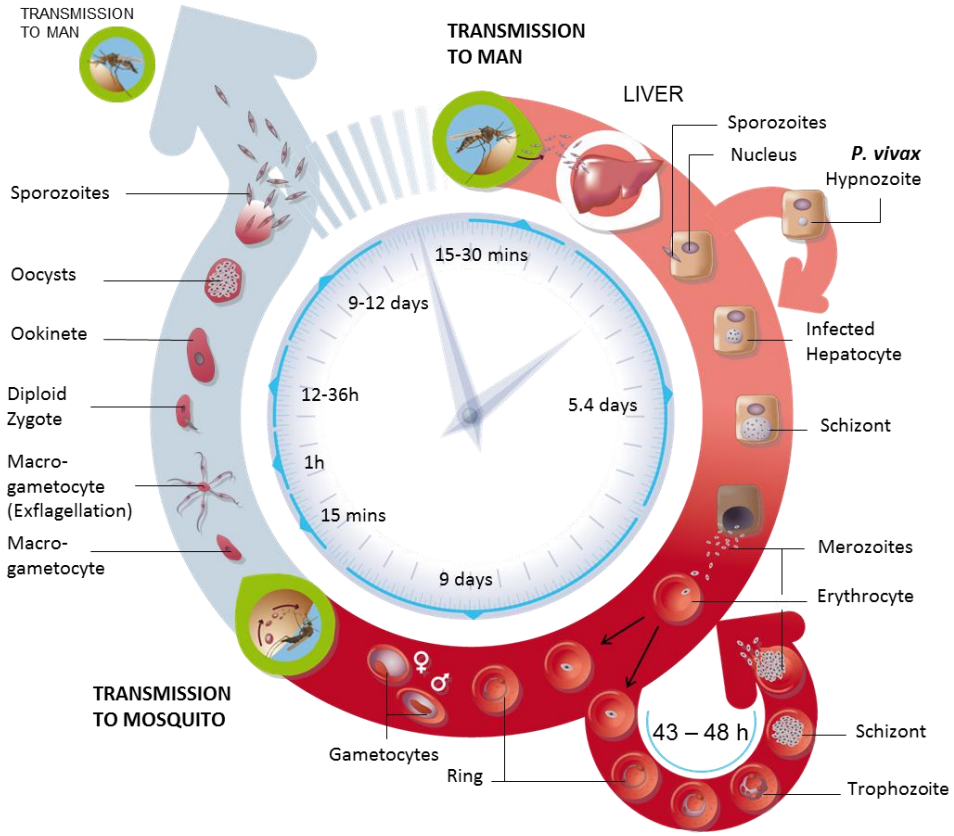

The life cycle of *Plasmodium* spp. is occurring in two hosts. After a blood meal of the Anopheles spec. mosquito, the parasite infects human hepatocytes and proliferates into merozoites. While an infection with *P. vivax* or *Plasmodium ovale* can lead to a sporozoite differentiation into hypnozoites in all other cases merozoites will directly infect RBC and replicate via schizogony. This assexually replication can be repeated several times. Other merozoites develop into male and female gametocytes that infect mosquitoes when taken up by the next blood meal. The sexual stages mature into the mosquito gut where they fuse and form an ookinete. The ookinete develops into the oocyst which releases new sporozoites that migrate to the insect's salivary glands Source: modified from (11).

Due to the increased prevention and vector control, the global malaria mortality rates have been reduced by 29% and even by 35% among children under 5 since 2010 (1). Nevertheless, continuous outbreaks of vector resistance associated with the spread of resistance among parasites to classical antimalarial treatments are the reason for the devastating effects of this disease. Therefore continuous discovery and development of novel antimalarials are needed to combat malaria (12,13).

1.2 Conquer malaria

The primary way to overcome malaria is the vector control via insecticide-treated mosquito nets (ITNs) and indoor residual spraying (IRS) in areas of high risks. The most effective and affordable insecticide is 1,1,1-Trichloro-2,2'bis(p-chlorophenyl) ethane DDT, the first synthetic organic (14). It was intensively used to combat malaria in 1940s to 1970s before it was banned in 1972 because of its impact on the environment and human health (14). However after several years of debating 2006 WHO gave again a clean bill to use of DDT to combat malaria in Africa due of the great burden of malaria and the current expensive and ineffective vector control strategies (15,16).

The alternative, long-lasting insecticidal nets (LLINs) are containing pyrethroids, which lead to a protection of up to 3 years and is highly recommended especially for young children and pregnant women in endemic areas. Between 2010 and 2015, the use of these ITNs increased in sub-Saharan Africa there by 80%. However, mosquito resistances to pyrethroids are already reported and in some areas, even all 4 classes of insecticides show already a decreased effect (1).

1.2.1 Drug treatment

One of the oldest known antimalarials is the quinine, an alkaloid derived from the bark of the cinchona tree. It was brought in the 17th century from Peru to Europe and was first isolated in the 19th century from French researchers Pierre Joseph Pelletier and Joseph Bienaimé Caventou. However, the first synthetic antimalarial drug, methylene blue, was introduced 1891 by Guttmann and Ehrlich. Methylene blue is a specific inhibitor of the glutathione reductase and interferes with the haemozoin

polymerisation (17). Because its uncommen side effects (green urine and blue sclera) it was discarded as antimalarial and replaced with chloroquine (CQ)(18). However because of its potential to reverse CQ resistance, today methylene blue is again considered as potential drug against *Plasmodium* spp. (18). In 1940 CQ took over as the new antimalarial drug of choice (19). Already in 1934, Hans Andersag discovered the quinine-related CQ (20), which was massively used worldwide. All 4-aminoquinolines, including quinine, CQ, mefloquine, amodiaquine and the quinoline-methanols, are supposed to interfere with the plasmodial heme detoxification inside the digestive vacuole (DV) killing thereby the parasite (21,22). Despite the advantages of CQ, such as high efficacy, low production costs and low toxicity, the need for new drugs raises because of the appearance of CQ-resistant *Plasmodium* strains in the late 1950s (2). The resistance is mediated through mutations in the *P. falciparum* chloroquine resistance transporter (*Pf*CRT) located on the DV membrane allowing the efflux of CQ (23,24).

Figure 3 – Occurrence of antimalarial drug resistance of *P. falciparum*.

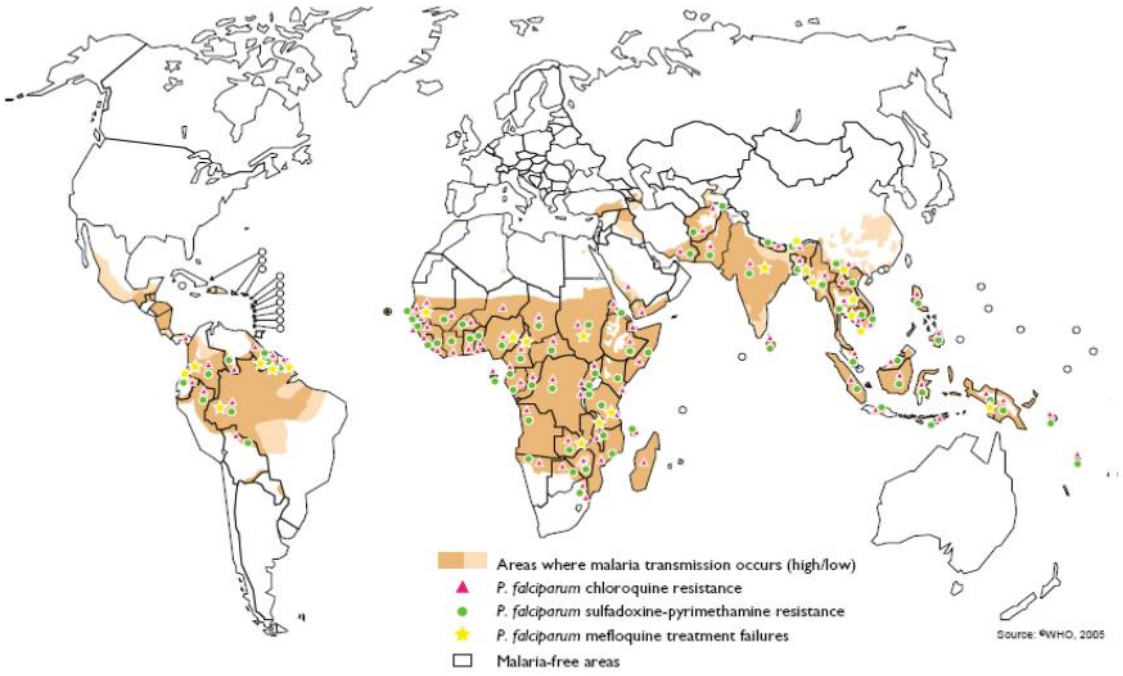

The resistance of *P. falciparum* to the still in use antimalarial drugs, such as chloroquine, sulfadoxine-pyrimethamine and mefloquine are already widespread as seen in the global map from 2005 (25).

However, antifolates were discovered as an alternative, acting through the inhibition of the biosynthesis of tetrahydrofolate (the active form of folate, vitamin B9), solely

present in the parasite. Antibiotics like sulfadoxine (a sulfonamide antibiotic) inhibit the enzyme dihydropteroate synthetase, while pyrimethamine serves as an inhibitor of the dihydrofolate reductase and dihydropteroate synthase (26,27). To enhance the effect both drugs were used in combination to inhibit two different steps in the same biosynthesis. Nevertheless, in 1970 the first resistances were noted in Thailand and from there spread rapidly through Asia and to the African continent (Figure 3) (24,26).

Because of the fast spreading of resistances against all known antimalarials new drugs were urgently needed and in the 1970s isolated artemisinin from the Chinese herb qinghaosu seemed to be the solution. Artemisinin was effective against all multi-drug resistant parasites (28). There exist several artemisinin derivates, which all are reducing the blood parasitemia very rapidly. However, the drug half-life is very short which is the reason why is the drug only given in combination with other antimalarials, known as artemisinin combination therapy (ACTs)(29). The mode of action of artemisinin is still not cleared but it is suggested that artemisinin gets activated by iron which in turn inhibits *Pf*ATP6 (a calcium pump) which leads to parasites death (30). Recently was demonstrated that artesunate, an artemisinin derivative, is inhibiting a novel membrane bound GST (*Pf*GST2/*Pf*EXP1) (31). Untill today ACTs are the treatment of choice for uncomplicated malaria. Nevertheless, parasites with resistance to artemisinin were identified already in 5 countries of South East Asia (Cambodia, Laos, Myanmar, Thailand and Viet Nam). Fortunately, ACTs seem still successful when used in combination with other drugs. However, the search for new antimalarial drugs has to continue and novel drug targets have to be discovered before the spread of the ACT-resistances.

Another strategy for new antimalarials is to block the parasite transmission by targeting the liver or the sexual stages of the parasite. Till today there is just one drug family available attacking also hypnozoites. The 8-aminoquinolines like as primaquine is the only available drug to use for relapsing malaria caused by *P. vivax* or *P. ovale*. The mechanism of action is still unclear but probably involves cytochrome P450s and monoamine oxidase, as well as the formation of reactive intermediates (32). However, due to the risk of hemolytic anaemia, glucose-6-phosphate-deficient patients infected with malaria should not be treated by

primaquine, as well as a pregnant woman. Since the combat against the liver and sexual stage could lead to a clinically relevant reduction of malaria, new drugs for these stages are important. Tafenoquine could be one of these promising agents showing already several benefits over primaquine (32).

1.2.2 Vaccination

The use of vaccination against malaria would lead a big step forward to the eradication of this disease. However, the complex live cycle with their multistage and the genetic diversity of *Plasmodium* spp. hinder the approaches to develop a vaccine hence there is currently no effective vaccination available. However, in 2015 the first malaria vaccine RTS,S/AS01 against *P. falciparum* was accepted for pilot implementations in 3 countries in sub-Saharan Africa. Before, large clinical trials in 7 countries in Africa were completed with positive evaluation by the European Medicines Agency (1).

RTS,S/AS01 targets pre-erythrocytic stages of the *Plasmodium* infection. This might result in a reduction of liver stage schizonts releasing merozoites, which will induce the blood stage proliferation. Previous field trials showed already a partial protective effect, with efficiencies around 30-50% (33). This seems rather disappointing but this pilot project could open the way to an increased attention on the discovery of vaccines. However the vaccination program with RTS,S/AS01 is intended to start in 2018 (1).

1.2.3 Innate Resistances

Knowing the long lasting history of human malaria it is certainly no surprise that this disease had a selective pressure on the human genome evolution. This was first recognised and described in 1949 by J.B.S. Haldane. He found a correlation between malaria-endemic regions around the Mediterranean Sea and the local frequency of thalassemia which seemed to mediate a protective effect against human malaria (34,35). Consequently, Haldane formulated his hypothesis of “balanced polymorphisms”, where the enhance fitness against malaria acquired from a heterozygote carrier phenotype would prevail over the disadvantages of the

homozygote phenotype, which causes the genetic disease. This hypothesis is today known as the “malaria hypothesis” and was first confirmed in 1954 for the sickle cell trait (36). Additionally to the sickle cell trait and thalassemia, there are several other red blood cells mutations which provide a certain resistance to malaria, like Glucose 6-phosphate dehydrogenase (G6PD) deficiency, pyruvate kinase deficiency, the absence of Duffy antigens and other haemoglobin (Hb) mutations (HbC, HbE). The precise mechanisms of action are despite years of research still unknown. However, two major reasons are discussed in the literature. On the one hand, the proliferation of the parasite within altered erythrocytes could be impaired because of limited access to Hb or the increased oxidative stress. On the other hand, an enhanced immune response could diminish the appearance of differently formed RBCs.

1.2.3.1 Sickle cell disease

Sickle cell trait is the term of heterozygote sickle cell anaemia, which was first described by J.B. Herrick in 1910 (37). It is driven by a single point mutation in the β chain of the Hb gene, resulting in the exchange of glutamate at position 6 to valine. A Hb molecule with such a mutation is termed HbS. As a result, the deoxygenated HbS tetramer gained a hydrophobic motif which mediates the binding between a β1 of one HbS molecule to the β2 chain of another. This results in an aggregation of HbS molecules to long polymers which disrupt the erythrocytic shape and their flexibility generating cellular dehydration and oxidative stress (38). Patients having sickle cell disease suffer primarily from vaso-occlusions and hemolytic anaemia.

In 2013 about 3.2 million people were diagnosed with the sickle-cell disease and another 43 million with sickle-cell trait (39). The highest occurrence of this HbS mutation is in sub-Saharan Africa which involves around 80% of all sickle cell diseases in children (40). The heterozygote HbAS form consisting of one WT Hb gene (HbA) and one HbS gene show protection against malaria, respectively. This is demonstrated by a lower parasite density in infected HbS children compared to HbAA children as well as by a decrease in severe malaria and mortality of 50-90%. This occurrence has been analysed for more than 50 years (36,41,42) and the respective mode of action has been studied as well.

However, a precise mechanism has not been identified yet and all hypotheses relating to a protective role against malaria fall into three main categories. Early work suggested both, erythrocytes containing HbS are less supportive for *P. falciparum* proliferation under low oxygen tensions as well as a reduction of the parasite invasion event into HbS carrying erythrocytes under low oxygen levels (43,44). Further it has been observed that HbS cells deposit oxidized, denaturated haemoglobin at the inner site of the erythrocytic membrane (45), which occurs to a higher extent in HbS- than in HbA-red blood cells (RBC) and is even forced by the release of non-heme iron that also binds to the RBC membrane (46,47). Due to this denaturating, pro-oxidative environment, the intracellular proliferation of the malaria parasite might be attenuated (48). Secondly, an increased degree of phagocytosis of the respective infected erythrocytes could explain the low parasitemia in HbS carriers (49,50). Recently, data have been accumulated which suggest that HbS might be involved in pathophysiological consequences of *P. falciparum* by reducing the amount of proteins such as *Pf*EMP1 encoded by the var-gene family on the surface of the erythrocyte which leads to a higher level of sequestration (51,52). Indeed in a very recent study by Cyrklaff and colleagues (53), it has been implicated that HbS carrying erythrocytes influence the actin cytoskeleton and the Maurer's cleft formation and thereby impair the vesicle transport towards the erythrocytic surface. More recently, it has been suggested that HbS is mediating a higher tolerance of the host as shown by a non-reduction of the parasite quantity or virulence (54,55). Although these experiments were of some controversial nature as already outlined by (56), the focus was on how the parasite is proliferating in an elevated oxidative environment. Humans who are sickle cell carriers have higher levels of free, non-protein bound heme in the blood circulation (57), which is potentially toxic, due to its oxidative nature. It has been suggested that increased levels of human heme oxygenase 1 (HO-1) might detoxify free heme to CO, biliverdin and iron that binds subsequently to the protein ferritin H chain in HbS blood and thereby renders complicated (cerebral) malaria (54). However, it remains questionable whether the protective nature of the increased level of free heme in HbS carriers is related to a higher tolerance to an increased level of oxidative stressor-mediated by HO-1 or to a higher susceptibility of the parasite by a decreased parasitemia (36) within a pro-oxidative environment.

1.2.3.2 Thalassemia

Similar to the sickle cell trait, thalassemia is also hemoglobinopathies driven by the decrease in synthesis of α- or β-globin (α- and β-thalassemia). In 2013 about 208 million cases were noted with about 4.7 million severe forms of thalassemia and resulting in 25,000 deaths (39,58). It mostly occurs around the Mediterranean Sea, Middle Eastern, South Asian and sub-Saharan Africa correlating with the distribution of malaria infections. In some of this regions, α-thalassemia occurs even in up to 50% of the population (59). This is indicating the former propose of Haldane, that milder forms of thalassemia provide a certain protection against malaria (34).

The α-thalassemia disorder involves the genes HBA1 and HBA2 encoding for the Hb α-chains on chromosome 16. The severity of the disease depends on if one (-α/αα), two(--/αα; -α/-α), three (--/-α) or all four (--/--) genes are inactive either by deletion or point mutations. Because of the followed excess of β- or γ-chains in new-borns unstable HbH tetramers consisting of 4 beta chains are formed. The formation of γ-chains tetramers in a homozygote α^0 fetus often results in a soon death because of the high affinity to oxygen, which hinders the transport of oxygen to the tissues. Nevertheless, α-thalassemia shows a protective effect against *P. falciparum* infection around 40% (60–64). The mechanism of action is still unknown but it has been reported that the parasite density in blood is not different than for (αα/αα) children (60,61,63–65). This rejects the possibility of impaired growth or an enhanced removal of iRBC by the immune system as a possible mode of action (60,66). Currently, a discussion of a weakened cytoadherence as the reason for the protective effect has been initiated (59).

The decrease of active β-globin driven by gene mutation is the cause of β-thalassemia. Up today there are around 300 mutations described (67). The most common are HbE where the glutamic acid at position 26 is exchanged for a lysine. HbE carriers usually show no clinical effects (68,69), but provide an resistance advantage towards *P. vivax* infections, and to a lesser extent to *P. falciparum* (70–72).

1.2.3.3 Duffy antigen negative

The Duffy antigen chemokine receptor (DARC), also known as Fy glycoprotein (FY) is a glycoprotein receptor on the surface of red blood cells (73). The receptor serves for several chemokines and is important for the merozoite invasion into RBC of *P. vivax* and *Plasmodium knowlesi* (74,75). In 1950 the first antigen (Fya) of the DARC-family was discovered, followed several other resulting in a total of six: FyA, FyB, Fy3, Fy4, Fy5 and Fy6 (76,77). However, the mediated resistance is dependent mainly on two of these antigens, FyA and FyB. A single nucleotide substitution polymorphism (SNIP) (DARC 46 T → C) in the promoter region of the Duffy antigen gene results in the suppression of their expression. Duffy negative includes individuals which have this mutation on both alleles (78).

Similar to *P. falciparum, P. vivax* is distributed around tropical countries. However, in West and Central Africa, a low occurrence is noticed. In parallel up to 90% of the population of this area shows a lack of Duffy receptors (75,79). It is believed that the heavy burden of *P. vivax* forced the selection of a Duffy-negative population over the time, resulting in the elimination of *P. vivax* in this region (80).

Nevertheless, there is evidence that *P. vivax* is able to infect Duffy negative RBC as it was shown for populations in Western Kenya, the Brazilian Amazon region and Madagascar (81–83). Although the resistance is not protecting completely against *P. vivax* infection it remains a good example of innate resistance against malaria.

1.2.3.4 Pyruvate kinase deficiency

A recent example of the malaria hypothesis is the pyruvate kinase (PK) deficiency mediated resistance towards malaria (84). PK catalyses the last step of anaerobic glycolysis converting phosphoenolpyruvate (PEP) into pyruvate releasing ATP. Because of the absence of mitochondria in mature erythrocytes, this step is responsible for creating about 50% of the RBC total ATP production (85). Therefore PK deficiency leads to a decreased ATP concentration resulting in a shorter erythrocyte lifespan (85).

PK deficiency was first described in 1961 and is caused by mutations in the PK, liver and RBC (PKLR) gene on chromosome 1q21 (86,87).Today more than 200

mutations are known which result in clinical symptoms like nonspherocytic hemolytic anaemia in homozygous and compound heterozygotes patients (88,89). With one out of 20,000 persons who have PK deficiency this disease is the second most common enzymopathy after G6PD deficiency (90).

Recently a geographical co-distribution between malaria and PK deficiency was shown by Machado and colleagues demonstrating the highest prevalence in the Middle East and sub-Saharan Africa (84). The protective effect was already revealed for in vivo malaria infection in the murine models and under culture conditions using human PK-deficient blood (91). The mediated resistance and the co-distribution with human malaria suggest that it might be a selective pressure resulting in the development of PK deficiency variants (92,93).

1.2.3.5 Glucose 6-phosphate dehydrogenase deficiency

The most common enzymopathy is a G6PD deficiency with more than 400 million cases worldwide (94). Although G6PD mutations are distributed all over the world the main prevalence is in Africa, southern Europe and Asia, as well as the Middle East and southern Pacific islands (Figure 4). This is remarkably similar to the world distribution of malaria leading to the idea of a G6PD deficiency mediated protective effect (80).

G6PD deficiency was first known as favism because of the pathological symptoms like hemolytic anaemia occurring after the consumption of fava beans (95). In 1956 G6PD deficiency was described for the first time, seeing low levels of G6PD in patients with hemolytic anaemia using the antimalarial drug primaquine. Subsequently, the correlation of favism and G6PD deficiency was published (96).
G6PD is catalysing the first step of the pentose phosphate pathway (PPP) providing the reduced form of nicotinamide adenine dinucleotide phosphate (NADPH). NADPH is the reducing agent in many enzymatic reactions and is playing a key role in protection against oxidative stress via the glutathione system. Especially in erythrocytes which lack mitochondria, the PPP is the only source of NADPH making the G6PD essential to counterbalance oxidative stress (97).

The G6PD deficiency is a X-linked, hereditary genetic disease with a gene location at the telomeric region of the long arm (98,99). Because of the X-linked pattern the disease occurs more in males who are either G6PD deficient or not. Females, however, have two alleles and can be heterozygote mosaics because of the X chromosome inactivation (lyonization) (100).

Figure 4 – World distribution of G6PD deficiency.

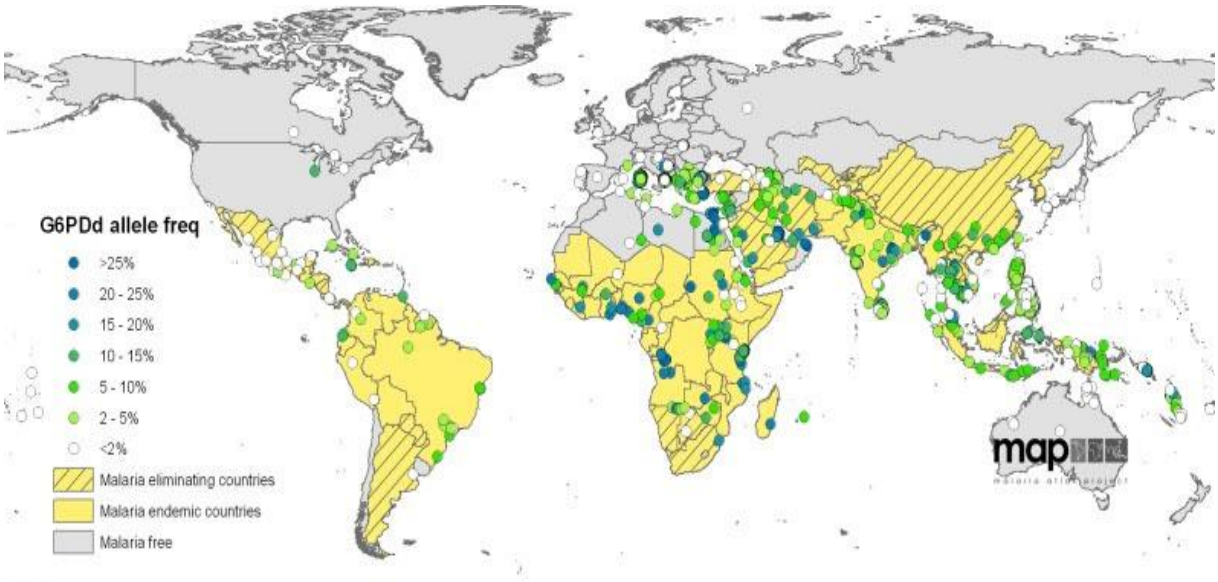

World prevalence of G6PD deficiency using coloured data points compared to the malaria distribution as background map (101).

G6PD is active as a tetramer or dimer with a $NADP^+$ molecule in each subunit. The quaternary structure is essential for the enzyme activity and therefore, it is no surprise that often G6PD deficiency is due to mutations interfering with the enzyme conformation (100). There are about 140 different mutations described which are all located in the enzyme coding sequence (102). Most of them are single base exchanges leading to various biochemical and clinical different phenotypes. However, mostly G6PD deficient individuals show no clinical symptoms when not exposed to oxidative stress triggers like drugs, infection or fava beans (103). In some severe cases, patients develop neonatal jaundice or acute hemolytic anaemia which could lead to permanent neurological damage or death (104).

As already suspected G6PD deficiency mediates resistance against malaria. It was already seen, that individuals with this condition have a protection up to 50% against

severe *P. falciparum* malaria (105,106). More recent studies show a protective effect also against *P. vivax* infection (107,108). In both infections, a lower parasite density was found. However no mechanism of action for G6PD deficiency mediates malaria resistance is known, there are several theories which are discussed, like an enhanced phagocytosis (109–111) or the impairment of parasite growth because of increased oxidative stress. It was already refuted that the reason is an increase of antibodies against *P. falciparum* merozoite surface protein 2 (MSP2). G6PD deficient individuals showed even a lower level of MSP2 IgG3 antibodies (112). Moreover it is still discussed if the protective effect is given for male hemizygote or just for female heterozygote individuals (106,113–117).

1.3 Oxidative stress

1.3.1 Formation of reactive oxygen species

Reactive oxygen species (ROS) is a term to describe by oxygen- (O_2) derivates driven free radicals, such as superoxide anion ($O_2^{\bullet-}$), alkoxyl radical (RO•), peroxyl radical (ROO•), and the highly toxic hydroxyl radical (HO•), as well as nonradicals like hydrogen peroxide (H_2O_2), singlet oxygen ($^1O_2$), hypochlorous acid (HOCl) and ozone (O_3). Reactive nitrogen species (RNS) are similar reactive molecules containing nitrogen, such as nitric oxide. They are by-products of the normal cell metabolism or driven by exogenous sources like drugs, xenobiotics or pollutants. ROS can be important signalling molecules for cell proliferation and differentiation (118,119) as well as harmful to the cell and tissues leading to apoptosis and cell death (120). Therefore the balance of ROS formation and detoxification is essential for the cellular homoeostasis and depends on pro- and antioxidant enzymatic reactions as well as antioxidant molecules.

One of the main sources of ROS production is the mitochondrion. Through the inner mitochondrial membrane, electrons are translocated via the electron transport chain (ETC) reducing in their final step O_2 to water and so finally producing adenosine triphosphate (ATP) via the ATP-synthase complex. Here about 1-2% of the electrons pass through and produce in the presence of metal ions (present in Complex I and

Complex III) ROS, such as $O_2^{\bullet-}$ and H_2O_2 via the Fenton and/or Haber-Weiss reactions leading to the dangerous HO• (121,122):

$$Fe^{3+} + O_2^{\bullet-} \rightarrow Fe^{2+} + O_2$$

$$Fe^{2+} + H_2O_2 \rightarrow Fe^{3+} + OH^- + OH\bullet$$

$$O_2^{\bullet-} + H_2O_2 \rightarrow HO\bullet + OH^- + O_2$$

Also the endoplasmic reticular (ER) can be responsible for the increase of ROS for e.g. through monooxygenases like cytochrome P450 (CYP) (123). CYPs are important for the detoxification of the ER and catalyse the oxygenation of an organic substrate by reducing O_2 to water.

$$RH + O_2 + NADPH + H^+ \rightarrow ROH + H_2O + NADP^+$$

When the reaction of O_2 and the organic substrate not tightly coupled, electron equivalents derived from NADPH can react directly with O_2 forming a CYP–oxygen complexes which will dissociate and form ROS as $O_2^{\bullet-}$ and H_2O_2 and HO• (123–125).

Furthermore, another significant source of cellular ROS are the peroxisomes, which are ubiquitous subcellular organelles. They are responsible for the β-oxidation of fatty acids, biosynthesis of ether phospholipids as well as the metabolism of ROS. Certain enzymes like the flavin oxidases catalyse the reaction of O_2 with organic substrates. In this oxidative reaction ROS can be generated. It is already described that peroxisomes are responsible for H_2O_2, $O_2{\cdot}^-$ and $^1O_2$ cellular production (126). Thus peroxisomes are present in almost all eukaryotic cells (127,128) some organisms suffered its evolutionary loss, such as several parasitic lineages including *Plasmodium* spp (129).

The last important source to mention are the NADPH oxidase (NOX) complexes which are the only enzymes, whose biological function is the production of ROS. The first NOX described was the phagocyte NOX2 (NOX2/gp91phox) which is highly expressed in granulocytes and monocyte-macrophages (reviewed in (119). Here ROS generation is used for the active killing of microorganisms. However, up today six more NOX homologous were found, which are localised in almost every tissue.

Interestingly, though, a defence function is just described for NOX2. The active generation of ROS suggests that this molecule has to have an important role for cell development and survival. Besides host defence, NOX driven ROS production has been associated with the posttranslational processing of proteins, cellular signalling, regulation of gene expression, and cell differentiation (119).

Despite the advantages of ROS generation, an increase of this molecules results in dangerous cell damage. In normal cells, intracellular levels of ROS are maintained in balance with intracellular biochemical antioxidants and when this balance is disrupted it can be called an oxidative stress situation. In this case, ROS reacts with several molecules like carbohydrates, proteins, lipids, or nucleic acids, resulting in consequences such as lipid peroxidation or unfolded protein response (UPR) in the ER. If the oxidative stress level is too high and too much damage occurs, a cell will undergo apoptosis or programmed cell death.

1.3.2 The oxidative defence system of erythrocytes

The primary biological function of erythrocytes is the transport of O_2 from the lungs to all blood tissues. Therefore the cytoplasm is rich of haemoglobin, which can bind O_2 via its iron-containing heme group. To use the whole cytosolic capacity RBC lacks mostly all organelles as well as the nucleus. Although RBCs are not exposed to ROS-driven by the above-mentioned organelles like mitochondrion, ER and peroxisomes RBCs are continuously exposed to both cellular and extracellular ROS (130). One of the main intracellular sources of ROS in RBS is the autoxidation of Hb under hypoxic conditions, leading to the formation of $O_2^{\bullet-}$ which will rapidly convert to H_2O_2. Because of the iron-containing heme group the generation of HO• via the Fenton and/or Haber-Weiss reactions is also possible. New approaches show that RBCs contain a ROS producing NOX and therefore enzymatically catalysing ROS. It is suspected that these RBC-NOX are involved in sickle cell disease, although RBC-NOX were also found in healthy erythrocytes (131). Xenobiotic floating in the blood stream is exogenous exposure of RBCs to ROS as well as free heme after haemolysis as well as free radicals released via neutrophils and macrophages into the plasma (132). However, experiments showed that as well as intracellular as well as extracellular generated ROS are rapidly neutralised by the RBC antioxidant

system (132). To do so RBCs have a comprehensive antioxidant system (Figure 5) involving both non-enzymatic antioxidants like glutathione and ascorbic acid and enzymatic antioxidants including superoxide dismutase, catalase (133) glutathione peroxidase (134) and PRDX-2 (135,136).

Figure 5 – Oxidative defence system of red blood cells.

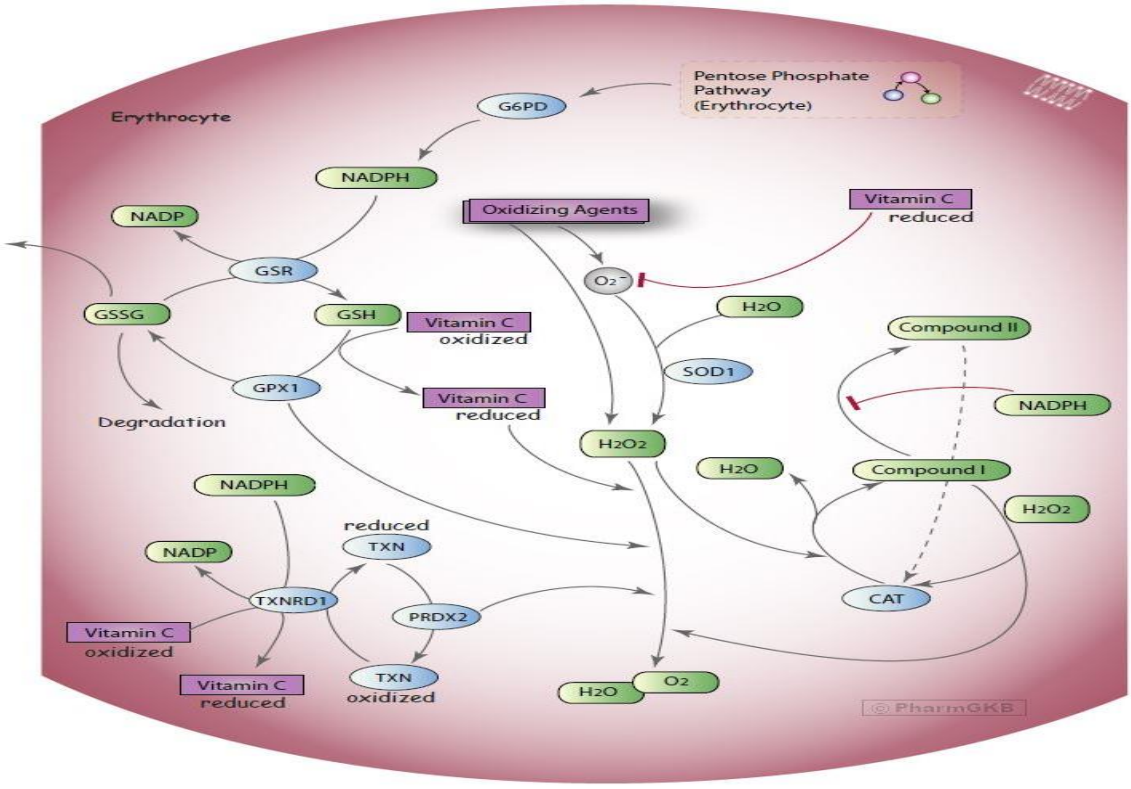

The oxidative defence system of RBCs consisting of superoxide dismutase, catalase the glutathione and thioredoxin system as well as peroxiredoxin-2 and the essential vitamin C. Source: (137).

Via autoxidation or Fenton reactions resulted cytosolic $O_2^{\bullet-}$ is converted to H_2O_2 by superoxide dismutase. This can be either neutralized by the glutathione (GSH) system or via TXN both NADPH-dependent systems. GSH is a small tripeptide (γ-L-Glutamyl-L-cysteinylglycine) which serves as an important antioxidant due to its thiol group. On the other hand, TXN is a small redox protein which facilitates the reduction of other proteins. Both GSH and thioredoxin reductase (TXNR1) are able to reduce vitamin c (ascorbic acid) which subsequently neutralises $O_2^{\bullet-}$, H_2O_2 and oxygen free radicals (137).

GSH is also important together with peroxiredoxin 2 (PRDX2) to stabilise haemoglobin by preventing and reversing oxidation that causes disulphide cross-links between globin chains. The in this way resulting a change of haemoglobin structure is the potential reason for the formation of the typical G6PD deficient RBCs appearance the 'Heinz bodies'. Finally, RBCs contain a catalase (CAT) which is NADPH-independent and is able to catalyse H_2O_2 to H_2O and O_2.

1.3.3 The oxidative defence system of P. falciparum

During the erytrocytic stage of *P. falciparum*'s life cycle the parasite has to adept himself to the oxidative environment of the host cell. Therefore he needs an effective oxidative defence system which protects him from ROS driven by the RBC, as well as from the host immune response and his own ROS products driven by the degradation of Hb (138). The parasite uptakes Hb from the RBCs cytosol and digests it inside the DV. The released highly reactive heme is than bound as a non-toxic criystal, the haemozoin. However, small amounts of free heme are released into the parasites cytosol where it reacts with O_2 to $O_2^{\bullet-}$ and H_2O_2 which can lead to oxidative damage and parasites death (139). Another main source of ROS in *P. falciparum* is the mitochondrion as already described above. Nevertheless *Plasmodium* spp. does not possess a peroxisome (129) or NOX complexes.

The adaptation to this oxidative milieu is critical to the parasites survival, therefore already in the early blood stages at least five different antioxidant proteins are expressed (140). However, Plasmodium lacks a catalase and glutathione peroxidase (141,142) and therefore it has established several other mechanisms to detoxify H_2O_2 and other ROS (Figure 6). Superoxide dismutases in the cytosol (*Pf*SOD1) and in the mitochondrion (*Pf*SOD2) catalyze the reaction from $O_2^{\bullet-}$ to H_2O_2. Cytosolic H_2O_2 either react with $O_2^{\bullet-}$ to the highly reactive HO• or can be neutralized by TRX dependent peroxidases, which are part of the main system to remain the redox homeostasis together with the GSH system (143). Both GSH and TRX antioxidant mechanisms are NADPH dependent and can be recycled by GSH or TRX reductases. Plasmodium is able to synthesis GSH *de novo* an important small molecule for the detoxification via *Pf*GST and glyoxalases. Plasmodium contains two *Pf*GSTs, one localised in the parasites cytosol detoxifying *e.g.* hemin and different

intracellular xenobiotics (144). *Pf*GST2 previously known as *Pf*EXP1 is localised in the parsitophorous vacuolar membrane and is contributing in the hemin/haematin detoxification (145). *Pf*GST2 was also shown to be a potential target of the antimalarial artesunate (31). GSH is also an important co-factor for the glyoxalases which is reacts with a toxic by-product of the glycolysis, methylglyoxal to D-lactate, which than can be secreted (146).

Figure 6 – Oxidative defence system of *P. falciparum*.

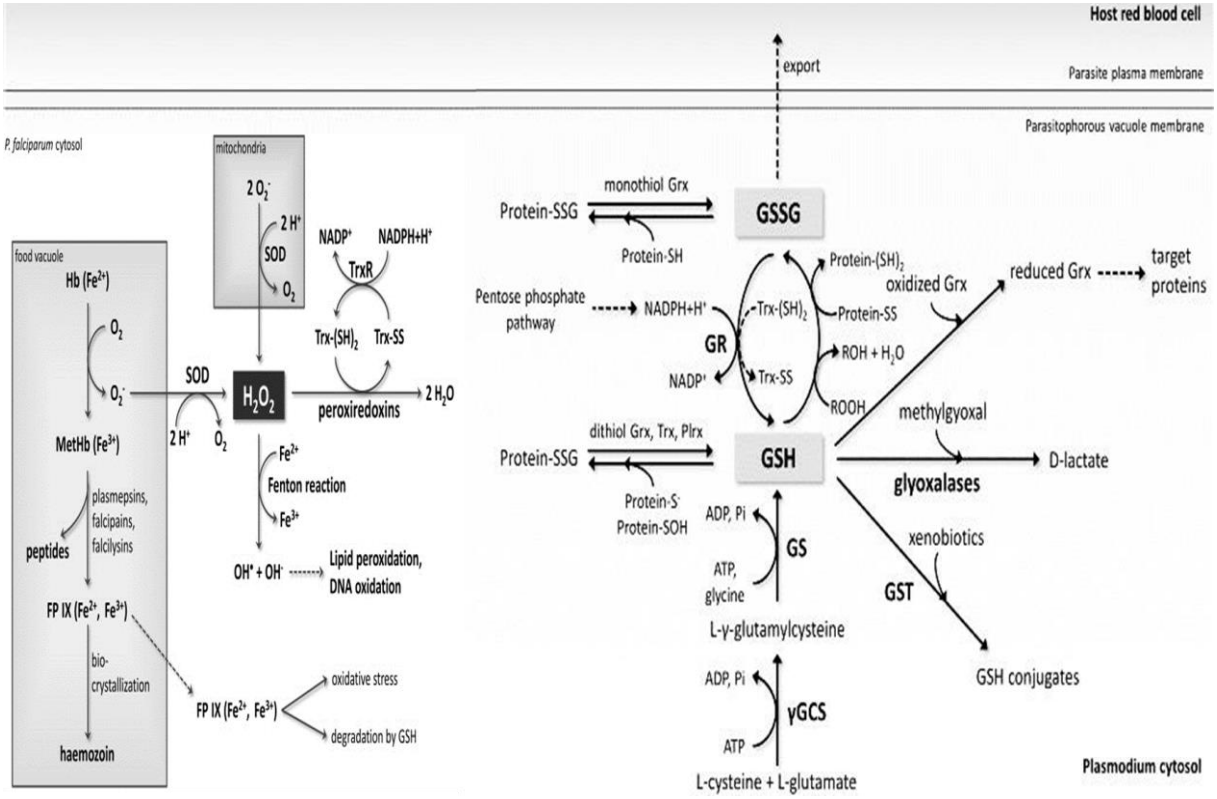

The oxidative defence system of *P. falciparum* is important to conter ROS driven from mitochondria and Hb digestion. Superoxide dismutase catalyze the reaction from $O_2^{\bullet-}$ to H_2O_2 which will be neutralized via the TRX system. The *de novo* synthesis of GSH is present in the parasite providing GSH as a co-factor for *Pf*GSTs and other detoxifying enzymes like glycolases. Source: modified from (147).

Interestingly *P. falciparum* contains the biosynthesis pathway for Vitamin B6, as well as the possibility for scavenging it from the blood plasma. Vitamin B6 is a co-factor in more than 100 enzymatic reactions and additionally is highly relevant to quench oxidative stress, due to its role in singlet oxygen ($^1O_2$) detoxification (148,149).

2 JUSTIFICATION AND OBJECTIVES

Malaria, caused by *Plasmodium spp*., remains with more than 400.000 deaths per year one of the most severe diseases of our time. The few existing antimalarial drugs are losing their efficacy due to the worldwide spreading of parasite's drug resistance. Therefore the discovery of new targets to interfere with is of the highest importance. However, some native resistances against human malaria are known for a long time among them, sickle cell trait or enzymopathies such as glucose-6-phosphate dehydrogenase deficiency. Although there are several hypotheses about the mode of action of a better innate immune response or the increased oxidative stress inside altered erythrocytes the protection mechanism is still unknown.

This work is focusing on the oxidative defence system of *P. falciparum* using transgenically modified parasites cultured in wild-type and abnormal red blood cells to discover the mode of action of the native resistance mediated through glucose-6-phosphate dehydrogenase deficiency. The abnormal blood is provided by ProSangue, Brazil.

To achieve a deeper insight of the protection mechanism of the glucose-6-phosphate dehydrogenase deficient erythrocytes this work had the following objectives:

- Amplification of open reading frames known to be involved in the redox mechanism of *P. falciparum* via PCR and cloning into the transfection vector pARL 1a-
- Transfection of all cloned genes of interests into *P. falciparum*
- Verification of the respective protein expression via Western-blot analysis and qRT-PCR
- Growth analysis of transgenic parasites in wild-type and glucose-6-phosphate dehydrogenase deficient erythrocytes
- Analysing the ROS level of wild-type and glucose-6-phosphate dehydrogenase deficient erythrocytes infected with transgenic *P. falciparum*
- Analysing the glutathione level of wild-type and glucose-6-phosphate dehydrogenase deficient erythrocytes infected with transgenic *P. falciparum*
- Compound screening against novel drug targets involved in the mode of action of the native resistance

3 MATERIALS AND METHODS

3.1 Cloning the genes of interests

3.1.1 Deoxyribonucleic acid amplification

The open reading frames (ORF) encoding for the proteins involved in oxidative stress mediation of *P. falciparum* had been identified in the plasmodial genome database by BLAST search analyses (Table 1). The identified open reading frames were amplified by polymerase chain reaction (PCR) using the Platinum PCR SuperMix, High Fidelity (Invitrogen) or if necessary by Reverse Transcriptase-PCR (RT-PCR) using the SuperScript™ III One-Step RT-PCR System with Platinum® Taq High Fidelity (Invitrogen). As template genomic Deoxyribonucleic acid (gDNA) or messenger ribonucleic acid (mRNA) were used, which were previously isolated from unsynchronized 3D7 culture, as described in (150). Employed primers are listed in Table 2. For later protein evaluation the antisense (AS) primers are containing either a myc-tag or a strep-tag followed by a STOP-codon, or just the STOP-codon after the GFP-OFR when desired.

Table 1 – List of the studied gene of interests.

Gene ID	Protein	Abbreviation	Introns	Gene size (bp)	Protein size (kDa)
PF3D7_0112200	multidrug resistance-associated protein 1	MRP1	-	5469	214.5
PF3D7_1229100	multidrug resistance-associated protein 2	MRP2	-	6327	248.3
PF3D7_0923800	thioredoxin reductase	TrxR	-	1854	68.6
PF3D7_1438900	thioredoxin peroxidase 1	TrxPx1	-	588	77.5
PF3D7_0814900	superoxide dismutase 1	SOD1	-	597	22.7
PF3D7_0623500	superoxide dismutase 2	SOD2	+	801	31.2
PF3D7_1345700	isocitrate dehydrogenase	IDH	-	1407	51.5
PF3D7_1419800	glutathione reductase	GR	+	1503	56.5
PF3D7_0512200	glutathione synthetase	GS	-	1968	77.4
PF3D7_0918900	gamma-glutamylcysteine synthetase	gGCS	-	3192	124.3
PF3D7_1419300	glutathione S-transferase	GST	+	636	23.2
PF3D7_1453800	glucose-6-phosphate dehydrogenase-6-phosphogluconolactonase	GluPho	+	2733	106.8

Listed are the gene ID of PlasmoDB.org as well as the protein name and used the abbreviation, if the gene contains introns as well as the size of the mRNA and of the resulting Protein.

Table 2 – List of used primers for cloning into the vector pARL 1a-.

Primer Name	Sequence 3'-5'
MRP1 kpnI S	GCGCGGTACCATGACGACATATAAAGAAAATGTTGG
MRP1 strep avrII AS	GAGACCTAGGTTATTTTTCGAACTGCGGGTGGCTCCAAGCGCTGTCG TCCATTTCTAACAAATGTG
MRP2 kpnI S	GCGCGGTACCATGATGAGACGGAGAAGCGTTTACAATTTCG
MRP2 myc avrII AS	GAGACCTAGGTTATAAATCTTCTTCTGATATTAATTTTTGTTCATTTAA TTGTTTTTCTTGAAGCAAGTTAGC
TrxR kpnI S	GCGCGGTACCATGAACAATGTAATTTCTTTCATTGG
TrxR strep avrII AS	GAGACCTAGGTTATTTTTCGAACTGCGGGTGGCTCCAAGCGCTTCCA CATTTTCCACCCCCACATCCTCC
TrxPx1 kpnI S	GCGCGGTACCATGGCATCATATGTAGGAAGAGAAGCTCC
TrxPx1 strep avrII AS	GAGACCTAGGTTATTTTTCGAACTGCGGGTGGCTCCAAGCGCTCAAC TTTGATAAATATTCACTAACACC
SOD1 kpnI S	GCGCGGTACCATGGTTATTACATTGCCCAAATTAAAGTACGC
SOD1 strep avrII AS	GAGACCTAGGTTATTTTTCGAACTGCGGGTGGCTCCAAGCGCTCTTT TGCATAGCTTTTTTTAAGTTTTCATTTGC
SOD2 kpnI S	GCGCGGTACCATGAATTTGAAGATTTTACTTTGTTCG
SOD2 strep avrII AS	GAGACCTAGGTTATTTTTCGAACTGCGGGTGGCTCCAAGCGCTACTT GAAATGGACAAATTATAATTGGC
IDH xmaI S	GAGACCCGGGATGGTACCATGGGAAAGCATATACGAATTTTAAAAAA TCAATACC
IDH strep avrII AS	GAGACCTAGGTTATTTTTCGAACTGCGGGTGGCTCCAAGCGCTTGTT GAATGTTCTTGGGGAGCATAAAAATTCC
GR kpnI S	GCGCGGTACCATGGTTTACGATTTAATTGTAATTGG
GR strep avrII AS	GAGACCTAGGTTATTTTTCGAACTGCGGGTGGCTCCAAGCGCTTTTC ATCCATGGCTGTAAGGTTAGAAATTCTTCTGC
GS kpnI S	GCGCGGTACCATGGAAAGAAAGGTAGATGAGTTTTATAAAG
GS strep avrII AS	GAGACCTAGGTTATTTTTCGAACTGCGGGTGGCTCCAAGCGCTATGT TCAGTTAAAAAAAAAGAATCC
gGCS kpnI S	GCGCGGTACCATGGGTTTTCTAAAAATCGGAACGCC
gGCS strep avrII AS	GAGACCTAGGTTATTTTTCGAACTGCGGGTGGCTCCAAGCGCTTGCA CTCAGTTCGTACATTTTTTTTGC
GST kpnI S	GCGCGGTACCATGGGAGATAATATAGTG
GST Y9F kpnI S	GCGCGGTACCATGGGAGATAATATAGTGTTATATTTTTTTGATGC
GST avrII myc AS	GAGACCTAGGTTATAAATCTTCTTCTGATATTAATTTTTGTTCGTATAC ACTTTCTTTTCTATTAG
GST avrII AS	GAGACCTAGGGTATACACTTTCTTTTCTATTAG
G6PD kpnI S	GCGCGGTACCATGGATTATGAGAATTTTGTAAAAAGTG
G6PD strep avrII AS	GAGACCTAGGTTATTTTTCGAACTGCGGGTGGCTCCAAGCGCTATTA ATATCTAACAAATCG
pARL Seq S	ATATCCGTTAATAATAAATACACGC
pARL Seq AS	CCAGTAGTGCAAATAAATTTAAGGG

Names and sequence are shown in 5' to 3' orientation of used primers including the encoded restriction sites and tags. Primers used for sequencing are named pARL Seq.

The reactions were prepared according to manufacturer specification applying an annealing temperature of 47 °C and elongation times corresponding to the size of the gene.

The gene size was confirmed by 1% TRIS-Acetate-EDTA buffer (TAE) agarose gel electrophoresis (151) using 1 kb ladder (Fermentas). The positive amplifications were purified via the PCR purification kit (Qiagen) like described in the recommendations and eluted in distilled sterile water.

3.1.2 Ligation and transformation

The purified PCR products together with the transfection vector pARL 1a-*Pf*ARG-GFP (152,153) (Figure 7) were digested with restriction endonucleases *kpn*I and *avr*II. The IDH-strep cloning was performed with the restriction enzymes *xmaI* and *avr*II provided by New England Biolabs (NEB, USA). The reaction was performed at the recommended conditions for two hours followed by PCR purification using the Qiagen purification kit (Qiagen, Germany) according to its recommendation. For the ligation of the gene of interests (GOI) into the vector the T4 DNA ligase (NEB)

Figure 7 – Vector map of pARL1a-hDHFR with *Pf*ARG-GFP

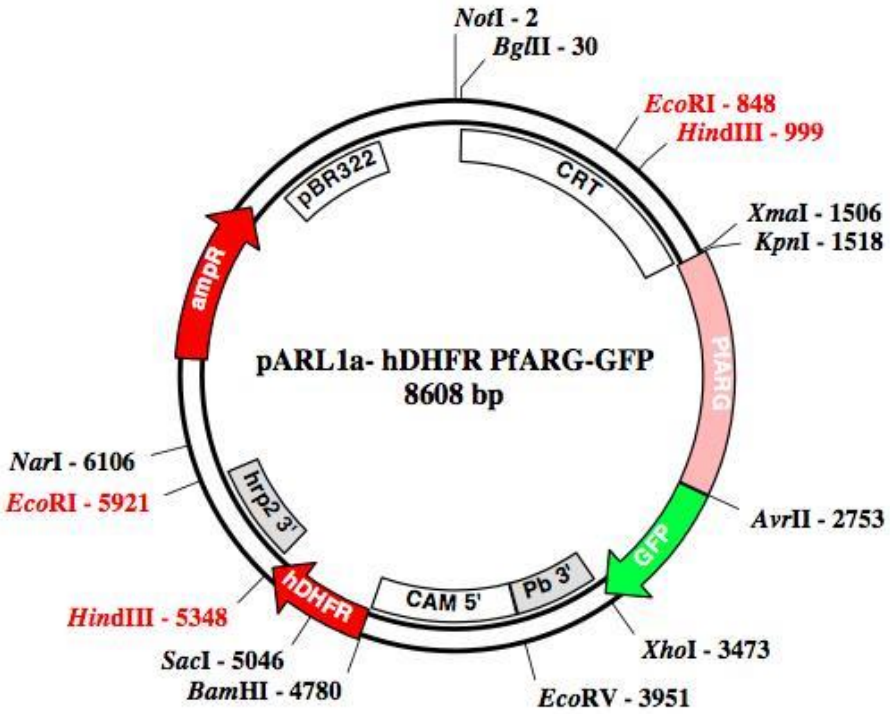

The plasmid used for transfection pARL 1a+. The vector contains the ampicillin resistance cassette and the human dihydrofolate reductase cassette (*h*DHFR), leading to resistance against ampicillin and for the transgenic parasites against the selection drug WR99210. The transcription of the introduced gene is *crt*-promoter driven. Source: modified from (154).

was used in a final reaction volume of 20 µL, using 1-2 µL of digested plasmid and up to 15 µL of the digested PCR product and incubated at 4 °C overnight. The ligation was afterwards transformed into chemical competent XL10-Gold ultra-competent cells (Agilent Technologies) as described in SAMBROOK; RUSSELL, 2001, followed by selection on Luria broth (LB) agar plates containing 50 µg/ml ampicillin.

The plasmids of the obtained colonies were purified via Plasmid Miniprep Kit I, peqGOLD (Peqlab) and the nucleotide sequence was confirmed by automated sequencing (Setor de Sequenciamento de DNA, Centro de Pesquisas sobre o Genoma Humano e Células-Tronco, Instituto de Biociências, Universidade São Paulo, Brazil) before using for transfection into *P. falciparum*.

3.1.3 Maxi preparation

For transfection, the respective constructs of the cloned plasmid are needed at high concentration. Therefore the positively sequenced vector is re-transformed into XL10-Gold ultracompetent cells and cultivated in a volume of 500 mL LB medium (151) overnight. The plasmid was purified with the Plasmid Maxi Kit (Qiagen). The obtained plasmid DNA was dissolved in TE buffer, after drying. DNA concentration was determined using a NanoDrop 2000c device (Thermo Scientific, USA) and divided into 120 µg aliquots, which were then precipitated with 2V ethanol (EtOH) 100% and 1/10V sodium acetate (NaAc) 3 M. The plasmid DNA was stored at -20 °C until used for transfection.

3.2 **Analysing proliferation of *Plasmodium falciparum***

3.2.1 Culture conditions

All *P. falciparum* strains wild type 3D7 (Wellcome Trust, Dundee) and transgenic lines were maintained in continuous culture as originally described by Trager and Jansen (155)TRAGER and JENSEN (1977)with modifications from Das Gupta et al., 2005 (156) at 37 °C in presence of 90% N_2, 5% O_2 and 5% CO_2 in O^+ WT or genetically modified blood provided by InCor-USPand/or ProSangue, Brazil.

3.2.2 Transfection of P. falciparum

The in 3.1 successfully cloned and precipitated pARL 1a- constructs were transfected into the malaria parasite *P. falciparum* 3D7 (148,154). Therefore the plasmid DNA was centrifuged for 30 min at 10.000 *g* and 4 °C before the supernatant was removed and the DNA pellet could be air-dried. The plasmid DNA was then resuspended in 50 µL of Tris-EDTA (TE) buffer (10 mM Tris-HCl; 1 mM EDTA; pH 7.5) and 200 µL cytomix (157). Parasite 3D7 culture at a parasitemia with at least 2% of ring stage parasites was centrifuged for 10 min at 450 *g* and 4 °C. The supernatant was removed and 250 µL of iRBC were added to the resuspended plasmid DNA and subsequently transferred to an electroporation cuvette (BioRad, Germany) and electroporated using the BioRad X-cell total system (BioRad, Germany) at 0.31 kV and 900 mF. After electroporation, the cells were transferred into pre-warmed RPMI medium and inoculated with 200 µl of fresh RBC. Four hours post transfection the culture medium was exchanged. Parasites were grown for 24 h without drug selection before the medium was supplemented with 5 nM of WR99210, where parasites were maintained in continuous culture for selection. To determine the effect of the selection drugs a MOCK line was generated, transfected with the plasmid pARL 1a- MOCK *h*DHFR, as previously described in Knöckel et al., 2012 (148) and used as a control.

3.2.3 Growth Assay with P. falciparum

To establish the influence of the transgenic parasites during proliferation in WT compared to genetically different erythrocytes (InCor and/or ProSangue, Brazil) flow cytometry analyses was applied. Therefore an initial parasitemia of 1% of the *P. falciparum* 3D7, MOCK or transgenic cell line was applied in normal or genetically different erythrocytes with a haematocrit of 2%. Exchange of culture media and selection drug was performed every second day for up to 5 weeks. Every second day 1 µl of the iRBC were collected in 1 mL PBS and 20 µg/mL ethidium bromide was added. After an incubated for 15 min in dark the cells were washed once with 1 mL PBS and again incubated for additional 4 h in dark. Afterwards, the cells were applied to the cytometer Guava EasyCyte Mini (EMD Millipore, Germany). The gates used to determine the parasitemia of the culture are shown in Figure 8. Parasite cultures

reaching a parasitemia levels over 5% were diluted and cumulative parasitemias were calculated by extrapolation of the observed ones and the corresponding dilution factors that were employed at each sub-culturing step. The analyses were evaluated from at least three independent triplicate assays using GraphPad Prism 4 (GraphPad Software, USA).

Figure 8 – Gate profile for the determination of the parasitemia.

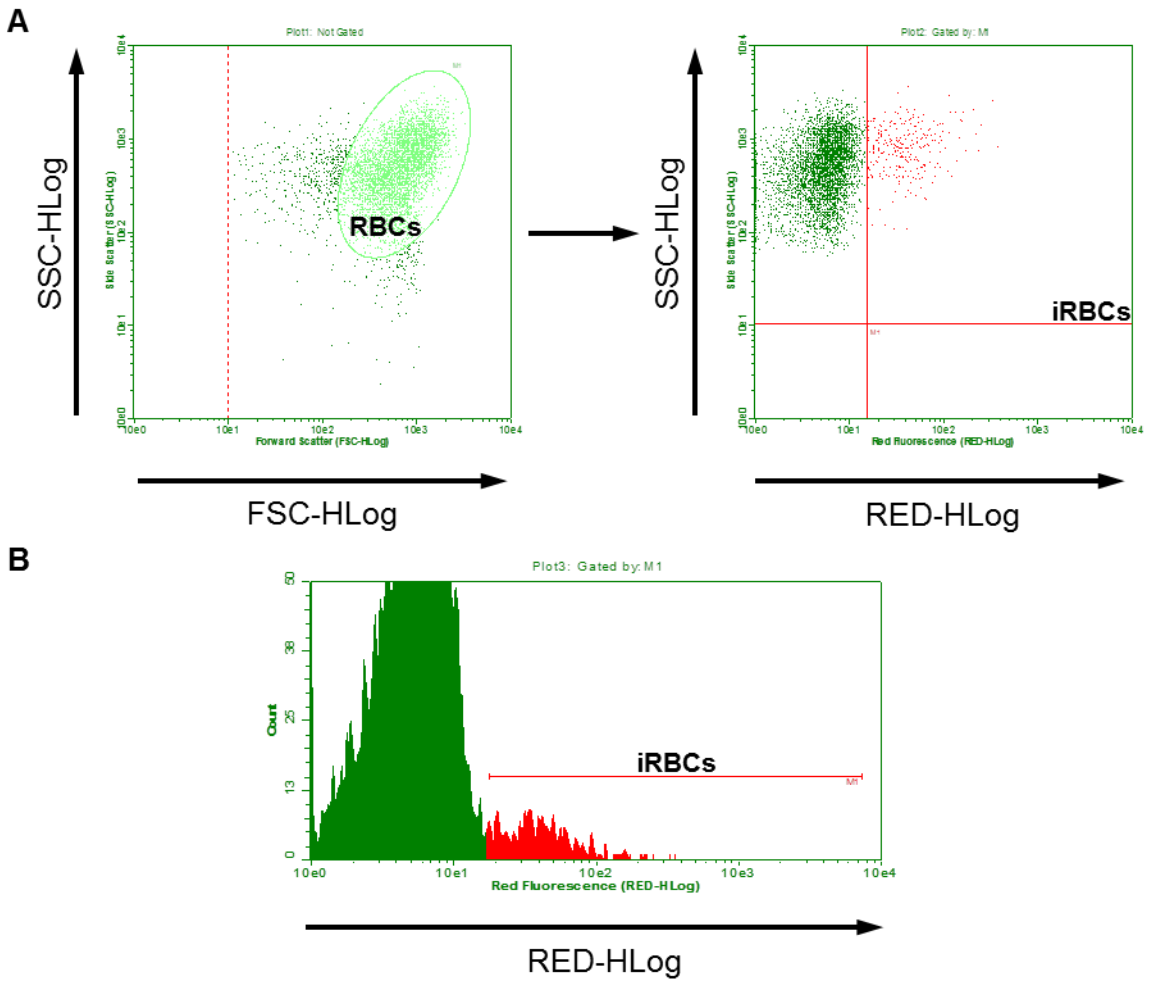

The mock line in G6PD deficient RBCs incubated with 20 µg/ml ethidium bromide for 15 min in dark. Counted were 15000 events via Guava EasyCyte Mini (EMD Millipore, Germany) and analysed through the CytosoftBlue software. **A** Flow cytometry SSC/FCS dot blot showing total RBCs, which were plotted using SSC-HLog and RED-HLog as an axis to determine the total parasitemia. **B** Histogram of resulted gated dot blot.

3.2.4 Verification of overexpression P. falciparum

3.2.4.1 Western Blot

The protein expression of the transgenic cell lines was verified via western blot analysis. Therefore an asynchronous culture of transgenic 3D7 parasites was isolated via saponin lysis (150). The isolated parasites were resuspended in 5x SDS-PAGE sample buffer (151) boiled for 5 min and centrifuged for 5 min at 14.000 *g*. The supernatant was separated by 10% SDS-PAGE as described above (3.5.3). With the Trans-Blot SD Semi-Dry Transfer Cell (BioRad, Germany) the proteins were transferred on a nitrocellulose membrane (BioRad, Germany) the using the protocol described in (151). The expressed proteins were detected via their strep- or GFP-tag by using a monoclonal anti strep- (1:5.000 dilution) or anti GFP-antibody (IBA, Germany; Pierce, USA) and a secondary anti-mouse horseradish peroxidase (HRP)-labelled antibody (1:10.000 dilution, Pierce, USA) and visualized on X-ray films using the SuperSignal West Pico detection system (Thermo Scientific, USA).

3.2.4.2 Quantitative real-time polymerase chain reaction

To analyse the overexpression of the transfected cell lines on the transcriptional level a quantitative real-time PCR (qRT-PCR) was performed. Infected erythrocytes were saponin lysed and total RNA was extracted using TRIZOL (Invitrogen) according to the manufacturer's instruction. Total cDNA was obtained by using a random primer (0.5 pmol/µL) in a RT-PCR using 50 ng of RNA. After this qRT-PCR with the specific primers using 5x HOT FIREPol EvaGreen qPCR Supermix (Solis BioDyne, Estonia) was performed in the Realplex2 Mastercycler EpGradient S (Eppendorf, Germany). The obtained results were analysed via the $2^{-\Delta CT}$ method normalising the results with the plasmodial housekeeping gene *Pf*Aldolase (Salanti et al. 2003). The experiments were performed in triplicate through three independent experiments.

Table 3 – List of used qRT-PCR primers.

Primer Name	Sequence 3'-5'
qRT GFP S	TCAGTGGAGAGGGTGAAGGT
qRT GFP AS	GTTGGCCATGGAACAGGTAG
qRT Aldolase S	TGTACCACCAGCCTTACCAG
qRT Aldolase AS	TTCCTTGCCATGTGTTCAAT

Names and sequence are shown in 5' to 3' orientation of used qRT-PCR primers for the GOI and the housekeeping gene *Pf*Aldolase.

3.3 Fluorescence microscopy

Live parasites were analysed by fluorescent microscopy using an Axio Imager M2 microscope (Zeiss, Germany) equipped with an AxioCam HRC digital camera (Zeiss, Germany). Infected RBCs were incubated with 10 µg/ml HOECHST 33342 (Invitrogen, USA) during 5 min for nucleus staining or with 5 µM 2′,7′-dichlorodihydrofluorescein (H_2DCF-DA) for 15 min to visualise oxidative stress. The images were analysed with the AxioVision 4.8 software.

3.4 Analysing oxidative stress

3.4.1 Fluorometric Assay

To characterise the redox level of the different cell lines oxidative stress was measured by flow cytometry using 5 µM 5-(and-6)-chloromethyl-2',7'-dichlorodihydrofluorescein diacetate, acetyl ester (CM-H_2DCFDA), as a marker for oxidative stress. Aliquots of 1 µL of an asynchrony culture, with a parasitemia higher than 5%, containing iRBC were collected in 1 mL PBS and 20 µg/ml ethidium bromide, as well as 5 µM CM-H_2DCFDA was added. After an incubated for 15 min in dark the cells were washed three times with 1 mL PBS before applying them to Guava EasyCyte Mini (EMD Millipore, Germany). The gates used to determine the parasitemia and the redox level of the culture are shown in Figure 9. However, the influence of extern stress was also evaluated by adding different concentration of H_2O_2. The change of fluorescence intensity was measured over 15 and 30 min and the geometric mean of fluorescence intensity (gMFI) was determined for ring (R), trophozoites (T) and total (R+T). The obtained data were analysed with GraphPad Prism 5 software.

Figure 9 – Gate profile for fluorometric analysis of the ROS level of iRBC.

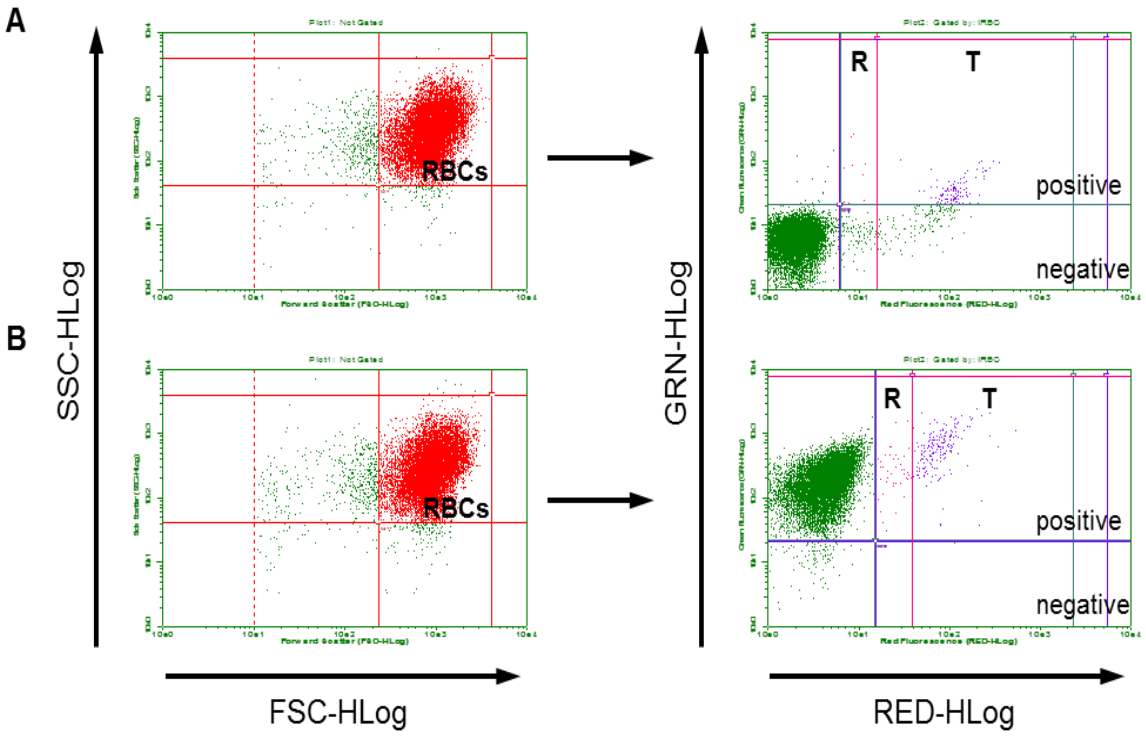

Flow cytometry SSC/FCS dot blot showing total RBCs, which were plotted using the GRN-Hlog and RED-Hlog as an axis. Analysed was the parasitemia in the ring (R) and trophozoites (T) as well as the ROS level using the gMFI of rings (R positive) and trophozoites (T positive). **A** MOCK line in G6PD deficient RBCs incubated with 20 µg/ml ethidium bromide and 5 µM CM-H2DCFDA for 15 min in dark. **B** MOCK line in G6PD deficient RBCs after additional incubation for 30 min with 0,17% H_2O_2. It were counted 15000 events via Guava EasyCyte Mini (EMD Millipore, Germany) and analysed through the CytosoftBlue software

3.4.2 Mass spectrometry

To analyse the oxidised and reduced glutathione (GSH/GSSG) ratio concentration within the different blood types, either infected with the different parasite cell lines, a liquid chromatography electrospray ionisation tandem mass spectrometry (LC-ESI-MS/MS) analyses were performed accordingly to (158). Therefore iRBC were cultured until a high parasitemia of around 10% and purified via µMACS CS Columns and the VarioMACS (Miltenyi Biotec, Germany) ensuring the presence of just late stage iRBC. The parasite pellet was stored at -80 °C before prepared for the LC-ESI-MS/MS analyses. Subsequently, it was added 1 mol/L *N*-ethylmaleimide (NEM) to each pellet, in order to prevent further unwanted oxidation of –SH groups, followed by 1 µg of the dipeptide Glu-Glu as an intern control. The cells were lysed by adding 250 µL of lysis buffer (Tris 20 mM pH 7.5; EDTA 5 mM;

Saponin 0.008%; Triton X-100 0.08%) and by two freezing and thawing cycles. Probes of 200 µL were applied to the API 3200 LC-MS/MS (AB Sciex, USA). Additionally, protein concentration was determined via Bradford analysis, which was used as a normalisation for the measured GSH concentration was normalised via the total protein concentration. Data were analysed by GraphPad Prism 5 software.

3.5 Analysing recombinant protein

3.5.1 Cloning into expression vector

To analyse the plasmodial *Pf*GST closer a recombinant expression construct was generated. Therefore wild type (WT) *Pf*GST and an already characterised inactive mutant, *Pf*GST-Y9F (159) were amplified via RT-PCR, as already described above. The utilised primers containing a C-terminal strep tag are listed in Table 2. The cloning was performed as mentioned in 3.1.2, but digested with *bsa*I (New England Biolabs, USA) and cloned into the *E. coli* expression vector pASK-IBA3 (IBA, Germany).

Table 4 – List of used primers for cloning into pASK IBA3.

Primer Name	Sequence 3'-5'
GST IBA3-S	GCGCGCGGTCTCGAATGGGAGATAATATAGTGTTATATTATTTTGATGC
GST Y9F IBA3-S	GCGCGCGGTCTCGAATGGGAGATAATATAGTGTTATATTTTTTTGATGC
GST IBA3 AS	GCGCGCGGTCTCAGCGCTGTATACACTTTCTTTTCTATTAG
IBA3 Seq S	AGAGTTATTTTACCACTCCCT
IBA3 Seq AS	GACGCAGTAGCGGTAAACG

Names and sequence are shown in 5' to 3' orientation of used primers for cloning into pASK IBA3 including sequencing primers (Seq).

3.5.2 Expression

The expression was performed in *E. coli* BLR(DE3) (Novagen, Germany), as previously described in (160). The expression was induced at an OD_{600} of 0.5 with 200 ng/mL Anhydrotetracycline (AHT) and incubated for 4 h at 37 °C. The following purification of the WT *Pf*GST-strep and *Pf*GST-Y9F-strep enzyme were done by Strep-tag®/Strep-Tactin® protein purification system according to the manufacturer's

recommendation (IBA, Germany). The protein was eluted in 5 mL of respective buffer (1 M Tris-HCl; 1.5 M NaCl; 10 mM EDTA; 25 mM D-desthiobiotin; pH 8.0).

3.5.3 **Sodium dodecyl sulphate polyacrylamide gel electrophoresis**

To analyse the purity of the eluted the protein concentration was determined by NanoDrop 2000c device (Thermo Scientific, USA) measurements and a 10% sodium dodecyl sulphate polyacrylamide gel electrophoresis (SDS-PAGE) was performed (151). The gel was stained with Coomassie Brilliant Blue.

3.5.4 The oligomeric state

3.5.4.1 Fast protein liquid chromatography

In order to investigate the formation of WT *Pf*GST and mutant, the strep-tagged protein was purified as described previously. Subsequently, 5 mg/mL of the protein were separated by fast protein liquid chromatography (FPLC) on a Superdex 200 10/30 column (GE Healthcare Life Sciences, USA) using Äkta Avant 150 (GE Healthcare Life Sciences, USA). The used buffer conditions for the exclusion chromatography contained 100 mM Tris-HCl, pH 8.0, 150 mM NaCl, 1 mM EDTA. The flow velocity was adjusted for 1 ml/min collecting 120 mL total volume. The molecular weight of the detected protein was determined on a calibrated Superdex 200 10/30 column (GE Healthcare Life Sciences, USA) (Figure 10).

3.5.4.2 Dynamic light scattering

A second method to analyse the oligomeric state of WT *Pf*GST and its mutant is the Dynamic Light Scattering (DLS), which measures hydrodynamic sizes of protein solutions using a laser beam and its scattered light. Fluctuations of the scattered light are detected at a scattering angle of 90° by a fast photon detector. Therefore a protein concentration of 0.5 mg/mL was adjusted. After a centrifugation of 10 min at maximum speed at 4 °C, a micro-cuvette was filled with 20 µl of the protein solution. The DLS device Zetasizer Nano Zs (Malvern, UK) performed 10 measurements of 30 seconds each. The data were analysed with the respective Malvern software.

Figure 10 – Calibration of Superdex 200 10/30 column with protein standards

Protein (weight per vial)	Molecular weight (M_r)	Stoke's radius[1] (Å)	Source
Aprotinin (10 mg)	6500	NA	Bovine lung
Ribonuclease A (50 mg)	13 700	16.4	Bovine pancreas
Carbonic anhydrase (15 mg)	29 000	NA	Bovine erythrocytes
Ovalbumin (50 mg)	44 000	30.5	Hen egg white
Conalbumin (50 mg)	75 000	NA	Chicken egg white
Blue Dextran 2000			

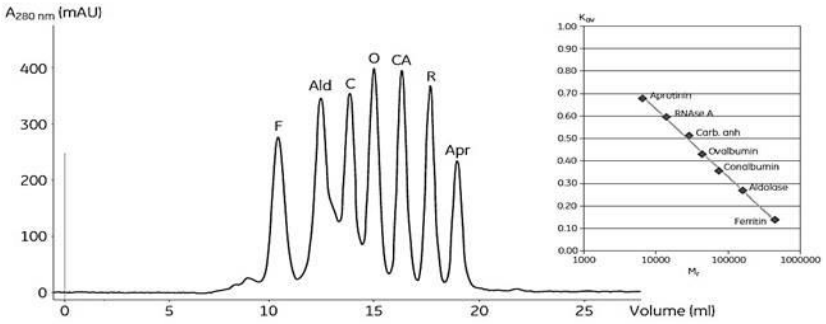

The table shows the protein standards and their molecular weight that were used to calibrate the Superdex 200 10/30 column. The graph indicates in which fraction the standard can be found corresponding the size of the protein. Source: GE Healthcare Life Sciences

3.5.5 Enzymatic Activity

To validate the *Pf*GST and mutant kinetic profile, we performed activity assays as described in Hiller et al., 2006. After expressing and purifying both as described in 0, followed by a FPLC separation (3.5.4.1), the concentration of the proteins was determined using Bradford analysis (151). To measure the enzyme activity the extinction coefficient of the product S-(2,4-dinitrophenyl)glutathione (e_{340}nm=9.6 $mM^{-1}cm^{-1}$) was used. The assays were performed for 20 min using 1 mM GSH and 0.5 mM 2,4-Dinitrochlorobenzene (CDNB) in 100 mM HEPES and 1 mM EDTA, pH 6.5. The reaction was started by adding 10 µg of *Pf*GST or *Pf*GST-Y9F and its absorbance was measured at 340 nm using a SpectraMax i3x multi-well plate fluorescence and luminescence reader (Molecular Devices, USA). Data were analysed via the software SoftMax Pro and the GraphPad Prism 5 software.

3.6 Compound screening and validation

3.6.1 Virtual screening and molecular docking

All the virtual screening calculations were performed by computer workstations equipped with eight-core AMD FX-8150 (3.60GHz each core) processors and double NVIDIA GTX 750ti graphics devices. Software used for VS were licensed by OpenEye Scientific Software, including FILTER 2.0.0, OMEGA 2.5.1.4, ROCS 3.2.1.4 and VIDA v4.3.0, using academic license.

Molport subset (6,835,345 unique compounds) of the ZINC library was cleaned and had their conformers generated and protonation adjusted by Omega2.3 (161–163). Chemical queries to filter compounds with substrate similarity using ROCS 3.2 (164) and compounds were ranked accordingly to Tanimoto-combo. Best thousand compounds were docked on the active site of *Pf*GST crystal structure post-treatment (165) using the AutoDock Vina, (Exhaustiveness value of 10, box was centered at the point 41.7, 43.5, -12.5 with sizes x=24, y=19 and z=25 Å), using Y9 and K14 as flexible. The obtained compounds were ordered at MolPort (ChemDiv, USA).

3.6.2 Compound validation in vitro

The WT *Pf*GST was expressed and purified as described in 0 followed by FPLC gel filtration (3.5.4.1). To validate the compounds against *Pf*GST an activity assay, as described in Hiller et al., 2006 (159), was performed in the presence of 100 µM drug. The activity was measured as explained in 3.5.5, in the presence and absence of GSH. The enzyme assay was started by adding the *Pf*GST and was measured at 340 nm for 20 min. Data were analysed via the GraphPad Prism 5 software.

3.6.3 Compound validation in vivo

For drug discovery against *P. falciparum* three drug concentrations (100 µM, 50 µM, 25 µM) were tested, as described in (166). Briefly, each well of a 96-well plate was seeded with 100 µl of a cell suspension (0.5% parasitemia and 2% haematocrit in RPMI 1640 containing 10% Albumax); in addition, several wells containing not

infected erythrocytes at a haematocrit of 2% serving as controls. The concentrations were tested in triplicates and in three independent assays and incubated for 96 h at 37 °C with a gas mixture of 5% O_2, 5% CO_2 and 90% N_2).

After the incubation 100 µl of SYBR Green, I (0.2 µl/mL of SYBR Green I) in lysis buffer (20 mM Tris-HCl, pH 7.5; 5 mM EDTA; 0.008% Saponin; 0.08% Triton X-100) was added to each well, whose contents were mixed until no visible erythrocyte sediment remained. After 1 h of incubation in the omission of light and at room temperature, fluorescence was measured using a SpectraMax i3x multi-well plate fluorescence reader (Molecular Devices, USA) at excitation and emission wavelength bands centred at 485 and 530 nm, respectively, and a gain setting equal to 50. Data were analysed via the SoftMax Pro and the GraphPad Prism 5 software.

4 RESULTS

4.1 Cloning and transfection

Table 5 shows, in summary, the as in 3.1 described cloned GOI with the corresponding tag and the vector of choice. The constructs were confirmed by sequencing before transfected into *P. falciparum* 3D7 strain as explained in 3.1. In Table 5 time and the voltage resulting from the transfection event are also listed.

Table 5 – Successfully cloned and transfected GOIs.

Construct	Vector	Time (ms)	Voltage (V)
MRP1-strep	-	-	-
MRP2-strep	-	-	-
TrxR	pARL 1a- WR	11,8	306
TrxPx1	pARL 1a- WR	11,8	307
SOD1-strep	pARL 1a- WR	13,6	307
SOD2-strep	pARL 1a- WR	15,1	306
IDH-strep	pARL 1a- WR	18,3	306
GR-strep	pARL 1a- WR	16,4	306
GS-strep	pARL 1a- WR	13,5	306
gGCS	pARL 1a- WR	14,3	306
GST-myc	pARL 1a- WR	12,9	307
GST Y9F-myc	pARL 1a- WR	12,9	307
G6PDH-strep	pARL 1a- WR	13,3	308

List of the successfully cloned GOIs into the vector pARL 1a- WR together with the resulting time and voltage conditions of the transfection events.

However, MRP1 and MRP2 were not possible to clone into pARL 1a- WR and were subsequently not transfected into *P. falciparum* 3D7 strain.

4.2 *P. falciparum* growth analysis

4.2.1 Growth assay of P. falciparum 3D7 strain in G6PD deficient blood

To establish the conditions of the growth assay in WT and G6PD deficient blood first 3D7 WT was cultivated for 8 days in both blood lines as described in 3.2.3. As shown in Figure 11A no difference was seen in the growth behavior between 3D7 in WT or G6PD deficient blood. To analyse if long time exposure influences the survival of the parasite the assay was continued for 32 days. Figure 11 B shows the effect of

long-term cultivation of 3D7 in WT or G6PD deficient blood. After 10 days the proliferation of 3D7 in G6PD deficient blood is slowing down and after 18 days the total parasitemia is reducing until day 28 where no parasites were detected for the next 4 days.

Figure 11 – Growth rate of 3D7 in WT and G6PD deficient blood

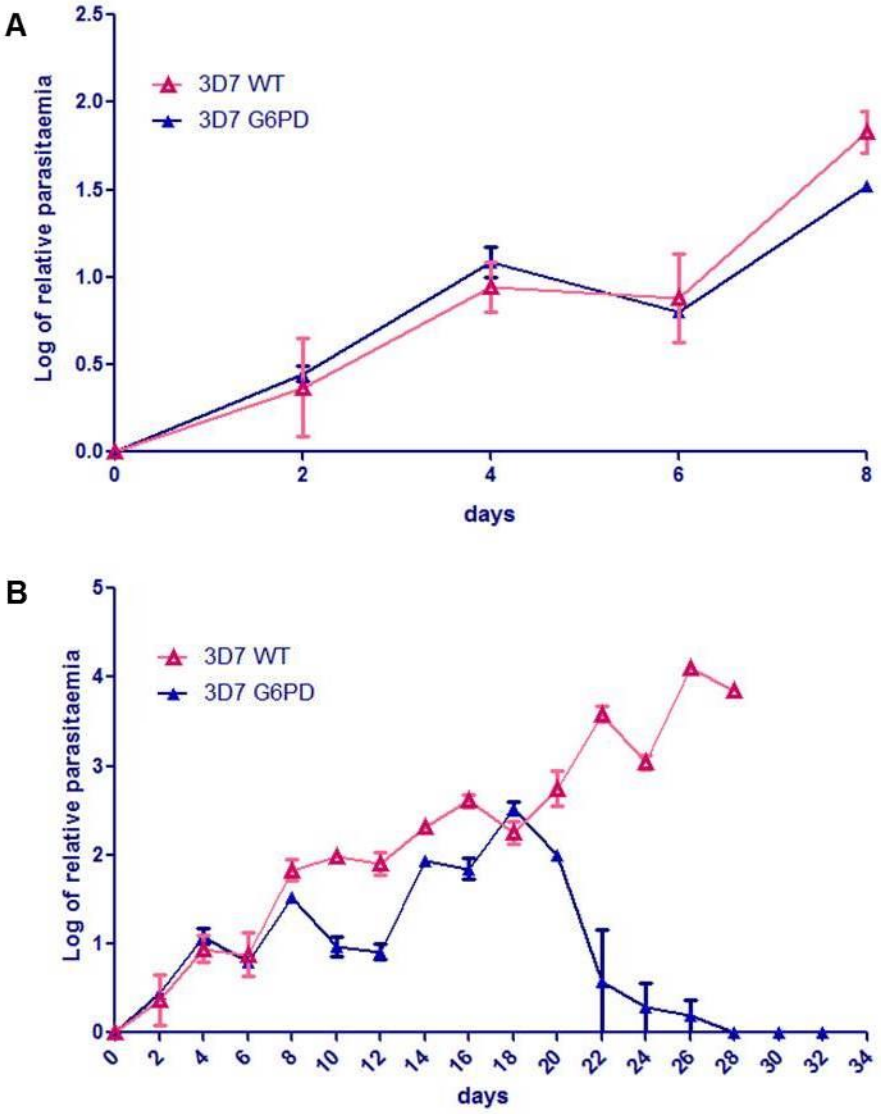

Growth assay of *P. falciparum* 3D7 strain in WT and G6PD deficient blood. The relative parasitemia (%) was measured by flow cytometry for 7 days (A) and 32 days (B) in duplicates and two independent experiments. Displayed is the logarithm of the relative parasitemia (%).

4.2.2 Growth assay of P. falciparum overexpress lines in G6PD deficient blood

The growth behavior of the transgenic cell lines was analysed in the same way for about 30 days. First, the influence of an enhanced protection inside the plasmodial mitochondrion was investigated (Figure 12). Therefore the cell line pARL 1a- WR *Pf*SOD2-strep was cultured in G6PD deficient blood together with the 3D7 and MOCK control line took daily samples. *Pf*SOD2 is responsible for the dismutation of the superoxide anion inside the mitochondrion. Figure 12 shows that there is no difference in proliferation of *P. falciparum* using G6PD deficient blood overexpressing *Pf*SOD2. The overexpressing line, as well as 3D7 and the MOCK line, show a similar proliferation until day 18 before the parasitemia starts to diminish up to day 24 and 25 where all three cell lines reveal no detectable parasitemia.

Figure 12 – Growth rate of pARL 1a- WR *Pf*SOD2-strep compared to 3D7 and MOCK in G6PD deficient blood.

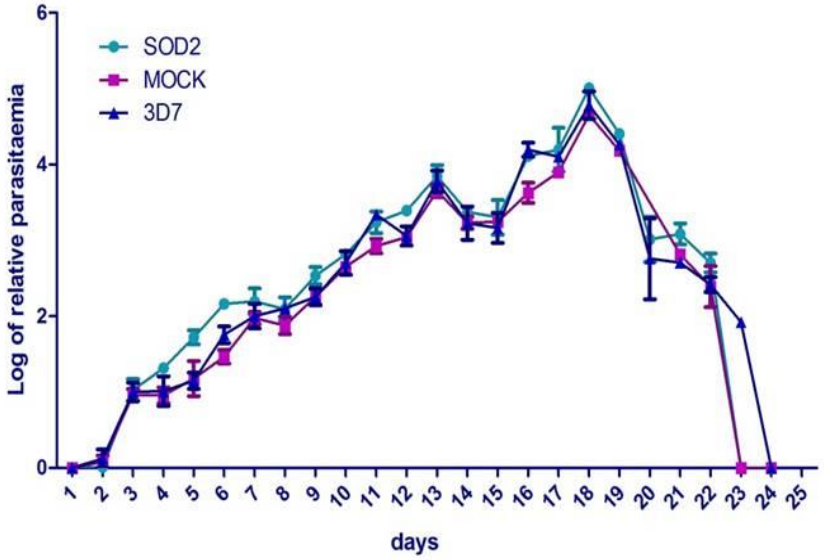

Growth analyses of *P. falciparum* pARL 1a- WR *Pf*SOD2-strep line (SOD2), as well as 3D7 and MOCK in G6PD deficient blood. The relative parasitemia (%) was measured by flow cytometry for 24 days in duplicates and two independent experiments. Displayed is the logarithm of the relative parasitemia (%).

To investigate the importance of a cytosolic localised enzyme the growth profile of the pARL 1a+ WR *Pf*GST -myc cell line was analysed. GSTs are important for the detoxification of a large variety of electrophilic substrates which are not usually present in the cell. These molecules are called xenobiotics (167,168). GSTs are

catalysing the conjugation of GSH to xenobiotics, which will be transported through a GST channel outside the cell.

Figure 13 shows the growth behavior of the *Pf*GST overexpressed line compared with 3D7 and the MOCK line. The overexpression of *Pf*GST generates an advantage in the proliferation of the parasite when cultured in G6PD deficient blood. While 3D7 and the MOCK line show no parasitemia after 23 days the pARL 1a+ WR *Pf*GST-myc cell line continues proliferating.

Figure 13 – Growth rate of pARL 1a- WR *Pf*GST-myc compared to 3D7 and MOCK in G6PD deficient blood.

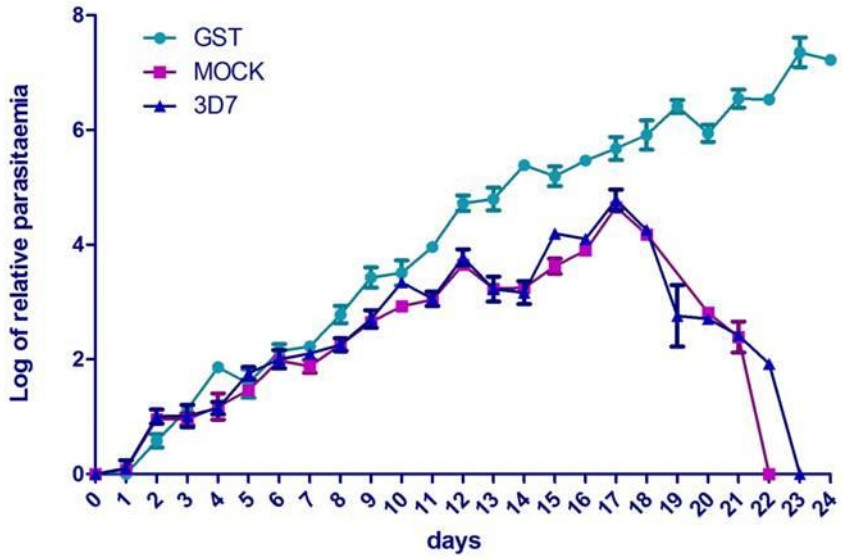

Growth analyses of *P. falciparum* pARL 1a- WR *Pf*GST -myc line (GST), as well as 3D7 and MOCK in G6PD deficient blood. The relative parasitemia (%) was measured by flow cytometry for 24 days in duplicates and two independent experiments. Displayed is the logarithm of the relative parasitemia (%).

Because of the growth advantage indicated by the *Pf*GST overexpression, the importance of *Pf*GST in the mode of action of G6PD deficiency mediated resistance against malaria was investigated.

4.2.3 Protein interference in G6PD deficient blood

To determine if the protective effect shown in Figure 13 results directly because of the overexpression of *Pf*GST, an already characterised *Pf*GST mutant was generated, *Pf*GST Y9F, with a remaining activity of 7% (159). Figure 14 shows the

crystal structure of PfGST with the generated mutation in red. The mutant was cloned as in 3.1 described and transfected into *P. falciparum* 3D7 strain as explained in 0. *Pf*GST exists as a dimer-tetramer transition state (169) allowing the application of protein interference (170).

Figure 14 – Crystal structure of *Pf*GST and the active site.

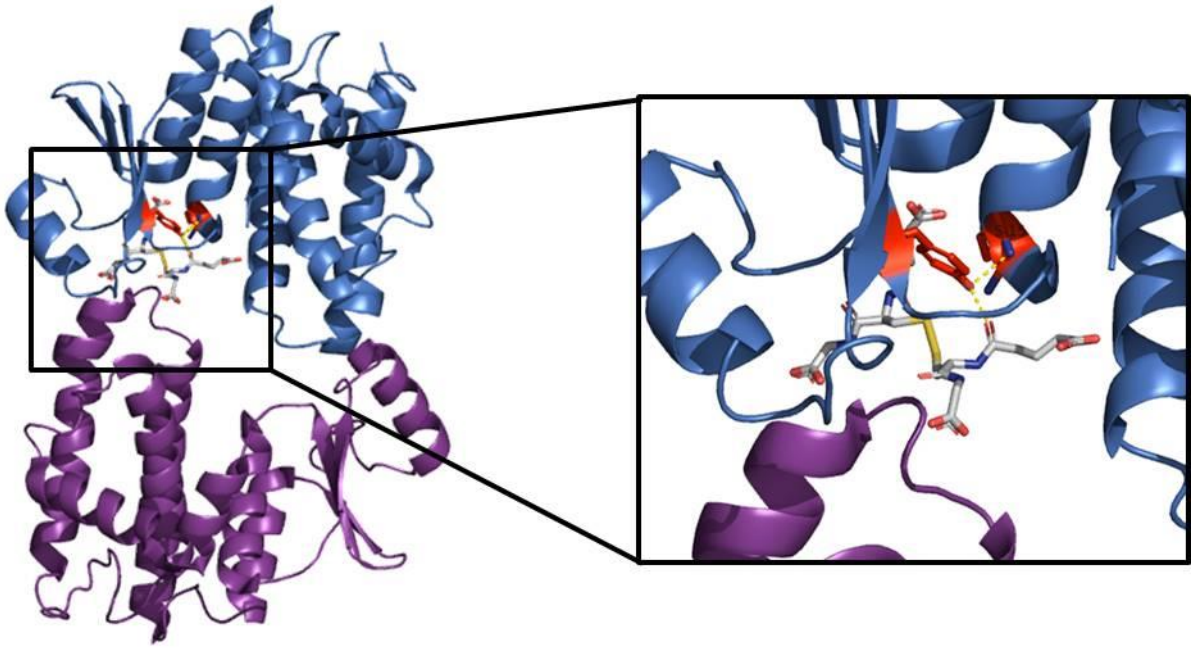

Shown is the *Pf*GST dimeric structure with GSH in active site generated by PyMol 1.7, based on the protein crystal 4ZXG. The residue *Pf*GST Y9 is highlighted in red (right). Source: modified from (159).

Figure 15 shows the growth behavior of overexpressed *Pf*GST Y9F compared to the *Pf*GST and MOCK cell line in G6PD deficient blood. Additionally, in Figure 16 the proliferation of *Pf*GST Y9F, *Pf*GST and MOCK cell lines are demonstrated during parasite culturing in WT blood.

It is clearly shown that the protective effect of the overexpressed *Pf*GST Y9F mutant is reversed in G6PD deficient blood compared to the *Pf*GST WT overexpressed line. Both, *Pf*GST Y9F mutant and MOCK line show a similar growth profile with no parasites detected after 22-24 days, while the *Pf*GST overexpressing line continues to grow even after 32 days.

However in WT blood is no difference in growth detected between the cell lines. The *Pf*GST overexpressing line as well as the *Pf*GST Y9F mutant and MOCK line continue growing even after 32 days.

Figure 15 – Growth curve overexpressed *Pf*GST-myc and *Pf*GST Y9F-myc compared to MOCK line in G6PD deficient blood.

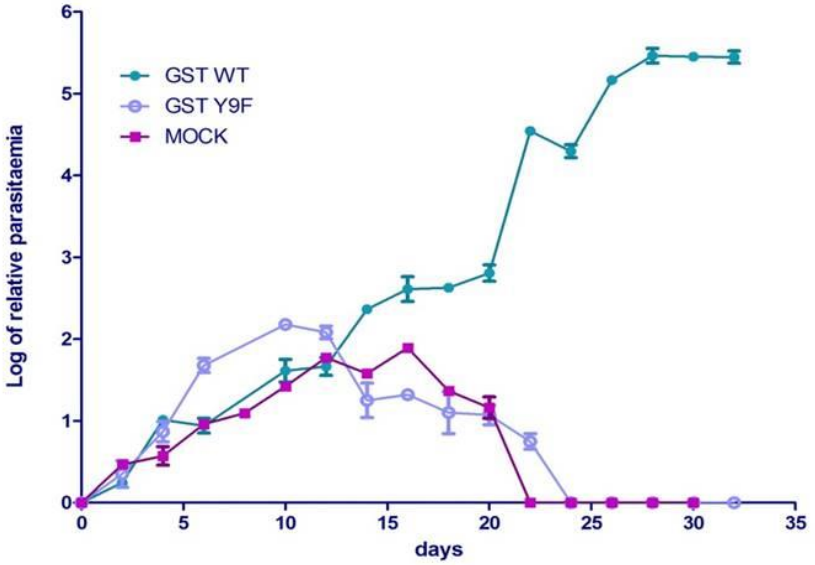

Growth analyses of *P. falciparum* pARL 1a- WR *Pf*GST -myc line (GST-WT), as well as pARL 1a- WR *Pf*GST Y9F-myc line (GST Y9F) compared to MOCK in G6PD deficient blood. The relative parasitemia (%) was measured by flow cytometry for 32 days in duplicates and two independent experiments. Displayed is the logarithm of the relative parasitemia (%).

Figure 16 – Growth curve overexpressed *Pf*GST-myc and *Pf*GST Y9F-myc compared to the MOCK line in WT blood.

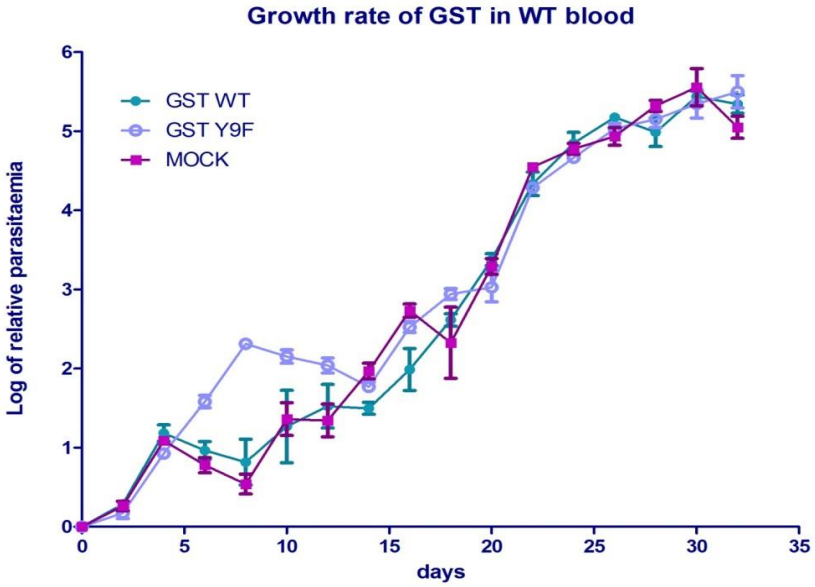

Growth analyses of *P. falciparum* pARL 1a- WR *Pf*GST -myc line (GST-WT), as well as pARL 1a- WR *Pf*GST Y9F-myc line (GST Y9F) compared to MOCK in WT blood. The relative parasitemia (%) was measured by flow cytometry for 32 days in duplicates and two independent experiments. Displayed is the logarithm of the relative parasitemia (%).

4.3 Verification of overexpression in *P. falciparum*

4.3.1 Western blot

To verify the expression of *Pf*GST-myc and *Pf*GST Y9F-myc in *P. falciparum* Western blot analysis was performed as described in 3.2.4.1 using an anti-myc antibody and anti-mouse HRP antibody. The respective analysis is shown in Figure 17. Isolated parasites of the MOCK cell line were used as a control.

Figure 17 – Western-blot of *Pf*GST-myc, MOCK and *Pf*GST Y9F-myc.

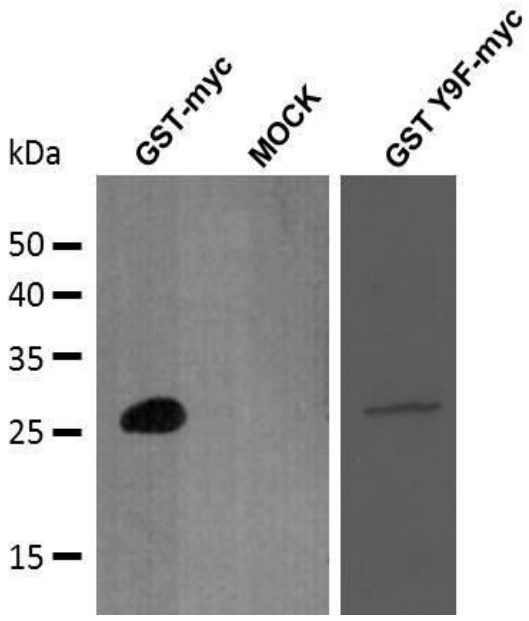

Western blot of *Pf*GST-myc, MOCK and *Pf*GST Y9F-myc with mouse anti myc antibody (1:5.000 dilution, Pierce, USA) and goat antibody antiMouse IgG with Horseradish Peroxidase (HRP) (1:10.000 dilution, Pierce, USA). The detection was done with SuperSignal West Pico detection system (Thermo Scientific, USA). The molecular masses are given on the right.

The western blot shows the expected size for the WT *Pf*GST-myc and *Pf*GST Y9F-myc (26 kDa). A respective signal was not detected in the MOCK cell line.

4.3.2 Quantitative real time polymerase chain reaction

To analyse the overexpression rate of *Pf*GST and *Pf*GST Y9F a quantitative real-time PCR was performed comparing with 3D7 and the MOCK line. Therefore a set of primers were used which amplify a 120 bp fragment of the on the mRNA encoding GFP (Figure 18 A).

Figure 18 – Transcription profile of *Pf*GST-myc.

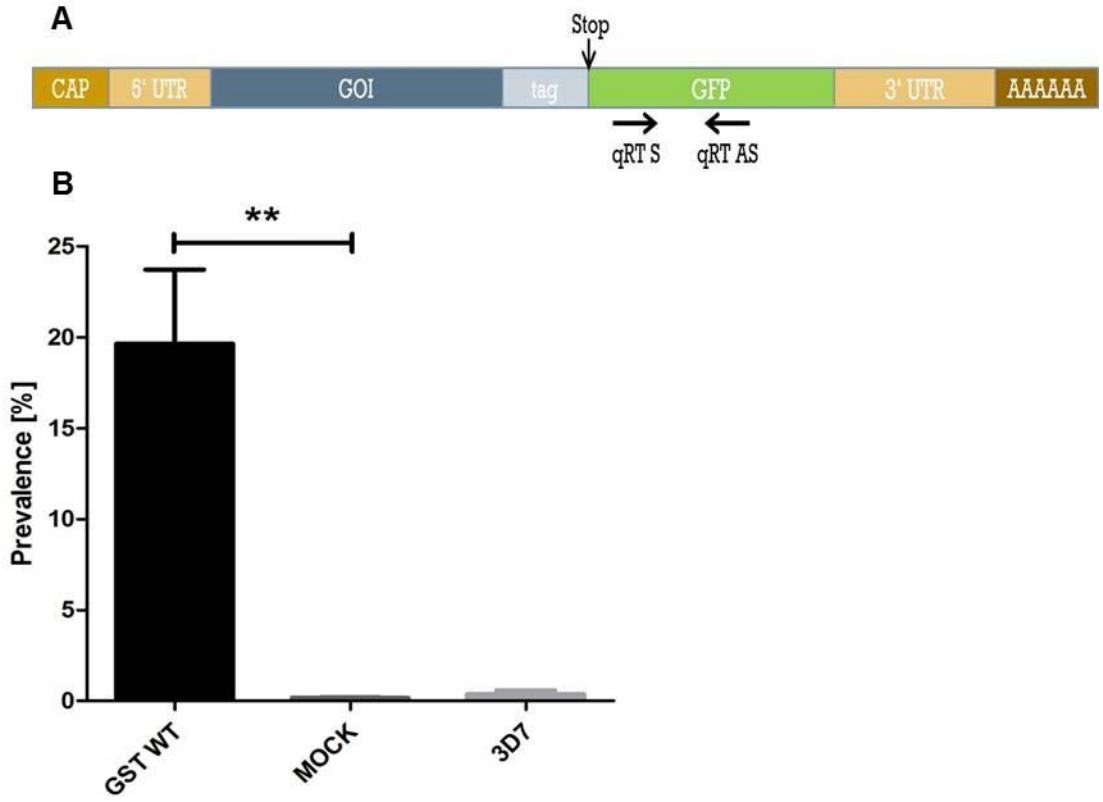

Transcription of *Pf*GST. **A** Schematic image of the transcribed mRNA and the location of the stop codon and qRT-PCR primer set. **B** Transcription profile of *Pf*GST compared with MOCK (two-tailed unpaired t-test (P-value = 0.0089)) and 3D7. Analyse was done via the $2^{-\Delta ct}$ method in triplicates and three independent experiments.

Figure 18 B shows the significant overexpression of *Pf*GST-myc compared to the MOCK line. For normalisation, the housekeeping gene *Pf*Aldolase was used. The results indicate a 135-fold ± 3,4 higher expression of *Pf*GST-myc compared to the MOCK line. However, there are still data missing for the *Pf*GST Y9F-myc mutant.

4.4 Localisation of *Pf*GST

To determine the localisation of *Pf*GST the ORF was cloned into the pARL 1a+ WR transfection vector as a C-terminal GFP fusion protein. The transfection was performed as previously described in 0. The transgenic cell line was analysed by live cell imaging using Hoechst 33342 as a nucleic acid stain as explained in 3.3.

Figure 19 – Cellular localisation of *Pf*GST**.**

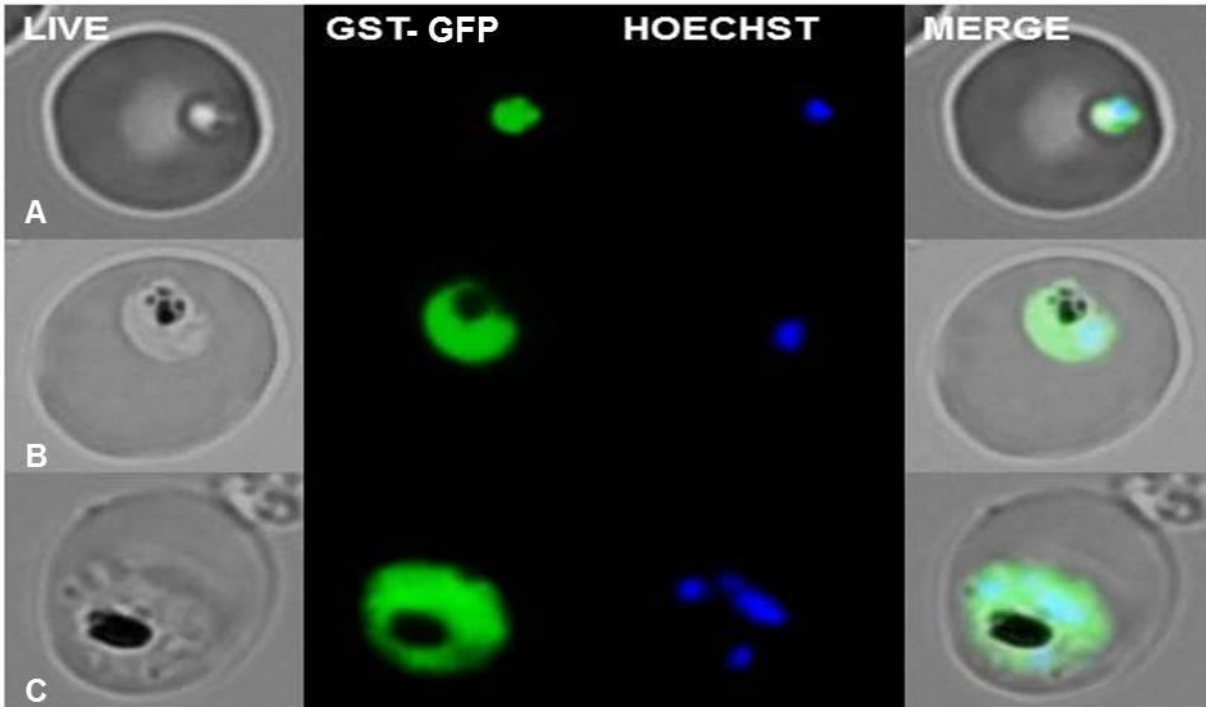

Visualised was the GFP signal in **A** ring stage, **B** trophozoites and **C** schizonts and co-localised with Hoechst 33342 (10µg/ml) to visualise the nucleus using an Axio Imager M2 microscope (Zeiss, Germany) equipped with an AxioCam HRC digital camera (Zeiss, Germany) with the AxioVision 4.8 software.

Figure 19 shows the localisation of *Pf*GST-GFP in cytosol of the parasite in the blood stages, ring, trophozoites and schizonts which confirm the predicted localisation (145)

4.5 Visualisation of cytosolic ROS in *P. falciparum*

To visualise ROS in the plasmodial cytosol the fluorometric dye H2DCFDA was used, which is known to react with several ROS including hydrogen peroxide, hydroxyl radicals and peroxynitrite. After entering the cells via diffusion the non-

fluorescent H2DCFDA dye is cleaved by intracellular esterases and reacts with ROS, to the highly fluorescent 2',7'-dichlorofluorescein (DCF).

Figure 20 – Visualisation of cytosolic ROS in MOCK cell line using WT blood.

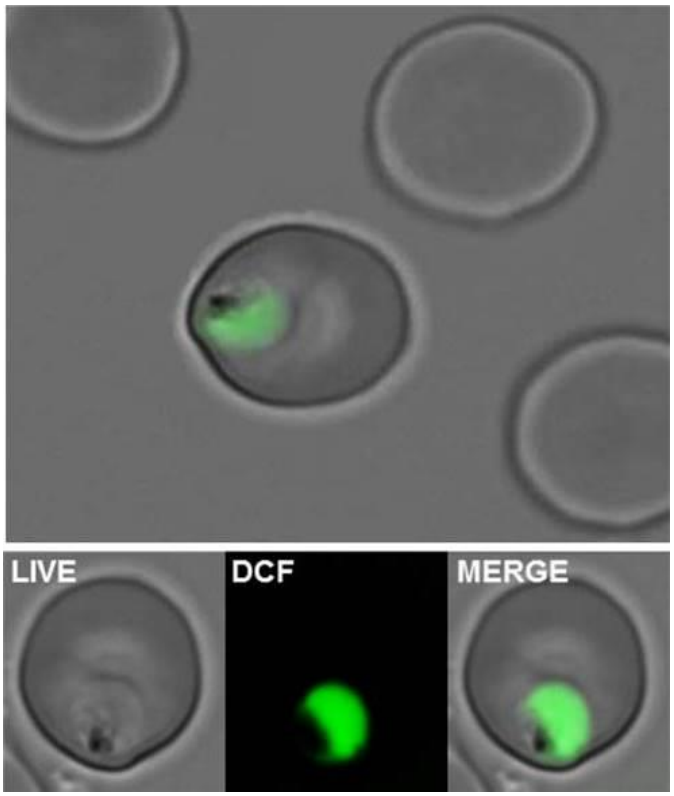

Live cell imaging of MOCK cell line in WT blood with H2DCF-DA. Cells were incubated for 15 min with 5 µM of H_2DCFDA before analysed via fluorescence microscopy using an Axio Imager M2 microscope (Zeiss, Germany) equipped with an AxioCam HRC digital camera (Zeiss, Germany) with the AxioVision 4.8 software.

As seen in Figure 20 an intensive fluorescence signal can be detected inside the parasite while RBC and the cytosol of the iRBC are showing no fluorescence signal at all. However, for analysing the ROS level of the transgenic cell lines in different blood types via flow cytometry, the chloromethyl derivative of H2DCFDA was used. CM-H2DCFDA is described to have a much better retention in live cells than H2DCFDA.

4.6 Oxidative stress in genetically different erythrocytes

To investigate the difference of the ROS level in the different blood types flow cytometric analysis was performed. Therefore 1 µL of WT and G6PD deficient RBCs

were dissolved 1 mL PBS with 5 µM CM-H2DCFDA and prepared as described in 3.4.1. Figure 21 is showing a representative flow cytometry histogram of the fluorescence intensity for both RBC types. While at normal conditions there is no substantial difference of the ROS levels (Figure 21 A), a significant shift is noticed when RBCs are stressed additionally with 0,17% H_2O_2 (Figure 21 B) for 30 min.

Figure 21 – ROS levels of WT and G6PD deficient RBCs.

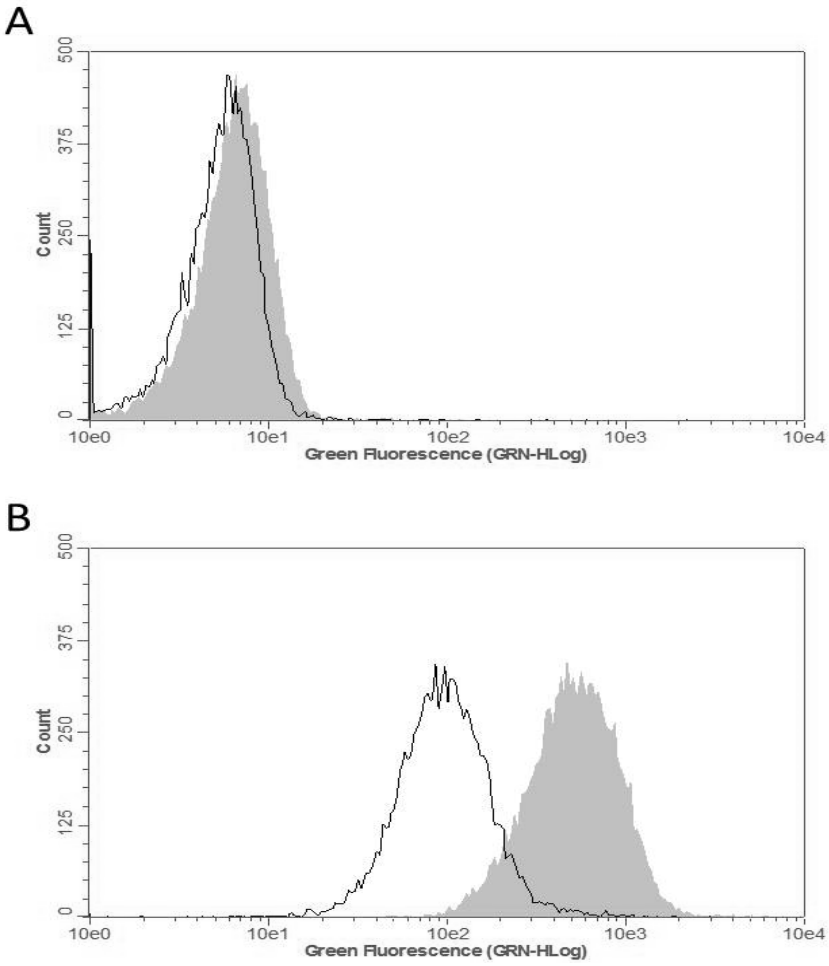

Flow cytometry histogram showing the ROS level of WT and G6PD deficient RBCs. **A** WT (black line) and G6PD deficient RBCs (grey filled) incubated with 5 µM CM-H2DCFDA for 15 min in dark. **B** WT (black line) and G6PD deficient RBCs (grey filled) after additional incubation for 30 min with 0,17% H_2O_2. It were counted 15000 events via Guava EasyCyte Mini (EMD Millipore, Germany) and analysed through the CytosoftBlue software.

4.7 Oxidative stress in *P. falciparum* infected erythrocytes

4.7.1 Determining oxidative stress in 3D7 and the MOCK cell line

To determine the ROS level in the different blood types and infected with the different cell lines a flow cytometric analysis was performed as described in 3.4.1. Figure 22 shows the difference of the ROS level of G6PD deficient blood infected with the MOCK cell line normalised with the ROS level of WT blood infected with the MOCK cell line according to the following equation:

$$\frac{\mathrm{gMFI}\ (\mathrm{MOCK_{G6PD}})}{\mathrm{gMFI}\ (\mathrm{MOCK_{WT}})}$$

Figure 22 – Relative difference of ROS level of G6PD deficient blood to WT blood both infected with the MOCK cell line.

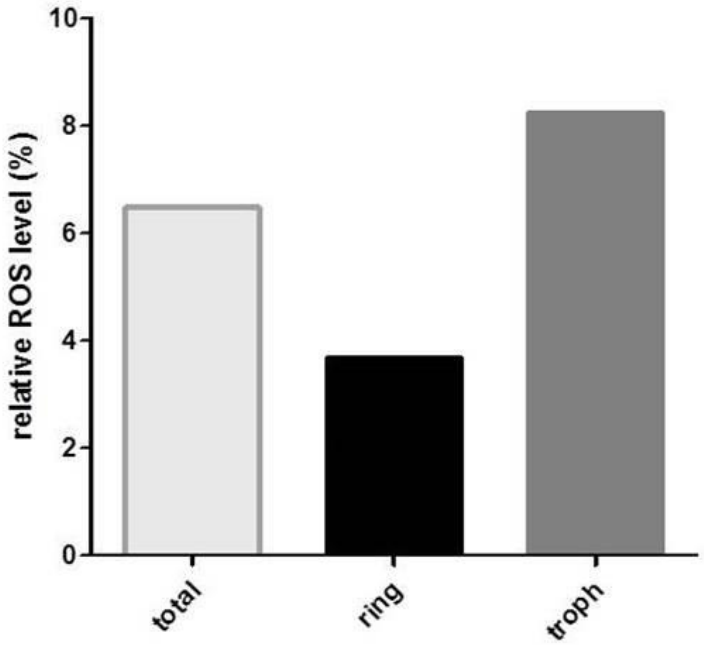

Shown is the proportion of the relative fluorescence of DCF in G6PD deficient blood infected with the MOCK cell line and to the relative fluorescence of DCF of WT blood infected with the MOCK line (gMFI ($MOCK_{G6PD}$)/ gMFI ($MOCK_{WT}$)) in percentage. Data were applied for total iRBC, as well as specific for ring and trophozoite stages.

It seems that infected G6PD deficient blood has a slightly higher oxidative stress level than infected WT RBCs. It can be mentioned that especially parasites in the trophozoite stage have a higher ROS level in G6PD deficient blood compared with ring stage parasites in the G6PD deficient blood.

To determine whether both, 3D7 infected WT and G6PD deficient RBC, are able to deal with enhanced oxidative stress, the cells were prepared as described in 3.4.1 and then incubated with different concentration of H_2O_2 (3,5%, 1,75%, 0,87%, 0,35%, 0,17%, 0,09%) for 10 min and 30 min and applied at the Guava EasyCyte Mini cytometer (EMD Millipore, Germany).

Figure 23 and Figure 24 shows the different relative fluorescence normalised by the not treated control (3D7 infected WT or G6PD deficient RBC).

$$\frac{\mathrm{gMFI}\ (3\mathrm{D7}_{\mathrm{WT}} + H_2O_2)}{\mathrm{gMFI}\ (\mathrm{MOCK}_{\mathrm{WT}} - H_2O_2)}\ or\ \frac{\mathrm{gMFI}\ (3\mathrm{D7}_{\mathrm{G6PD}} + H_2O_2)}{\mathrm{gMFI}\ (\mathrm{MOCK}_{\mathrm{G6PD}} - H_2O_2)}$$

Each graph represents one H_2O_2 concentration and compares the two different incubation times for the total iRBC, ring stage and trophozoite stage iRBC. In WT iRBC the addition of H_2O_2 does not change the relative ROS level as expected. In contrary, in most of the concentrations, the relative fluorescence in trophozoite iRBC was lower than in the not treated control. The highest difference was detected for the concentration of 1,75% and 0,09% H_2O_2 (up to 60%). There was also no significant difference observed for the two different time points in WT iRBC. However G6PD deficient iRBC were highly sensitive to the addition of H_2O_2. Up to 400% was noted when added 1,75% H_2O_2. All concentrations showed an increase in the relative ROS level and the incubation of 30 min improves the fluorescence signal of DCF. However, high concentrations of H_2O_2 do have a lytic effect on erythrocytes. To avoid this effect but to still see an increase of fluorescence after treating with H_2O_2 we decided to incubate for 30 min at a concentration of 0,17% H_2O_2.

Figure 23 – Relative difference of ROS level of WT blood infected with 3D7 before and after exposure to H_2O_2.

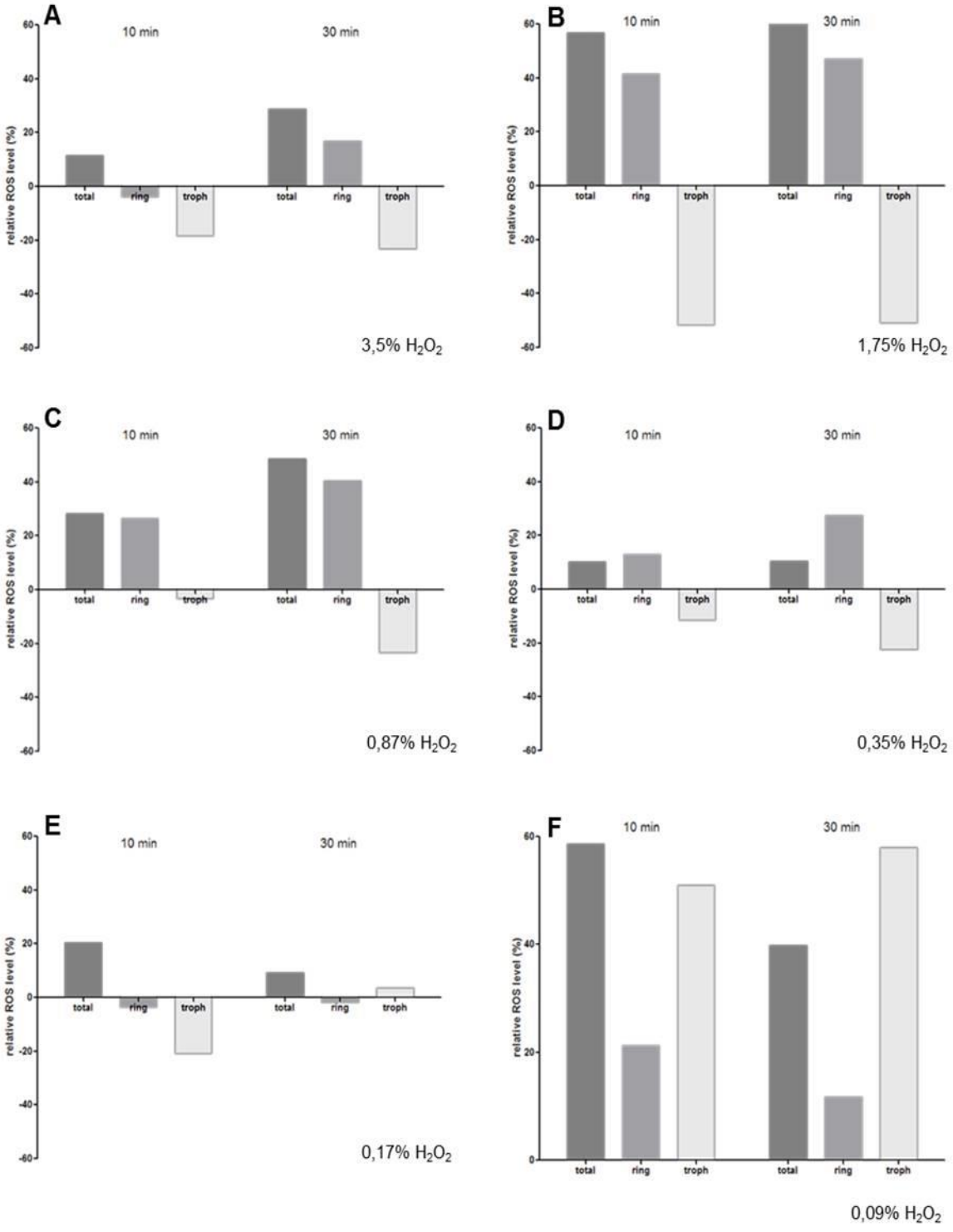

Relative difference of ROS level of WT iRBC with 3D7 treated with different concentrations of H_2O_2 for 10 min and 30 min. Shown is the difference of the relative fluorescence of DCF in WT iRBC treated with **A** 3,5% H_2O_2 **B** 1,75% H_2O_2 **C** 0,87% H_2O_2 **D** 0,35% H_2O_2 **E** 0,17% H_2O_2 **F** 0,09% H_2O_2 and normalized with not H_2O_2 treated WT iRBC. Data were applied for total iRBC, as well as specific for ring and trophozoite stages.

Figure 24 – Relative difference of ROS level of G6PD deficient blood infected with 3D7 before and after exposure to H_2O_2.

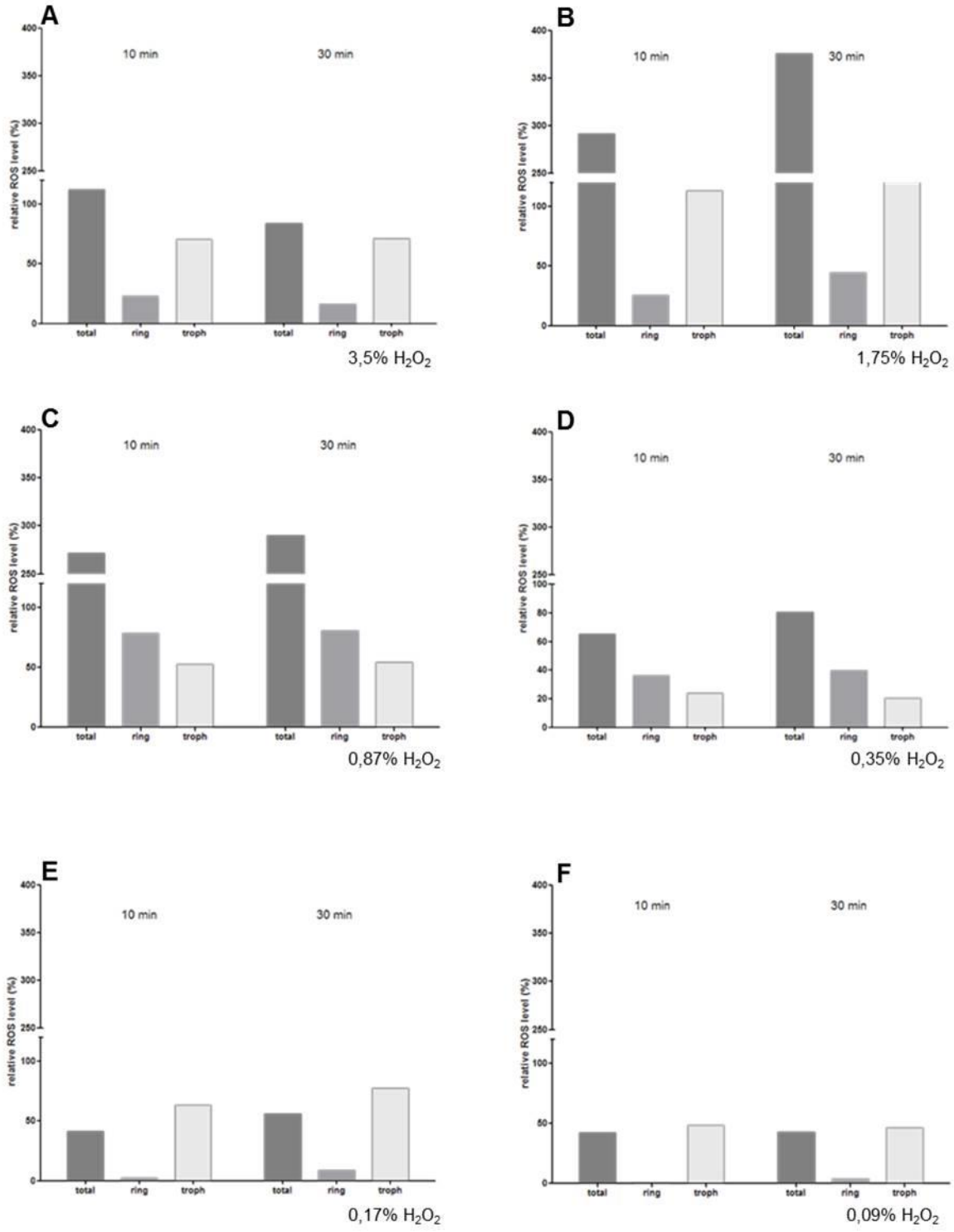

Relative difference of ROS level of G6PD deficient iRBC with 3D7 treated with different concentrations of H_2O_2 for 10 min and 30 min. Shown is the difference of the relative fluorescence of DCF in G6PD deficient iRBC treated with **A** 3,5% H_2O_2 **B** 1,75% H_2O_2 **C** 0,87% H_2O_2 **D** 0,35% H_2O_2 **E** 0,17% H_2O_2 **F** 0,09% H_2O_2 and normalized with not H_2O_2 treated G6PD deficient iRBC. Data were applied for total iRBC, as well as specific for ring and trophozoite stages.

Figure 25 – Optimisation of WT iRBC and G6PD deficient iRBC exposed to H_2O_2.

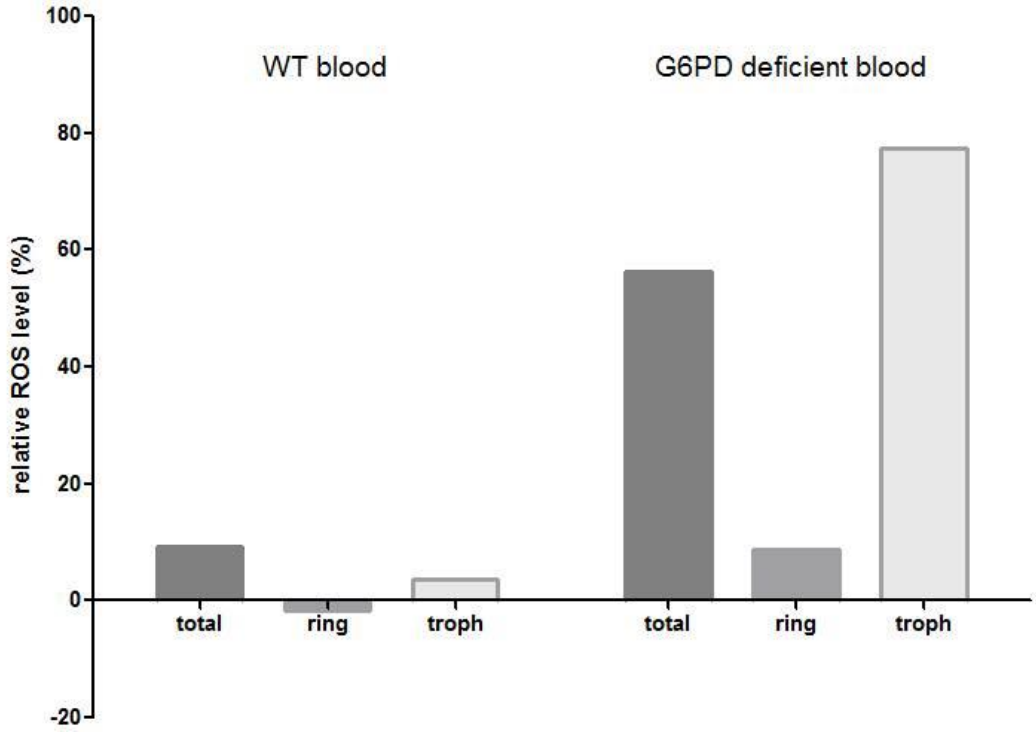

Relative difference of ROS level of WT and G6PD deficient iRBC with 3D7 treated with 0,17% of H_2O_2 for 30 min and normalised with not H_2O_2 treated WT and G6PD deficient iRBC. Data are demonstrated for total iRBC, as well as specifically for ring and trophozoite stages.

Figure 25 shows WT iRBC and G6PD deficient iRBC in comparison after treating with 0,17% of H_2O_2 and incubating for 30 min.

4.7.2 PfGST mediated protection against oxidative stress

To analyse the protective effect of *Pf*GST the overexpressing lines pARL 1a-WR *Pf*GST -myc, pARL 1a- WR *Pf*GST Y9F-myc and the MOCK line were prepared as described in 3.4.1. The samples were measured using the Guava EasyCyte Mini cytometer (EMD Millipore) and subsequently incubated for 30 min at 0,17% H_2O_2 and measured again. The fold-induction values were determined from parasites overexpressing *Pf*GST-myc and *Pf*GST mutant Y9F-myc (Figure 26), using the following equation, for both ring and trophozoite stages:

$$\frac{\mathrm{gMFI}\ (\mathrm{GST\ or\ Y9F_{WT\ or\ G6PD}} + H_2O_2)}{\mathrm{gMFI}\ (\mathrm{MOCK_{WT}}\ or\ G6PD + H_2O_2)}$$

Figure 26 – *Pf*GST and mutant mediated protection against oxidative stress normalised by the respective MOCK line.

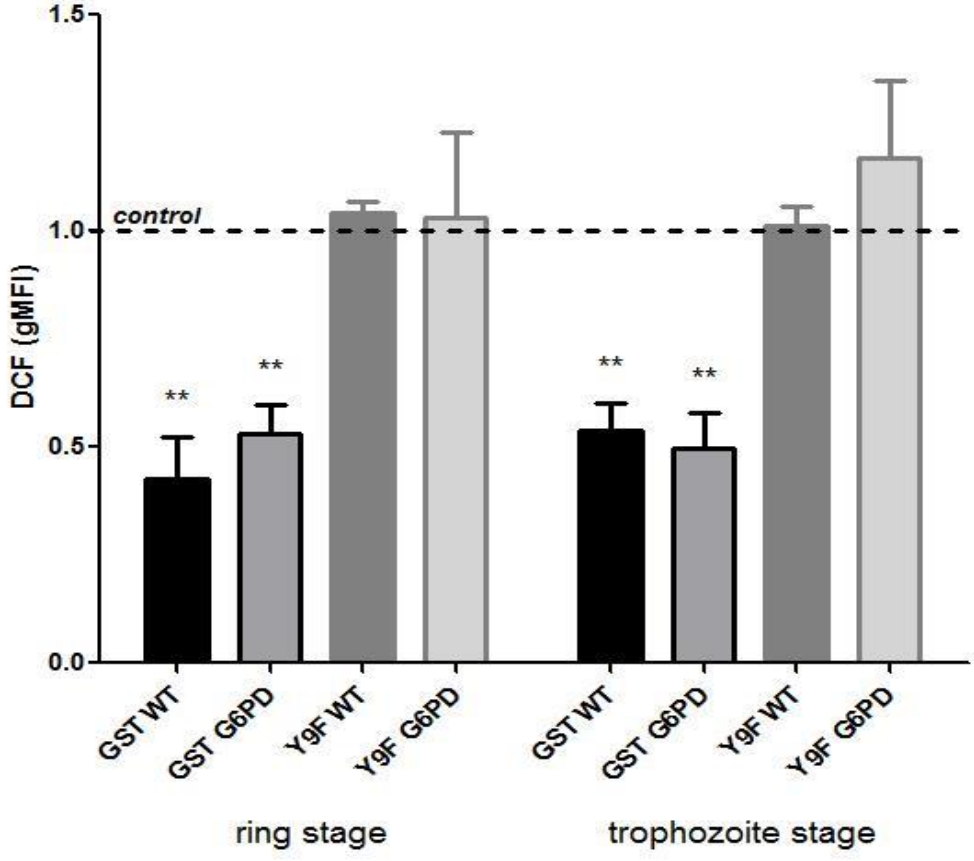

The fold-induction values of DCF (gMFI) were determined for the overexpressed *Pf*GST-myc and *Pf*GST Y9F-myc for ring and trophozoite stages and normalised by the respective MOCK line (control=1) after 30 min incubation with 0,17% H_2O_2. Samples were taken in duplicates of three independent experiments.

The overexpression of *Pf*GST protects the parasite when exposed to ROS such as H_2O_2. This is evident in ring and trophozoite stages by the relative fluorescence of the *Pf*GST overexpression, which is in both blood types lower than the MOCK control (control=1). However, there is no protective effect on the parasite overexpressing the *Pf*GST Y9F mutant.

4.8 Determination of free GSH level in *P. falciparum*

To measure the GSH concentration in the respective transfection lines in both blood types a LC-ESI-MS/MS analysis was performed like described in 3.4.2. The measured GSH concentration was normalised via the total protein concentration of the sample.

Figure 27 – GSH concentration of WT iRBC and G6PD deficient iRBC.

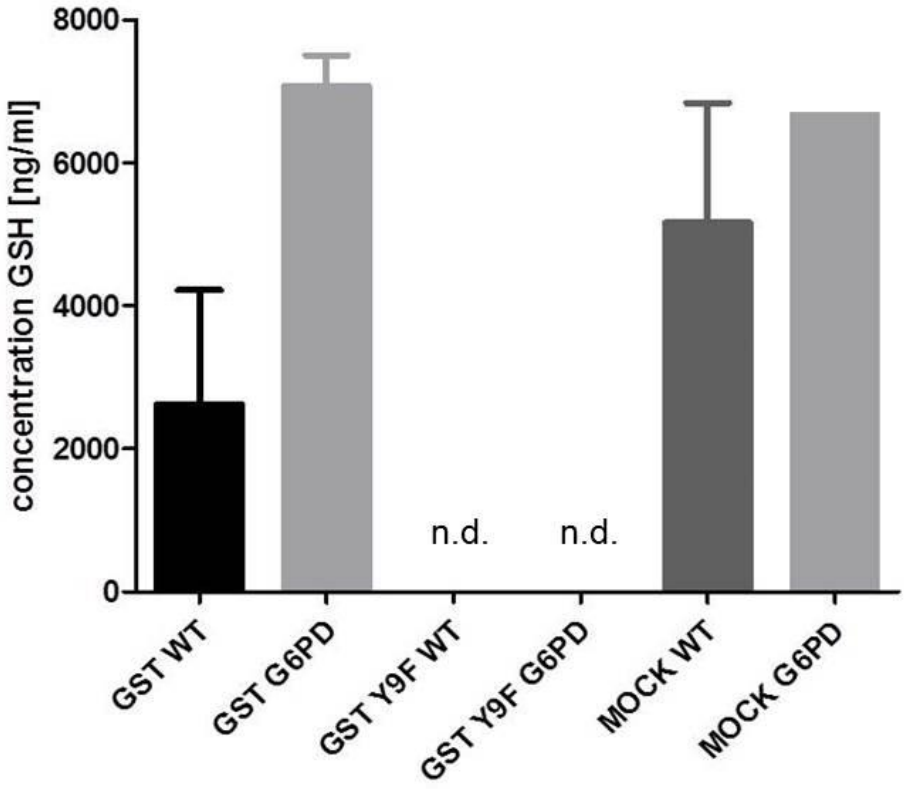

The concentration of GSH in the different cell lines in WT and G6PD deficient blood. The concentration was determined using LC-ESI-MS/MS analyses. Normalisation was done at total protein concentration. GST-WT n=2; GST G6PD n=2; GST Y9F WT n=1; GST Y9F G6PD n=1; MOCK WT n=2; MOCK G6PD n=1.

*Pf*GST-myc overexpressing line seems to have a lower free GSH level in WT blood than compared to the MOCK cell line. However, for the G6PD deficient blood, the free *Pf*GST-myc overexpressing line has a lower free GSH level in WT blood than the MOCK cell line. However, for the G6PD deficient blood, the free GSH level is not significantly different compared to MOCK-infected G6PD deficient RBC. Additionally, there was no free GSH detected in the overexpressing *Pf*GST Y9F mutant cell line.

4.9 *Pf*GST activity assays

To analyse the *Pf*GST biochemically, WT and *Pf*GST Y9F mutant were cloned in the expression vector pASK-IBA3 and expressed in the *E. coli* strain BLR DE3 according to 3.5.1 and 0. A SDS-PAGE was performed to verify the purity of the proteins (Figure 28 A).

Figure 28 – Purification of *Pf*GST and *Pf*GST Y9F.

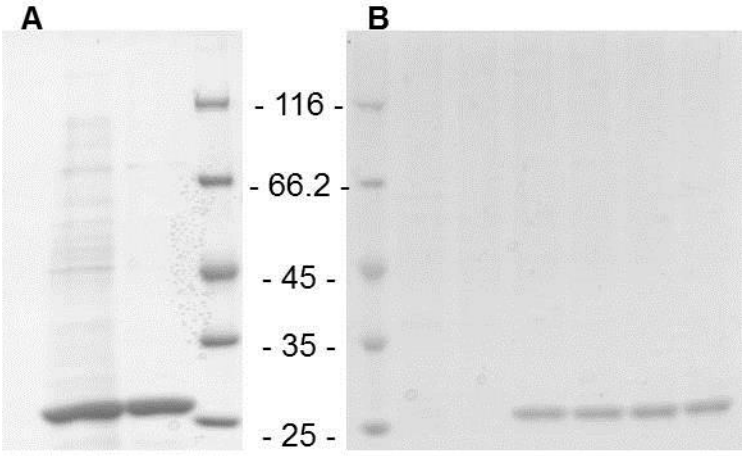

A *Pf*GST Y9F (left) and *Pf*GST WT (right) after Strep-tag®/Strep-Tactin® protein purification. **B** From right 4 fractions of *Pf*GST Y9F followed by 2 fractions *Pf*GST WT after FPLC purification. As ladder, the Unstained Protein Molecular Weight Marker (Thermo Scientific, USA) was used.

Through the Strep-tag®/Strep-Tactin® protein purification, the WT *Pf*GST-strep (25 kDa) can be purified while the WT *Pf*GST (25 kDa) while the *Pf*GST Y9F (25 kDa) still contains some impurity. Therefore the protein-tag purification was followed by gel-filtration to purify both *Pf*GST WT and mutant protein (Figure 28 B).

The purified enzymes were used for activity assays performed as described in 3.5.5. The assay was started by adding the enzyme and the measurement of the activity

was carried out at 340 nm for 20 min. Figure 29A shows the increase in absorption over the entire time while in Figure 29B the linear area is shown with the resulting slopes. The mutant shows compared to the WT *Pf*GST almost no activity as already shown in Hiller et al., 2006.

Figure 29 – Activity assay of *Pf*GST and *Pf*GST Y9F.

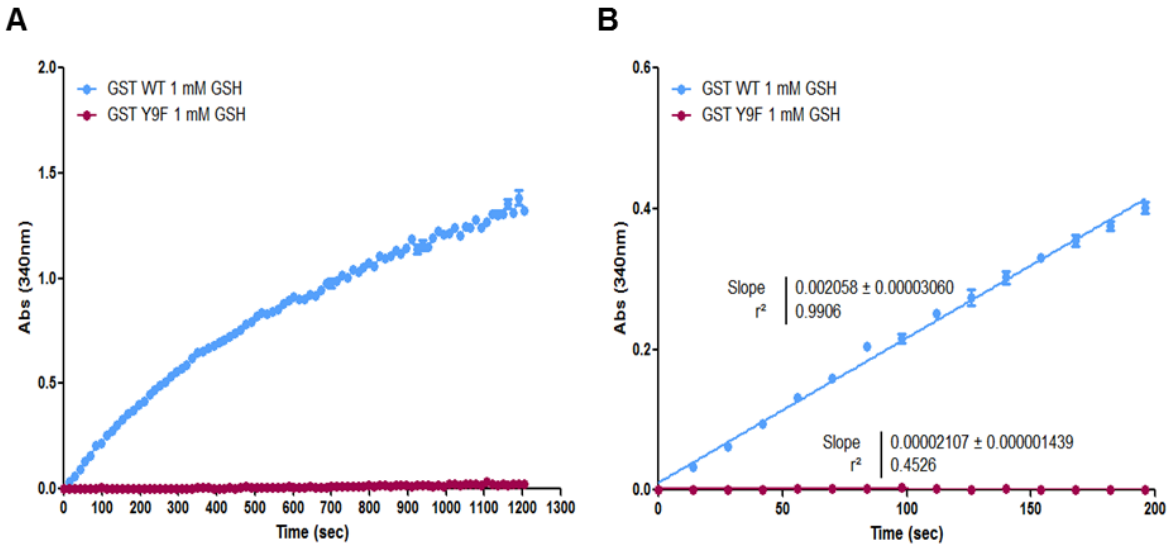

A Activity of *Pf*GST and *Pf*GST Y9F.using 10 µg of purified protein measured for 20 min in triplicates and was repeated in three independent experiments. **B** Linear area of the activity curve for calculating the slope (*Pf*GST WT 0.0021 ± 0.00003; *Pf*GST Y9F 0.000021 ± 0.000001).

4.9.1 The oligomeric state

*Pf*GST is active as a dimer and, therefore it is important that the oligomeric stage remains unchanged also in the *Pf*GST Y9F mutant, in order to ensure the activity. To confirm that the mutant *Pf*GST Y9F has the same oligomeric state as the WT *Pf*GST the protein conformation was analysed by FPLC and DLS Figure 30. FPLC analysis of *Pf*GST shows a peak at fraction 80 and 90 as well as for *Pf*GST Y9F. Corresponding to the calibration of the column fraction 80 harbours protein size of about 50 kDa and fraction 90 of about 25 kDa, which confirms both a dimeric and monomeric conformation. The determination of the oligomeric state via DLS shows that *Pf*GST reveals a size of 53.6 kDa and a diameter of 1,422 nm, while for *Pf*GST Y9F a size of 73.3 kDa and a diameter of 1,782 nm.

Figure 30 – Determination of oligomeric state via FPLC**.**

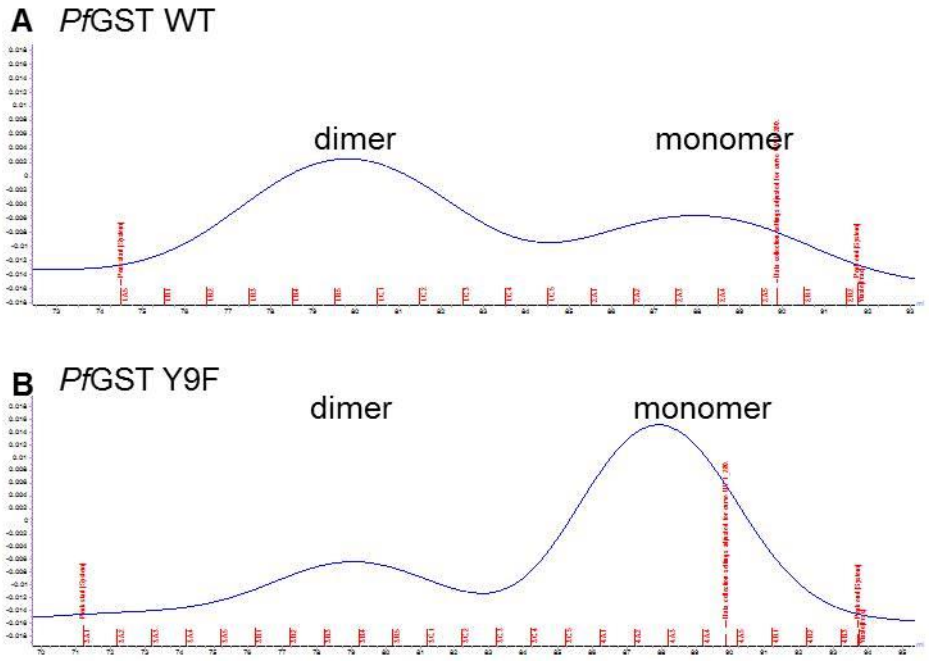

A *Pf*GST analyse showing a peak at fraction 80 and 90. **B** *Pf*GST Y9F analyse showing a peak at fraction 80 and 90. Corresponding the calibration of the column fraction 80 consists a protein size of about 50 kDa and fraction 90 of about 25 kDa

Figure 31 – Determination of oligomeric state via DLS.

A

	Diam. (nm)	% Int.	Width (nm)	MW (kDa)	Width (kDa)	Start (mL)	End(mL)
Peak 1:	6,527	47,4	1,422	53,6	1,52	0.00	0.00
Peak 2:	543,7	42,0	141,3	1,67e6	7,14e4	0.00	0.00
Peak 3:	119,8	10,6	33,08	4,85e4	2390	0.00	0.00

B

	Diam. (nm)	% Int.	Width (nm)	MW (kDa)	Width (kDa)	Start (mL)	End(mL)
Peak 1:	7,464	74,4	1,782	73,3	2,57	0.00	0.00
Peak 2:	443,9	24,1	105,3	1,04e6	3,59e4	0.00	0.00
Peak 3:	5560	1,5	0,000	3,85e8	0,00	0.00	0.00

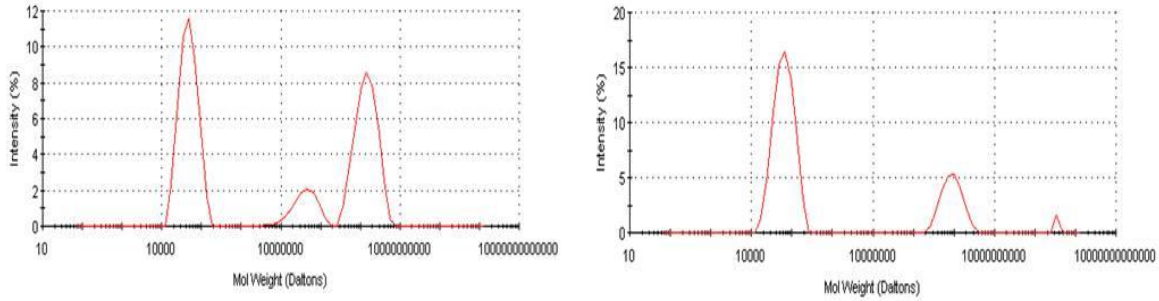

A *Pf*GST analyse showing a size of 53.6 kDa and a diameter of 1,422 nm. **B** *Pf*GST Y9F a size of 73.3 kDa and a diameter of 1,782 nm.

4.10 Computationally designed compounds against *Pf*GST

Another possibility to study *Pf*GST is by using specific drugs against the enzyme. Here for we designed 3 compounds (ISA1 to 3) starting from the compound codes (smiles list) of MolPort library of compounds from the Zinc Library of purchasable compounds as described in 3.6.1. In order to select compounds that would fit in the active site of *Pf*GST some features, which are considered as essential for the binding were used for designing of a pharmacophore. Chemical features considered information of the amino acid residues Y9 and K15, as well the chemical information from superimposed structures of GSTs, co-crystallised with substrates found in the PDB databases (159). The top hundred deriving from the docking were submitted for visual inspection of the poses and the final filter was based on the solubility and availability of the compounds for purchasing. Out of these, we chose three compounds to test on the recombinant enzymes as well as on *P. falciparum* cell culture (Figure 32).

Figure 32 – Designed compounds against *Pf*GST.

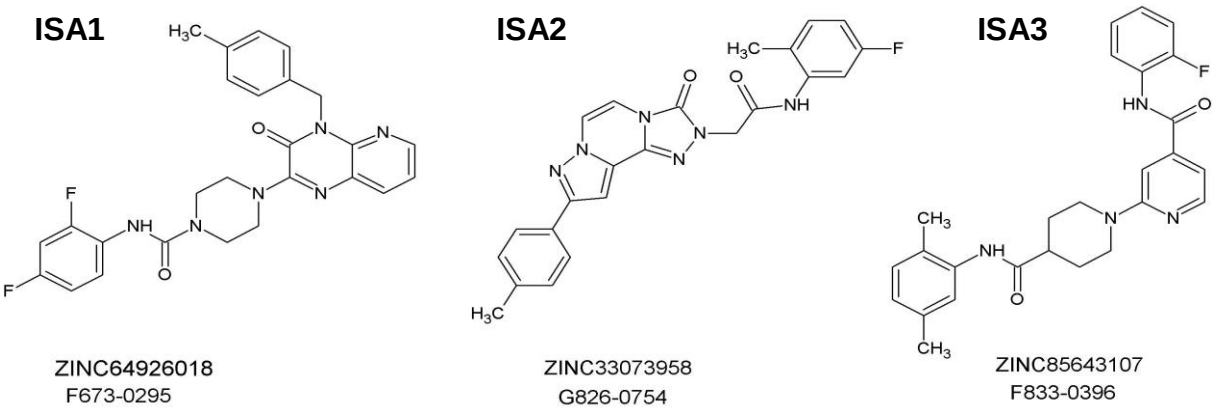

Compounds obtained through molecular docking, which was tested on recombinant enzymes as well as on *P. falciparum* cell culture. Shown are the codes of the ZINC database and of the supplier MolPort.

4.10.1 Validation of the compounds on recombinant enzymes

To test the in Figure 32 shown compounds an activity assay with recombinant *Pf*GST was performed as described in 3.6.2. Figure 33 shows the enzymatic activity of these drugs at a final concentration of 100 µM. Compound (Comp.) 1 to 3 does not

Figure 33 – Inhibiting effect of the compounds 1 to 3 against *Pf*GST.

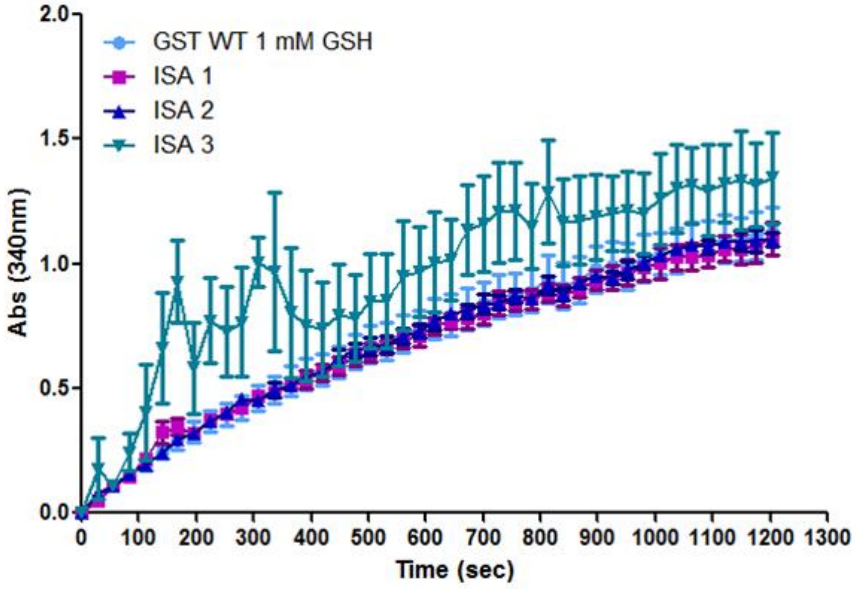

*Pf*GST activity assay together with and three different potential inhibitors (Comp.1 to 3) using 100 µM drug concentration. Data are plotted with SD of three independent experiments with triplicate measurements each.

Figure 34 – Prodrug activity of the compounds 1 to 3 with recombinant *Pf*GST.

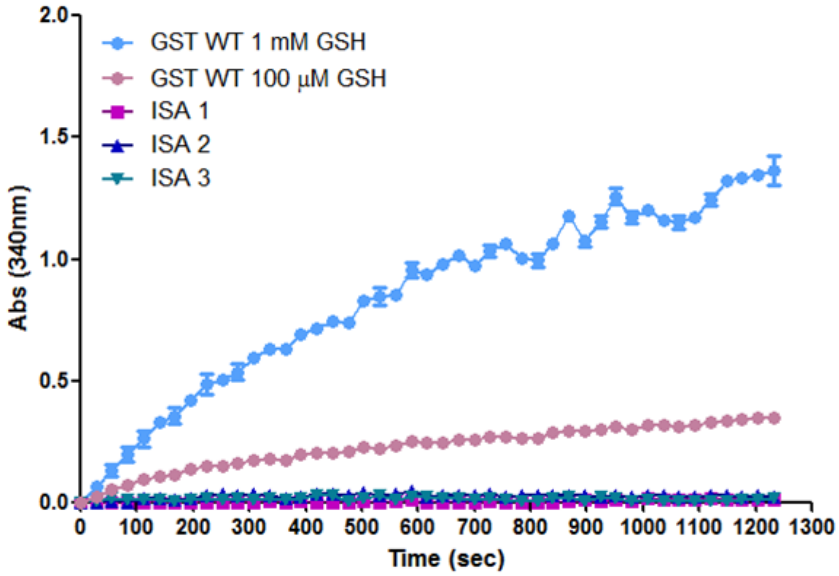

*Pf*GST activity assay together with and three different potential inhibitors (Comp.1 to 3) using 100 µM drug concentration instead of GSH as substrate. As a control, the normal assay conditions were tested and additional a condition with just 100 µM GSH. Data are plotted with SD of three independent experiments with triplicate measurements each.

have any effect on the enzyme activity as the curves are the same with and without the selected drug.However, a pro-drug activity of these compounds cannot be excluded. In order to test the pro-drug activity hypothesis, the compounds were used as a substrate by replacing the GSH in the activity assay. In Figure 34 the enzymatic activity is shown using the compounds at a final concentration of 100 µM without GSH. As control, the normal assay conditions were tested and additional a condition with just 100 µM GSH.

Nevertheless, no activity was detected using the compound as a substrate, indicating that the compound does not specifically inhibit *Pf*GST. However, an antimalarial effect could still be provided by this compound on cellular level. Therefore they had been tested against *P. falciparum*.

4.10.2 Validation of the compounds ISA1 to 3 against P. falciparum.

Although no inhibitory effect was shown of the compounds ISA1 to 3 against the recombinant enzyme *Pf*GST an antimalarial effect of them could be possible.

Figure 35 – Antimalarial activity of ISA1 to 3 against *P. falciparum*.

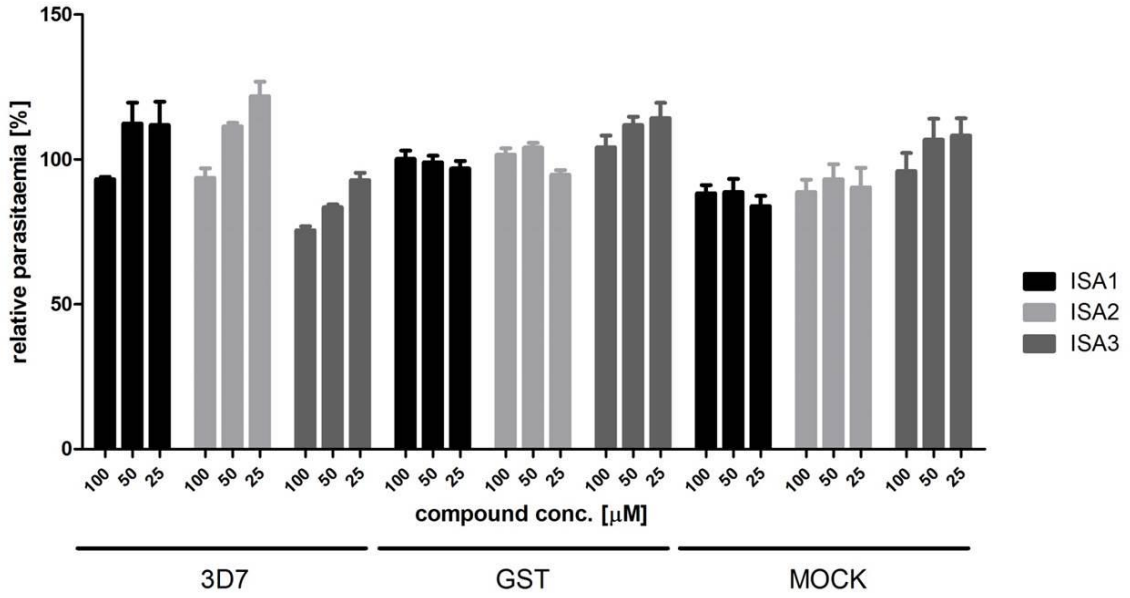

The antimalarial effect of the compounds ISA1 to 3 was tested on *P. falciparum* strain 3D7, *Pf*GST overexpressing and MOCK line using concentrations of 100, 50, and 25 µM. Parasites were incubated for 96 h before analysed by adding SYBR Green I (0.2 µl/mL lysis buffer). Values are normalised by the 3D7 control with DMSO and plotted with standard errors mean (SEM) of three independent experiments with triplicate measurements each.

Therefore three concentrations of the compounds (100, 50, 25 µM) were tested on three different cell lines (3D7, *Pf*GST and MOCK) in a SYBR Green I fluorescence the assay as described by Smilkstein et al., 2004 (166) for 96 h. As seen in Figure 35 the compounds do not inhibit the parasites growth and further analysis was not continued.

5 DISCUSSION

5.1 Oxidative stress and its influence of *P. falciparum*

During the life cycle of *P. falciparum* the parasite is growing and developing inside human erythrocytes. This asexual proliferation during the blood stage requires high adaptation of the parasite to the environment of the host cell. Erythrocytes, which are responsible for the transport of O_2, are permanently exposed to reactive species via both endogenous and exogenous sources. Although RBCs have a very effective ROS detoxification system, some blood diseases cause a shorter life span of the cell and to clinic symptoms like anaemia such as in sickle cell disease, Thalassemia and G6PD deficiency due to elevated oxidative stress levels. Interestingly, these diseases are mediating a natural resistance against human malaria. However the precise protection mechanisms are still unknown.

Additionally, the plasmodial infection is increasing the ROS level of erythrocytes e.g. the concentration of OH• and H_2O_2 were found twice as high as compared to not infected RBC (171). The accelerated aging and death of iRBCs and the development of anaemia have been associated with altered ROS levels (172).

However, in the comprehensive intraerythrocytic development the parasite undergoes constant metabolic changes and at the same time modifies the host cell. This results in a delicate homeostasis of pro- and antioxidants. Interference of this balance can lead to parasite's and RBC's death.

Part of the host immune response towards parasite infection is the activation of phagocytes (macrophages and neutrophils), which are generating ROS and RNS affecting the homeostasis inside the iRBC and thereby killing the parasite (173). The same concept is used by several anti-malarial drugs such as chloroquine, primaquine and artemisinins (174–176), which introduce oxidative stress inside the parasite leading to its elimination.

Because of the great impact of oxidative stress towards parasite proliferation in this work the relation between proliferation of *P. falciparum* inside erythrocytes with increased ROS levels were analyzed by using G6PD deficient RBCs. Taking in account that G6PD deficient erythrocytes cannot cope with elevated oxidative stress (103,104) the question was raised whether the increased ROS levels are inhibiting parasites' development and proliferation. Therefore we asked the following question:

If the increased level of oxidative stress in G6PD deficient RBC prevents parasites development and proliferation, would an enhanced defence system of the parasite reverse this effect?

5.2 Survival of *P. falicparum* in G6PD deficient RBCs

To answer this question the ORFs encoding for proteins involved in the detoxification of ROS in *P. falciparum* had been identified in the plasmodial genome database (Table 1) and had been subsequently cloned into the transfection vector pARL 1a- and transfected indo the *P. falciparum* 3D7 strain as showed in 4.1. Additional a control cell line was generated, containing the pARL 1a- verctor without any GOI (MOCK line). However the cloning and transfection of the two putative GSH transporters MRP1 and MRP2 was not successful and was excluded from the following work.

Before analyzing the generated transfection cell lines, the proliferation profile of 3D7 in WT and G6PD deficient blood was investigated. Already in 1983 Roth and colleagues were able to show that *in vitro* culturing of *P. falciparum* in G6PD deficient RBC shows a growth disadvantage compared to WT blood (177). They showed that after 5 days of culturing *P. falciparum* in blood of hemi- and heterozygote G6PD deficient patients had approximately only a third of parasitemia compared to blood derived from healthy malaria patients. G6PD deficiency is a X-chromosome linked disease and therefore we used for this work just blood of male G6PD deficient donors to avoid contamination with healthy RBC, which was kindly provided by ProSangue, Brazil. However as shown in Figure 11 after 5 days of culturing there was no significant difference in growth. Therefore the culturing time was extended by another 3 days. After this time a difference in proliferation of approximately 30% was detected. This delay compared to the data obtained by Roth and colleagues could be occurred probably because all cell lines were cultured regularly in WT RBCs and then diluted in G6PD deficient blood. Nevertheless the culturing time was prolonged to about 30 days to evaluate whether proliferation of *P. falciparum* is stopped. After 20 days of culturing the parasitemia starts to decrease until almost no parasites were detected. However *P. falciparum* cultured in WT blood reveal normal proliferation.

In order to verify whether the reason for parasite's death was the elevated oxidative stress level the transgenically modified malaria parasites were cultured in G6PD deficient blood in comparison to the MOCK line. First the cell line overexpressing *Pf*SOD2 was analysed. *Pf*SOD2 is localized in the parasite's mitochondrion and catalyzes the reaction from $O_2^{\bullet-}$ to H_2O_2. The mitochondrion is one of the main sources of ROS because this organelle harbours the electron transfer chain (ETC) system. Alterations in the redox balance of cells normally results in an increase of ROS in the mitochondria (120). Consequently enrichment of the plasmodial mitochondrion with *Pf*SOD2 could diminish the ROS level inside the mitochondria and protect the parasite form early cell death. However the growth curve of *Pf*SOD2 overexpressing parasites shows that there is no protecting effect (Figure 12). The similar proliferation profile with the MOCK line could be explained in several ways. First *Pf*SODs producing H_2O_2 which is released in the parasites cytosol. Here the parasite has to detoxify this reagent via the TXN cycle. If the *Pf*SOD2 is producing more H_2O_2 it could be possible that the TXN cycle is saturated. An overexposure of H_2O_2 could lead to an increase of Fenton-reactions resulting in the occurrence of the highly reactive OH•. This could actually lead to higher ROS levels than in the MOCK line and could result even in a decreased proliferation in WT blood. On the other hand *Pf*SOD2 is an NADPH dependent enzyme. Because in this cell line the NADPH level is not increased therefore the *Pf*SOD2 activity might be limited due to insufficient availability of the co-factor. IDH is providing the reduction equivalent via the Krebs cycle. To determine whether the increased H_2O_2 level or the lack of NADPH is the reason for the missing proliferation advantage several other experiments should be done, like culturing in WT blood or co-transfection with IDH overexpression plasmid. However due to the presence of various ROS defence systems in the malaria parasite we continued to analyse another ROS detoxification system and tested a further transgenic cell line. We omitted also to verify the cytosolic *Pf*SOD1 since this enzyme is also generating H_2O_2.

G6PD deficient erythrocytes are exposed to elevated ROS levels which results in cellular damage like lipid peroxidation or DNA and protein oxidation therefore we were interested in the investigation of an enzyme which could protect and decontaminate the cell. The primary function of *Pf*GST is the detoxification of endogenous and exogenous electrophilic molecules by GSH conjugation which

increases thereby their solubility of the molecule (178). Important is also the ability of *Pf*GST to bind the cytotoxic hemin (144). These GSH conjugates (GS-X) will subsequently be transported out of the cell via GS-X/GSSG pumps. *Pf*GST is an important part of the defence against oxidative stress. For example, *Pf*GST is able to neutralize H_2O_2 because of its GSH peroxidase activity and detoxifies some of the secondary ROS products such as lipid peroxidation products (179,180,178).

Therefore the proliferation of the *Pf*GST overexpressing line was evaluated in G6PD deficient blood and compared to the growth behavior of the MOCK line. Interestingly the overexpression of *Pf*GST shows a protective effect in G6PD deficient RBC. Unlike the MOCK line the *Pf*GST overexpressing cell line does not reveal a reduction of parasitemia. To investigate the relationship between growth advantage and the overexpression of *Pf*GST the analysis of the remaining enzymes of the parasites oxidative defence system were omitted so far. Further the localization of *Pf*GST was confirmed via a *Pf*GST-GFP fusion protein expression which indicated a cytosolic localisation within the parasite as also suggested by bioinformatic prediction tools (145).

5.3 *Pf*GST – The crux of G6PD deficiency mediated malaria resistance?

To make sure that *Pf*GST is protecting the parasite against the unfavourable milieu of G6PD RBC, the positive effect was reversed by generating an inactive *Pf*GST mutant (*Pf*GST Y9F) and overexpressing it in *P. falciparum* 3D7. The mutant was already described by Hiller et al., 2006. However the inactivity of the mutant was confirmed via recombinant expression and subsequent activity assays (shown in 4.9). However it was important to verify whether the mutant is still able to keep the oligomeric state of the *Pf*GST WT. The plasmodial *Pf*GST is active as a dimer with a shared active site and creates inactive tetramer structures under low ROS levels. In order to analyse if overexpression of *Pf*GST Y9F could reverse the growth benefit by binding to endogen *Pf*GST the oligomeric state of the mutant was analysed by FPLC and DLS. Both analyses showed that *Pf*GST Y9F is still able to build dimers but remains predominantly as a monomer quite the opposite of *Pf*GST WT. Nevertheless the growth profile was analysed and compared to MOCK and *Pf*GST cell line as well as in WT blood. It was expected that the *Pf*GST Y9F mutant will not just return the

positive effect but even show a worse proliferation profile because of the protein interference between endogenous *Pf*GST WT and overexpressed *Pf*GST Y9F diminishing the total *Pf*GST activity inside the parasite. As shown in 4.2.3 the mutant does not reveal any growth advantage suggesting that the previous effect was indeed due to the protective effect of *Pf*GST overexpression. However the *Pf*GST Y9F shows the same proliferation profile as the MOCK line. Although this was not expected the analysis of the oligomeric state could explain this effect. If *Pf*GST Y9F did not interfere with the endogenous *Pf*GST WT the MOCK line and *Pf*GST Y9F line will have the same *Pf*GST activity level. This could be analysed with *Pf*GST activity assays of plasmodial extract of the respective cell lines. Additionally the expression profile was analysed by qRT-PCR and Western blot. The *Pf*GST gene transcription is significantly increased compared to the MOCK line and *Pf*GST could also be detected via Western blot analysis (see 3.2.4). However *Pf*GST Y9F was also verified by Western blot analysis but there is still missing a quantitative verification through qRT-PCR. If *Pf*GST Y9F is just poorly overexpressed this could also explain why the mutant has no more significant impact in parasite death. Nevertheless the overexpressed *Pf*GST Y9F cell line indicates the importance of the *Pf*GST in the survival of the parasite in G6PD deficient blood. However the question remains if the increased ROS level in G6PD deficient cells is responsible for the impaired growth of *P. falciparum*.

5.4 Elevated ROS in G6PD deficient RBCs impairs parasites growth?

To analyse the ROS level in G6PD deficient cells compared to WT RBCs the fluorescence dye (H*2*DCF-DA and CM-H2DCFDA) was used which reacts with several ROS including hydrogen peroxide, hydroxyl radicals and peroxynitrite. The dye is entering the cell via diffusion and then cleaved by intracellular esterases and therefore remaining intracellular. After oxidation via ROS the dye is converted to the highly fluorescent 2',7'-dichlorofluorescein. In this work H*2*DCF-DA and CM-H2DCFDA were used, the latter provides better retention in live cells and was therefore used in flow cytometry analysis while H2DCF-DA was used for fluorescence microscopy.

Fluorescence microscopy of MOCK infected WT RBC showed a clear fluorescence signal inside the parasite after 5 min incubation with H2DCF-DA (Figure 20). This implicates that the parasite is exposed toward higher ROS levels than the WT RBC. This is could be explained by the parasites digestion of Hb. Thereby free heme is released into the parasites cytosol where it reacts with O_2 to $O_2^{\bullet-}$ and H_2O_2 (139).

However the difference of the ROS level of WT and G6PD deficient cells were also determined. Both blood types were incubated for 15 min with CM-H2DCFDA and subsequently analysed by flow cytometry. The histogram (Figure 21) is showing no significant difference between both RBC populations. This confirms with previous reports that G6PD deficient cells equal normal RBC as long not exposed to oxidative stress (103,104). Therefore both WT and G6PD deficient RBC were exposed to 0,17% H_2O_2 to imitate an oxidative environment. A significant shift occurred confirming that G6PD deficient RBC cannot recompense an increased oxidative pressure. On the other hand normal erythrocytes showed also a slight shift but are able to compensate the increase of ROS.

MOCK infected G6PD deficient RBCs showed already a slight increase in the ROS level compared to infected WT RBCs (Figure 22). However this increase is minor, suggesting that the increase of oxidative stress inside G6PD deficient RBC is not sufficient to impair the parasites development. Therefore again an oxidative environment was simulated. Previous tests showed that the use of 0,17% H_2O_2 is simulating an oxidative environment which has impact on the RBCs' ROS level but is neither lysing WT RBCs nor G6PD deficient RBCs (Figure 23Figure 24Figure 25). Consequently the analyse of the protective effect of *Pf*GST overexpression in G6PD deficient cells has been done simulating an oxidative environment supplementing with 0,17%. Comparing the ROS level of *Pf*GST overexpressing cell lines in WT and G6PD deficient blood towards the respective MOCK line a significant lower ROS level was detected in both blood types. The protective effect was also analysed stage specific between ring and trophozoite stage. Both are showing the same decrease in ROS concentration which can be explained due to the continuous overexpression of *Pf*GST driven by the *crt*-promoter. On the other hand the *Pf*GST Y9F overexpressed mutant shows the same ROS level in both blood types and in both parasite stages confirming the before obtained results of the growth profile.

The enhanced proliferation of *Pf*GST overexpressing *P. falciparum* in G6PD deficient RBCs and the diminished ROS level in this cell line let us propose the following resistance mechanism (Figure 36).

Figure 36 – *Pf*GST enhanced parasites growth in G6PD deficient RBCs

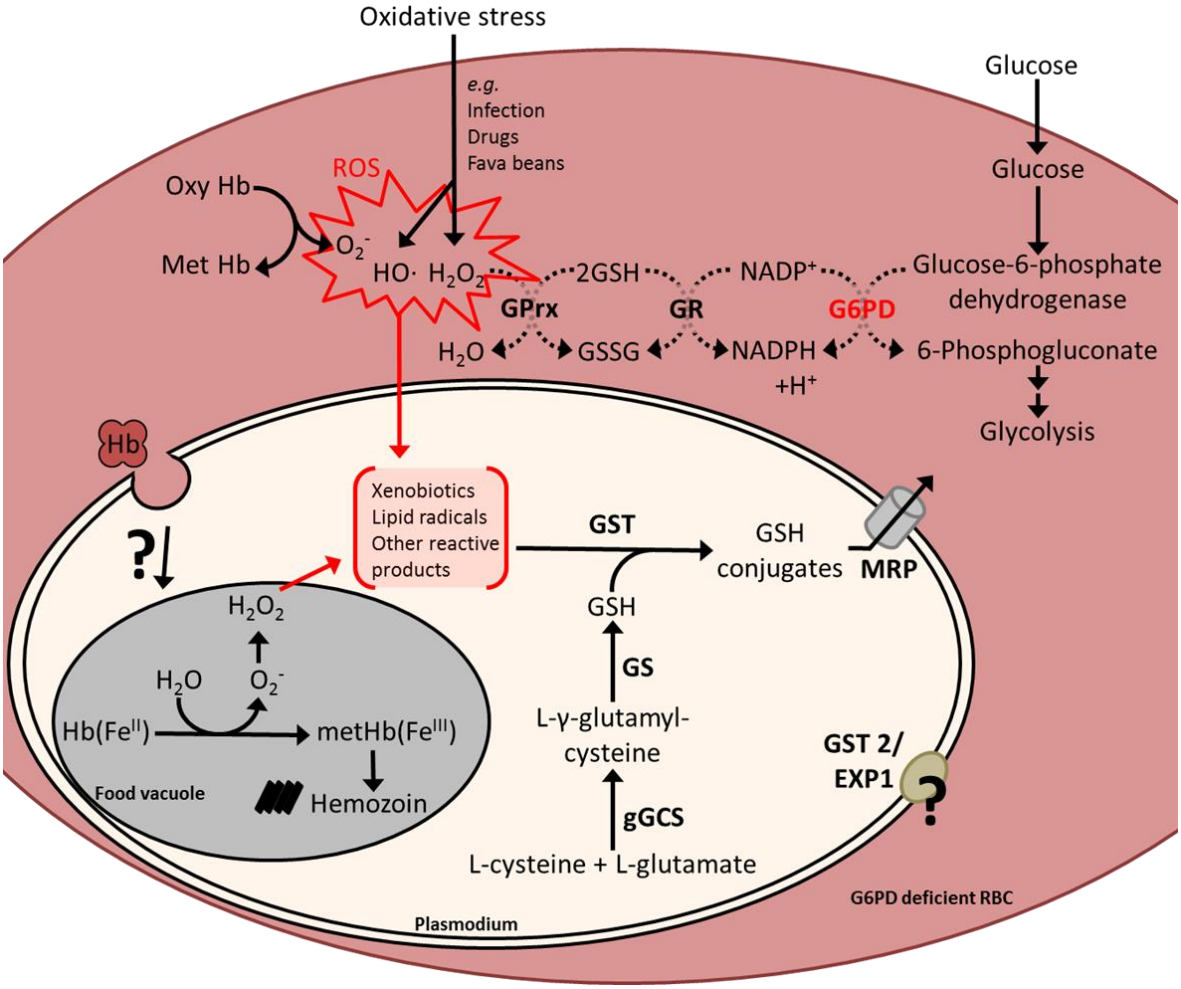

Proposed mode of action of G6PD deficientcy mediates malaria resistance. Exogenous ROS trigers the increase of ROS production inside G6PD deficient RBCs. Because of the limited NADPH production the redox homeostasis is disturbed resulting in an increase of ROS, lipid peroxidation and the formation of oxidated biomolecules inside the parasite. *Pf*GST is neutralizing access of H_2O_2 and detoxifing oxidated biomolecules through coppeling GSH and exporting GS-X conjugates via MRP transportes. The involvment of the membran bound *Pf*GST2/*Pf*EXP1 is still unknown.

P. falciparum is able to grow and prolifarate in G6PD deficent RBCs. The increased ROS level during an infection is not sufficient to impair the parasites development and proliferation. However exposure of these iRBC in an oxidative enviorment is significantly increasing the ROS production. We propose that during the infection, the RBC milieu is increasing the ROS formation, e.g. due to the release of free heme.

This increse disrubs the redosx balance of the RBC and starts a chain reaction producing ROS and oxidating biomolecules like lipids, proteins or DNA. An overexpression of *Pf*GST can detoxify the oxidated biomolecules via GSH conjugates which will be subsequently exported by MRPs. On the other hand *Pf*GST is neutralizing H_2O_2 because of its GSH peroxidase activity.

To analyse if the GSH conjugates are the important reaction or, if just the increase of peroxidase activity plays a role we analysed the GSH concentrations of the cell lines via LC-ESI-MS/MS. Expected was a decrese of GSH in the *Pf*GST overexpressing cell lines compared to the MOCK line if GSH conjugates would be the key point in the mediated growth advantage.

5.5 *Pf*GST – A good drug target?

The impotence of *Pf*GST is known for a long time. However a correlation between *Pf*GST and G6PD deficiency has never been demonstrated as possible mode of action. To clarify the importance of *Pf*GST in this context we designed three compounds (ISA1-3) which showed an inhibitory effect of *Pf*GST *in silico*. This compound should reverse the growth benefit of the *Pf*GST overexpressing line and could been tested as novel anti-malarial drugs. However the compounds were primarily analysed in activity assays using recombinantly expressed *Pf*GST. No inhibition was observed for drug concentrations of 100 µM. An eventual pro-drug activity was also excluded since the enzyme does not accept the compound as substrate. Lastly also no antimalarial effect was detected. The compound failure in inhibiting *Pf*GST specific activity could be explained by insufficient calculations based on the similarity to previous known *Pf*GST binding compounds.

Nevertheless *Pf*GST seems an interesting drug target and has been analysed several times over the years (48,181). The plasmodial *Pf*GST is structurally different from all other known *Pf*GST classes (182,183) which makes the protein an attractive drug target.. Additionally the inhibition of the *Pf*GST would impair several important functions, like detoxification of xenobiotic, the ROS control and the detoxification of hemin (159,183,184). Therefore plasmodial *Pf*GST seems a very promissing novel

drug target. Some promessing inhibitors with antiplamodial activity has been already demonstrated (185,186).

However it has to be considered that while G6PD deficiency can provide protection against malarial infection, it can also cause hemolysis induced by pro-oxidant antimalarial drugs like primaquine (187,188). Primaquine is till today the only drug available attacking hypnozoites and preventing relapsing malaria caused by P. vivax or P. ovale. Because of the high correlation between G6PD deficiency and malaria infections new antimalarials should be also potent in those patients without causing hemolytic anaemia as side effects.

6 CONCLUSION

*Pf*GST is one of the most abundant protein in *P. falciparum* and highly important for parasites survival. Its main function is the detoxification of hydrophobic and endogenous/exogenous electrophilic compounds, eliminating cytotoxic hemin by coupling GSH and neutralization of H_2O_2. In this we work reinforce the importance of *Pf*GST showing its role in enhancing parasite's growth in G6PD deficient RBCs, which are known to mediate malaria resistance. Those cells are more susceptible to oxidative stress resulting in the formation of Heinz body, erythrocyte destruction and subsequent hemolytic anemia. Under normal conditions G6PD deficient erythrocytes can cope with low levels of ROS as indicated by no difference in ROS concentration, RBC appearance and leading to no clinical symptoms.

P. falciparum infected G6PD deficient RBCs show just a slight increase in intracellular ROS compared to WT blood but have a comparable growth behavior in the first days of culturing. However after long term culturing (more than 15 days) the proliferation of the pathogen is decreasing. This effect was reversed by overexpression of plasmodial *Pf*GST, leading to an equivalent growth in G6PD deficient blood as in WT blood. Moreover *Pf*GST overexpressing decreases the ROS occurrence in both blood types. This result leads to the proposal that after long term culturing, elevated exogenous ROS alters the redox homeostasis of G6PD deficient RBCs leading to lipid peroxidation and oxidation of DNA and proteins. Overexpression of the plasmodial *Pf*GST is protecting the parasite by detoxifing oxidised biomolecules via coupling GSH and exporting GS-X conjugates via MRP outside of the cell. Additionally *Pf*GST is able to neutralize the access of H_2O_2 and thereby increasing the fitness of *P. falciparum* inside G6PD deficient RBCs.

However there are several other enzymes which have been reported to be involved in the defence of oxidative stress including a recently identified membrane-bound *Pf*GSTF2/*Pf*EXP1. In order to verify whether *Pf*GST is the only enzyme to enable *P. falciparum* to proliferate normally in G6PD-deficient RBCs further analyses of other ROS detoxifying pathways are required.

*

REFERENCES*

1. WHO. World Malaria Report 2016 [Internet]. 2016 [cited 2017 Mar 13]. Available from: http://apps.who.int/iris/bitstream/10665/252038/1/9789241511711-eng.pdf?ua=1

2. Cox FEG. History of human parasitology. Clin Microbiol Rev [Internet]. 2002 Oct [cited 2017 Feb 13];15(4):595–612. Available from: http://www.ncbi.nlm.nih.gov/pubmed/12364371

3. Majori G. Short history of malaria and its eradication in Italy with short notes on the fight against the infection in the mediterranean basin. Mediterr J Hematol Infect Dis [Internet]. 2012 [cited 2017 Mar 13];4(1):e2012016. Available from: http://www.ncbi.nlm.nih.gov/pubmed/22550561

4. Ross R. On some Peculiar Pigmented Cells Found in Two Mosquitos Fed on Malarial Blood. Br Med J [Internet]. 1897 Dec 18 [cited 2017 Mar 13];2(1929):1786–8. Available from: http://www.ncbi.nlm.nih.gov/pubmed/20757493

5. Shortt HE, Garnham PCC. Pre-erythrocytic stage in mammalian malaria parasites. Nature [Internet]. 1948 Jan 24 [cited 2017 Mar 13];161(4082):126. Available from: http://www.ncbi.nlm.nih.gov/pubmed/18900752

6. Krotoski WA, Collins WE, Bray RS, Garnham PC, Cogswell FB, Gwadz RW, et al. Demonstration of hypnozoites in sporozoite-transmitted Plasmodium vivax infection. Am J Trop Med Hyg [Internet]. 1982 Nov [cited 2017 Mar 13];31(6):1291–3. Available from: http://www.ncbi.nlm.nih.gov/pubmed/6816080

7. Pain A, Böhme U, Berry AE, Mungall K, Finn RD, Jackson AP, et al. The genome of the simian and human malaria parasite Plasmodium knowlesi. Nature [Internet]. 2008 Oct 9 [cited 2017 Mar 13];455(7214):799–803. Available from: http://www.ncbi.nlm.nih.gov/pubmed/18843368

8. Morrison DA. Evolution of the Apicomplexa: where are we now? Trends Parasitol [Internet]. 2009 Aug [cited 2017 Mar 13];25(8):375–82. Available from: http://linkinghub.elsevier.com/retrieve/pii/S1471492209001433

9. Kishore U. Target pattern recognition in innate immunity [Internet]. Springer Science+Business Media; 2009 [cited 2017 Mar 13]. 202 p. Available from: https://books.google.com.br/books?id=p5Oay0xBypwC&pg=PA175&lpg=PA175&dq=40,000+merozoites,+which+will+then+be+released+into+the+blood+stream&source=bl&ots=nQNuwx7Oyh&sig=gy3wrCnA00BBiNAfep4Gq_a36zk&hl=de&sa=X&ved=0ahUKEwiDw_T2h9TSAhVCGpAKHSwVDWQQ6AEINDAF#v=onepage&q=40%2C000 merozoites%2C which will then be released into the blood stream&f=false

10. Biryukov S, Stoute JA. Complement activation in malaria: friend or foe? Trends Mol Med [Internet]. 2014 May [cited 2017 Mar 13];20(5):293–301. Available from: http://linkinghub.elsevier.com/retrieve/pii/S1471491414000021

11. Delves M, Plouffe D, Scheurer C, Meister S, Wittlin S, Winzeler EA, et al. The Activities of Current Antimalarial Drugs on the Life Cycle Stages of

Plasmodium: A Comparative Study with Human and Rodent Parasites. Beeson JG, editor. PLoS Med [Internet]. 2012 Feb 21 [cited 2017 Mar 13];9(2):e1001169. Available from: http://dx.plos.org/10.1371/journal.pmed.1001169

12. Kronenberger T, Lindner J, Meissner KA, Zimbres FM, Coronado MA, Sauer FM, et al. Vitamin B6-dependent enzymes in the human malaria parasite plasmodium falciparum: A druggable target? Biomed Res Int. 2014;2014.

13. Lindner J, Meissner KA, Schettert I, Wrenger C. Trafficked proteins - Druggable in plasmodium falciparum ? Int J Cell Biol. 2013;

14. Beard J, Australian Rural Health Research Collaboration. DDT and human health. Sci Total Environ [Internet]. 2006 Feb 15 [cited 2017 Apr 9];355(1–3):78–89. Available from: http://www.ncbi.nlm.nih.gov/pubmed/15894351

15. Raghavendra K, Barik TK, Reddy BPN, Sharma P, Dash AP. Malaria vector control: from past to future. Parasitol Res [Internet]. 2011 Apr 13 [cited 2017 Apr 9];108(4):757–79. Available from: http://www.ncbi.nlm.nih.gov/pubmed/21229263

16. Sadasivaiah S, Tozan Y, Breman JG. Dichlorodiphenyltrichloroethane (DDT) for indoor residual spraying in Africa: how can it be used for malaria control? Am J Trop Med Hyg [Internet]. 2007 Dec [cited 2017 Apr 9];77(6 Suppl):249–63. Available from: http://www.ncbi.nlm.nih.gov/pubmed/18165500

17. Schirmer RH, Coulibaly B, Stich A, Scheiwein M, Merkle H, Eubel J, et al. Methylene blue as an antimalarial agent. Redox Rep [Internet]. 2003 Oct 19 [cited 2017 Apr 9];8(5):272–5. Available from: http://www.tandfonline.com/doi/full/10.1179/135100003225002899

18. Suwanarusk R, Russell B, Ong A, Sriprawat K, Chu CS, Pyaephyo A, et al. Methylene blue inhibits the asexual development of vivax malaria parasites from a region of increasing chloroquine resistance. [cited 2017 Apr 9]; Available from: https://www.ncbi.nlm.nih.gov/pmc/articles/PMC4267499/pdf/dku326.pdf

19. Greenwood D. The quinine connection. Journal of Antimicrobial Chemotherapy. 1992.

20. Solomon VR, Lee H. Chloroquine and its analogs: a new promise of an old drug for effective and safe cancer therapies. Eur J Pharmacol [Internet]. 2009 Dec 25 [cited 2017 Mar 13];625(1–3):220–33. Available from: http://linkinghub.elsevier.com/retrieve/pii/S001429990900870X

21. Roepe PD. Molecular and physiologic basis of quinoline drug resistance in *Plasmodium falciparum* malaria. Future Microbiol [Internet]. 2009 May [cited 2017 Mar 13];4(4):441–55. Available from: http://www.ncbi.nlm.nih.gov/pubmed/19416013

22. Bray PG, Mungthin M, Hastings IM, Biagini GA, Saidu DK, Lakshmanan V, et al. PfCRT and the trans-vacuolar proton electrochemical gradient: regulating the access of chloroquine to ferriprotoporphyrin IX. Mol Microbiol [Internet].

2006 Oct [cited 2017 Mar 13];62(1):238–51. Available from: http://www.ncbi.nlm.nih.gov/pubmed/16956382

23. Fidock DA, Nomura T, Talley AK, Cooper RA, Dzekunov SM, Ferdig MT, et al. Mutations in the P. falciparum digestive vacuole transmembrane protein PfCRT and evidence for their role in chloroquine resistance. Mol Cell [Internet]. 2000 Oct [cited 2017 Mar 13];6(4):861–71. Available from: http://www.ncbi.nlm.nih.gov/pubmed/11090624

24. Ecker A, Lehane AM, Clain J, Fidock DA. PfCRT and its role in antimalarial drug resistance. Trends Parasitol [Internet]. 2012 Nov [cited 2017 Mar 13];28(11):504–14. Available from: http://www.ncbi.nlm.nih.gov/pubmed/23020971

25. WHO. World malaria report 2005 [Internet]. World Health Organization; 2005 [cited 2017 Mar 19]. 294 p. Available from: http://www.who.int/malaria/publications/atoz/9241593199/en/

26. Sridaran S, McClintock SK, Syphard LM, Herman KM, Barnwell JW, Udhayakumar V. Anti-folate drug resistance in Africa: meta-analysis of reported dihydrofolate reductase (dhfr) and dihydropteroate synthase (dhps) mutant genotype frequencies in African Plasmodium falciparum parasite populations. Malar J [Internet]. 2010 Aug 30 [cited 2017 Mar 13];9(1):247. Available from: http://www.ncbi.nlm.nih.gov/pubmed/20799995

27. Gesase S, Gosling RD, Hashim R, Ord R, Naidoo I, Madebe R, et al. High Resistance of Plasmodium falciparum to Sulphadoxine/Pyrimethamine in Northern Tanzania and the Emergence of dhps Resistance Mutation at Codon 581. Gregson A, editor. PLoS One [Internet]. 2009 Feb 24 [cited 2017 Mar 13];4(2):e4569. Available from: http://dx.plos.org/10.1371/journal.pone.0004569

28. Mutabingwa TK. Artemisinin-based combination therapies (ACTs): Best hope for malaria treatment but inaccessible to the needy! Acta Trop [Internet]. 2005 Sep [cited 2017 Mar 13];95(3):305–15. Available from: http://linkinghub.elsevier.com/retrieve/pii/S0001706X05001592

29. Nosten F, White NJ. Artemisinin-based combination treatment of falciparum malaria. Am J Trop Med Hyg [Internet]. 2007 Dec [cited 2017 Mar 13];77(6 Suppl):181–92. Available from: http://www.ncbi.nlm.nih.gov/pubmed/18165491

30. Shandilya A, Chacko S, Jayaram B, Ghosh I, Haak J. A plausible mechanism for the antimalarial activity of artemisinin: A computational approach. Sci Rep [Internet]. 2013 Aug 29 [cited 2017 Mar 13];3:33–8. Available from: http://www.nature.com/articles/srep02513

31. Lisewski AM, Quiros JP, Ng CL, Adikesavan AK, Miura K, Putluri N, et al. Supergenomic network compression and the discovery of EXP1 as a glutathione transferase inhibited by artesunate. Cell [Internet]. 2014 Aug 14 [cited 2017 Apr 5];158(4):916–28. Available from: http://linkinghub.elsevier.com/retrieve/pii/S0092867414009258

32. Campo B, Vandal O, Wesche DL, Burrows JN. Killing the hypnozoite – drug

discovery approaches to prevent relapse in *Plasmodium vivax*. Pathog Glob Health [Internet]. 2015 May 18 [cited 2017 Mar 13];109(3):107–22. Available from: http://www.tandfonline.com/doi/full/10.1179/2047773215Y.0000000013

33. Alonso PL, Sacarlal J, Aponte JJ, Leach A, Macete E, Aide P, et al. Duration of protection with RTS,S/AS02A malaria vaccine in prevention of Plasmodium falciparum disease in Mozambican children: single-blind extended follow-up of a randomised controlled trial. Lancet [Internet]. 2005 Dec 10 [cited 2017 Mar 13];366(9502):2012–8. Available from: http://www.ncbi.nlm.nih.gov/pubmed/16338450

34. Haldane JBS. The rate of mutation of human genes. Hereditas [Internet]. 1949 Jul 9 [cited 2017 Mar 13];35(S1):267–73. Available from: http://doi.wiley.com/10.1111/j.1601-5223.1949.tb03339.x

35. Hedrick PW. Resistance to malaria in humans: the impact of strong, recent selection. Malar J. 2012;11:1.

36. Allison AC. Protection afforded by sickle-cell trait against subtertian malareal infection. Br Med J [Internet]. 1954 Feb 6 [cited 2017 Mar 13];1(4857):290–4. Available from: http://www.ncbi.nlm.nih.gov/pubmed/13115700

37. Herrick JB. Peculiar elongated and sickle-shaped red blood corpuscles in a case of severe anemia. 1910. Yale J Biol Med [Internet]. 1910 [cited 2017 Mar 13];74(3):179–84. Available from: http://www.ncbi.nlm.nih.gov/pubmed/11501714

38. Brittenham GM, Schechter AN, Noguchi CT. Hemoglobin S polymerization: primary determinant of the hemolytic and clinical severity of the sickling syndromes. Blood [Internet]. 1985 Jan [cited 2017 Feb 14];65(1):183–9. Available from: http://www.ncbi.nlm.nih.gov/pubmed/3965046

39. Vos T, Barber RM, Bell B, Bertozzi-Villa A, Biryukov S, Bolliger I, et al. Global, regional, and national incidence, prevalence, and years lived with disability for 301 acute and chronic diseases and injuries in 188 countries, 1990–2013: a systematic analysis for the Global Burden of Disease Study 2013. Lancet [Internet]. 2015 Aug 22 [cited 2017 Mar 14];386(9995):743–800. Available from: http://www.ncbi.nlm.nih.gov/pubmed/26063472

40. Rees DC, Williams TN, Gladwin MT. Sickle-cell disease. Lancet [Internet]. 2010 Dec 11 [cited 2017 Feb 14];376(9757):2018–31. Available from: http://www.ncbi.nlm.nih.gov/pubmed/21131035

41. Beet EA. Sickle cell disease in the Balovale District of Northern Rhodesia. East Afr Med J [Internet]. 1946 Mar [cited 2017 Mar 13];23:75–86. Available from: http://www.ncbi.nlm.nih.gov/pubmed/21027890

42. Allison AC. The distribution of the sickle-cell trait in East Africa and elsewhere, and its apparent relationship to the incidence of subtertian malaria. Trans R Soc Trop Med Hyg [Internet]. 1954 Jul [cited 2017 Mar 13];48(4):312–8. Available from: http://www.ncbi.nlm.nih.gov/pubmed/13187561

43. Friedman MJ. Erythrocytic mechanism of sickle cell resistance to malaria

(Plasmodium falciparum/hemoglobin S/in vitro culture/cyanate). 1978;75(4):1994–7.

44. Pasvol G, Weatherall DJ, Wilson RJ. Cellular mechanism for the protective effect of haemoglobin S against P. falciparum malaria. Nature [Internet]. 1978 Aug 17 [cited 2017 Mar 13];274(5672):701–3. Available from: http://www.ncbi.nlm.nih.gov/pubmed/353566

45. Browne P, Shalev O, Hebbel RP. The molecular pathobiology of cell membrane iron: the sickle red cell as a model. Free Radic Biol Med [Internet]. 1998 Apr [cited 2017 Mar 13];24(6):1040–8. Available from: http://www.ncbi.nlm.nih.gov/pubmed/9607615

46. Sheng K, Shariff M, Hebbel RP. Comparative oxidation of hemoglobins A and S. Blood [Internet]. 1998 May 1 [cited 2017 Mar 13];91(9):3467–70. Available from: http://www.ncbi.nlm.nih.gov/pubmed/9558406

47. Hebbel RP. Sickle hemoglobin instability: a mechanism for malarial protection. Redox Rep [Internet]. 2003 Oct 19 [cited 2017 Mar 13];8(5):238–40. Available from: http://www.ncbi.nlm.nih.gov/pubmed/14962356

48. Becker K, Tilley L, Vennerstrom JL, Roberts D, Rogerson S, Ginsburg H. Oxidative stress in malaria parasite-infected erythrocytes: Host-parasite interactions. International Journal for Parasitology. 2004.

49. Abu-Zeid YA, Abdulhadi NH, Hviid L, Theander TG, Saeed BO, Jepsen S, et al. Lymphoproliferative responses to Plasmodium falciparum antigens in children with and without the sickle cell trait. Scand J Immunol [Internet]. 1991 Aug [cited 2017 Mar 13];34(2):237–42. Available from: http://www.ncbi.nlm.nih.gov/pubmed/1866602

50. López C, Saravia C, Gomez A, Hoebeke J, Patarroyo MA. Mechanisms of genetically-based resistance to malaria. Gene. 2010.

51. Cholera R, Brittain NJ, Gillrie MR, Lopera-Mesa TM, Diakité SAS, Arie T, et al. Impaired cytoadherence of Plasmodium falciparum-infected erythrocytes containing sickle hemoglobin. Proc Natl Acad Sci U S A [Internet]. 2008 Jan 22 [cited 2017 Mar 13];105(3):991–6. Available from: http://www.pnas.org/cgi/doi/10.1073/pnas.0711401105

52. Fairhurst RM, Baruch DI, Brittain NJ, Ostera GR, Wallach JS, Hoang HL, et al. Abnormal display of PfEMP-1 on erythrocytes carrying haemoglobin C may protect against malaria. Nature [Internet]. 2005 Jun 23 [cited 2017 Mar 13];435(7045):1117–21. Available from: http://www.ncbi.nlm.nih.gov/pubmed/15973412

53. Cyrklaff M, Sanchez CP, Kilian N, Bisseye C, Simpore J, Frischknecht F, et al. Hemoglobins S and C Interfere with Actin Remodeling in Plasmodium falciparum-Infected Erythrocytes. Science (80-) [Internet]. 2011 Dec 2 [cited 2017 Mar 13];334(6060):1283–6. Available from: http://www.sciencemag.org/cgi/doi/10.1126/science.1213775

54. Ferreira A, Marguti I, Bechmann I, Jeney V, Chora Â, Palha NR, et al. Sickle

Hemoglobin Confers Tolerance to Plasmodium Infection. Cell [Internet]. 2011 Apr [cited 2017 Mar 13];145(3):398–409. Available from: http://linkinghub.elsevier.com/retrieve/pii/S0092867411003849

55. Haque A, Engwerda CR. An antioxidant link between sickle cell disease and severe malaria. Cell [Internet]. 2011 Apr 29 [cited 2017 Mar 13];145(3):335–6. Available from: http://linkinghub.elsevier.com/retrieve/pii/S0092867411004211

56. Rosenthal PJ. Lessons from Sickle Cell Disease in the Treatment and Control of Malaria. N Engl J Med [Internet]. 2011 Jun 30 [cited 2017 Mar 13];364(26):2549–51. Available from: http://www.ncbi.nlm.nih.gov/pubmed/21714653

57. Muller-Eberhard U, Javid J, Liem HH, Hanstein A, Hanna M. Plasma concentrations of hemopexin, haptoglobin and heme in patients with various hemolytic diseases. Blood [Internet]. 1968 Nov [cited 2017 Mar 13];32(5):811–5. Available from: http://www.ncbi.nlm.nih.gov/pubmed/5687939

58. Naghavi M, Wang H, Lozano R, Davis A, Liang X, Zhou M, et al. Global, regional, and national age–sex specific all-cause and cause-specific mortality for 240 causes of death, 1990–2013: a systematic analysis for the Global Burden of Disease Study 2013. Lancet [Internet]. 2015 Jan 10 [cited 2017 Mar 14];385(9963):117–71. Available from: http://www.ncbi.nlm.nih.gov/pubmed/25530442

59. Krause MA, Diakite SAS, Lopera-Mesa TM, Amaratunga C, Arie T, Traore K, et al. α-Thalassemia Impairs the Cytoadherence of Plasmodium falciparum-Infected Erythrocytes. Spielmann T, editor. PLoS One [Internet]. 2012 May 18 [cited 2017 Feb 14];7(5):e37214. Available from: http://www.ncbi.nlm.nih.gov/pubmed/22623996

60. Williams TN, Wambua S, Uyoga S, Macharia A, Mwacharo JK, Newton CRJC, et al. Both heterozygous and homozygous + thalassemias protect against severe and fatal Plasmodium falciparum malaria on the coast of Kenya. Blood [Internet]. 2005 Mar 15 [cited 2017 Feb 14];106(1):368–71. Available from: http://www.ncbi.nlm.nih.gov/pubmed/15769889

61. Mockenhaupt FP, Ehrhardt S, Gellert S, Otchwemah RN, Dietz E, Anemana SD, et al. +-thalassemia protects African children from severe malaria. Blood [Internet]. 2004 Oct 1 [cited 2017 Feb 14];104(7):2003–6. Available from: http://www.ncbi.nlm.nih.gov/pubmed/15198952

62. Wambua S, Mwangi TW, Kortok M, Uyoga SM, Macharia AW, Mwacharo JK, et al. The Effect of α +-Thalassaemia on the Incidence of Malaria and Other Diseases in Children Living on the Coast of Kenya. Pasvol G, editor. PLoS Med [Internet]. 2006 Apr 18 [cited 2017 Feb 14];3(5):e158. Available from: http://www.ncbi.nlm.nih.gov/pubmed/16605300

63. May J, Evans JA, Timmann C, Ehmen C, Busch W, Thye T, et al. Hemoglobin variants and disease manifestations in severe falciparum malaria. JAMA [Internet]. 2007 May 23 [cited 2017 Mar 13];297(20):2220–6. Available from: http://jama.jamanetwork.com/article.aspx?doi=10.1001/jama.297.20.2220

64. Allen SJ, O'Donnell A, Alexander ND, Alpers MP, Peto TE, Clegg JB, et al. alpha+-Thalassemia protects children against disease caused by other infections as well as malaria. Proc Natl Acad Sci U S A [Internet]. 1997 Dec 23 [cited 2017 Mar 13];94(26):14736–41. Available from: http://www.ncbi.nlm.nih.gov/pubmed/9405682

65. Veenemans J, Andang'o PEA, Mbugi E V, Kraaijenhagen RJ, Mwaniki DL, Mockenhaupt FP, et al. Alpha+ -thalassemia protects against anemia associated with asymptomatic malaria: evidence from community-based surveys in Tanzania and Kenya. J Infect Dis [Internet]. 2008 Aug 1 [cited 2017 Feb 14];198(3):401–8. Available from: https://academic.oup.com/jid/article-lookup/doi/10.1086/589884

66. Fowkes FJI, Allen SJ, Allen A, Alpers MP, Weatherall DJ, Day KP. Increased Microerythrocyte Count in Homozygous α+-Thalassaemia Contributes to Protection against Severe Malarial Anaemia. Pasvol G, editor. PLoS Med [Internet]. 2008 Mar 18 [cited 2017 Feb 14];5(3):e56. Available from: http://www.ncbi.nlm.nih.gov/pubmed/18351796

67. Thein SL. The molecular basis of β-thalassemia. Cold Spring Harb Perspect Med [Internet]. 2013 May 1 [cited 2017 Mar 13];3(5):a011700. Available from: http://www.ncbi.nlm.nih.gov/pubmed/23637309

68. Flint J, Harding RM, Boyce AJ, Clegg JB. The population genetics of the haemoglobinopathies. Baillieres Clin Haematol [Internet]. 1993 Mar [cited 2017 Feb 14];6(1):215–62. Available from: http://www.ncbi.nlm.nih.gov/pubmed/8353314

69. Weatherall DJ, Clegg JB. Inherited haemoglobin disorders: an increasing global health problem. Bull World Health Organ [Internet]. 2001 [cited 2017 Feb 14];79(8):704–12. Available from: http://www.ncbi.nlm.nih.gov/pubmed/11545326

70. Ray RN, Chatterjea JB, Chaudhuri RN. Observations on the resistance in hb e thalassaemia disease to induced infection with Plasmodium vivax. Bull World Health Organ [Internet]. 1964 [cited 2017 Feb 14];30:51–5. Available from: http://www.ncbi.nlm.nih.gov/pubmed/14122440

71. Kuesap J, Chaijaroenkul W, Rungsihirunrat K, Pongjantharasatien K, Na-Bangchang K. Coexistence of Malaria and Thalassemia in Malaria Endemic Areas of Thailand. Korean J Parasitol [Internet]. 2015 Jun [cited 2017 Feb 14];53(3):265–70. Available from: http://www.ncbi.nlm.nih.gov/pubmed/26174819

72. Hutagalung R, Wilairatana P, Looareesuwan S, Brittenham GM, Gordeuk VR. Influence of Hemoglobin E Trait on the Antimalarial Effect of Artemisinin Derivatives. J Infect Dis [Internet]. 2000 Apr [cited 2017 Mar 13];181(4):1513–6. Available from: https://academic.oup.com/jid/article-lookup/doi/10.1086/315373

73. Moore S, Woodrow CF, McClelland DB. Isolation of membrane components associated with human red cell antigens Rh(D), (c), (E) and Fy. Nature

[Internet]. 1982 Feb 11 [cited 2017 Mar 14];295(5849):529–31. Available from: http://www.ncbi.nlm.nih.gov/pubmed/6799838

74. Miller LH, Mason SJ, Dvorak JA, McGinniss MH, Rothman IK. Erythrocyte receptors for (Plasmodium knowlesi) malaria: Duffy blood group determinants. Science [Internet]. 1975 Aug 15 [cited 2017 Mar 14];189(4202):561–3. Available from: http://www.ncbi.nlm.nih.gov/pubmed/1145213

75. Miller LH, Mason SJ, Clyde DF, McGinniss MH. The Resistance Factor to *Plasmodium vivax* in Blacks. N Engl J Med [Internet]. 1976 Aug 5 [cited 2017 Mar 14];295(6):302–4. Available from: http://www.ncbi.nlm.nih.gov/pubmed/778616

76. Chown B, Lewis M, Kaita H. The duffy blood group system in caucasians: evidence for a new allele. Am J Hum Genet [Internet]. 1965 Sep [cited 2017 Mar 14];17:384–9. Available from: http://www.ncbi.nlm.nih.gov/pubmed/14334737

77. Cutbush M, Mollison PL, Parkin DM. A New Human Blood Group. Nature [Internet]. 1950 Feb 4 [cited 2017 Mar 14];165(4188):188–9. Available from: http://www.nature.com/doifinder/10.1038/165188b0

78. Zimmerman PA, Woolley I, Masinde GL, Miller SM, McNamara DT, Hazlett F, et al. Emergence of FY*A(null) in a Plasmodium vivax-endemic region of Papua New Guinea. Proc Natl Acad Sci U S A [Internet]. 1999 Nov 23 [cited 2017 Mar 14];96(24):13973–7. Available from: http://www.ncbi.nlm.nih.gov/pubmed/10570183

79. Schmid P, Ravenell KR, Sheldon SL, Flegel WA. DARC alleles and Duffy phenotypes in African Americans. Transfusion [Internet]. 2012 Jun [cited 2017 Mar 14];52(6):1260–7. Available from: http://doi.wiley.com/10.1111/j.1537-2995.2011.03431.x

80. Carter R, Mendis KN. Evolutionary and historical aspects of the burden of malaria. Clinical Microbiology Reviews. 2002.

81. Menard D, Barnadas C, Bouchier C, Henry-Halldin C, Gray LR, Ratsimbasoa A, et al. Plasmodium vivax clinical malaria is commonly observed in Duffy-negative Malagasy people. Proc Natl Acad Sci [Internet]. 2010 Mar 30 [cited 2017 Mar 13];107(13):5967–71. Available from: http://www.ncbi.nlm.nih.gov/pubmed/20231434

82. Ryan JR, Stoute JA, Amon J, Dunton RF, Mtalib R, Koros J, et al. Evidence for transmission of Plasmodium vivax among a duffy antigen negative population in Western Kenya. Am J Trop Med Hyg [Internet]. 2006 Oct [cited 2017 Mar 13];75(4):575–81. Available from: http://www.ncbi.nlm.nih.gov/pubmed/17038676

83. Cavasini CE, de Mattos LC, Couto Á, Couto V, Gollino Y, Moretti LJ, et al. Duffy blood group gene polymorphisms among malaria vivax patients in four areas of the Brazilian Amazon region. Malar J [Internet]. 2007 Dec 19 [cited 2017 Mar 13];6(1):167. Available from: http://www.ncbi.nlm.nih.gov/pubmed/18093292

84. Machado P, Manco L, Gomes C, Mendes C, Fernandes N, Salomé G, et al. Pyruvate kinase deficiency in sub-Saharan Africa: identification of a highly frequent missense mutation (G829A;Glu277Lys) and association with malaria. PLoS One [Internet]. 2012 [cited 2017 Mar 13];7(10):e47071. Available from: http://www.ncbi.nlm.nih.gov/pubmed/23082140

85. Grace RF, Zanella A, Neufeld EJ, Morton DH, Eber S, Yaish H, et al. Erythrocyte pyruvate kinase deficiency: 2015 status report. Am J Hematol [Internet]. 2015 Sep [cited 2017 Mar 14];90(9):825–30. Available from: http://www.ncbi.nlm.nih.gov/pubmed/26087744

86. Valentine WN, Tanaka KR, Miwa S. A specific erythrocyte glycolytic enzyme defect (pyruvate kinase) in three subjects with congenital non-spherocytic hemolytic anemia. Trans Assoc Am Physicians [Internet]. 1961 [cited 2017 Mar 14];74:100–10. Available from: http://www.ncbi.nlm.nih.gov/pubmed/13924348

87. Tanaka KR, Valentine WN, Miwa S. Pyruvate kinase (PK) deficiency hereditary nonspherocytic hemolytic anemia. Blood [Internet]. 1962 Mar [cited 2017 Mar 14];19:267–95. Available from: http://www.ncbi.nlm.nih.gov/pubmed/13919474

88. Warang P, Kedar P, Ghosh K, Colah R. Molecular and clinical heterogeneity in pyruvate kinase deficiency in India. Blood Cells, Mol Dis [Internet]. 2013 Oct [cited 2017 Mar 14];51(3):133–7. Available from: http://www.ncbi.nlm.nih.gov/pubmed/23770304

89. Pissard S, Max-Audit I, Skopinski L, Vasson A, Vivien P, Bimet C, et al. Pyruvate kinase deficiency in France: a 3-year study reveals 27 new mutations. Br J Haematol [Internet]. 2006 Jun [cited 2017 Mar 14];133(6):683–9. Available from: http://www.ncbi.nlm.nih.gov/pubmed/16704447

90. Ayi K, Min-Oo G, Serghides L, Crockett M, Kirby-Allen M, Quirt I, et al. Pyruvate Kinase Deficiency and Malaria. N Engl J Med [Internet]. 2008 Apr 24 [cited 2017 Mar 14];358(17):1805–10. Available from: http://www.ncbi.nlm.nih.gov/pubmed/18420493

91. Min-Oo G, Fortin A, Tam M-F, Nantel A, Stevenson MM, Gros P. Pyruvate kinase deficiency in mice protects against malaria. Nat Genet [Internet]. 2003 Dec 2 [cited 2017 Mar 14];35(4):357–62. Available from: http://www.ncbi.nlm.nih.gov/pubmed/14595440

92. Machado P, Pereira R, Rocha AM, Manco L, Fernandes N, Miranda J, et al. Malaria: looking for selection signatures in the human PKLR gene region. Br J Haematol [Internet]. 2010 Feb 8 [cited 2017 Mar 14];149(5):775–84. Available from: http://www.ncbi.nlm.nih.gov/pubmed/20377593

93. Alves J, Machado P, Silva J, Gonçalves N, Ribeiro L, Faustino P, et al. Analysis of malaria associated genetic traits in Cabo Verde, a melting pot of European and sub Saharan settlers. Blood Cells, Mol Dis [Internet]. 2010 Jan 15 [cited 2017 Mar 14];44(1):62–8. Available from: http://www.ncbi.nlm.nih.gov/pubmed/19837619

94. Peters AL, Noorden CJF Van. Glucose-6-phosphate Dehydrogenase Deficiency and Malaria: Cytochemical Detection of Heterozygous G6PD

Deficiency in Women. J Histochem Cytochem [Internet]. 2009 Nov [cited 2017 Mar 14];57(11):1003–11. Available from: http://www.ncbi.nlm.nih.gov/pubmed/19546473

95. Mehta AB. Glucose-6-phosphate dehydrogenase deficiency. Postgr Med J [Internet]. 1994 [cited 2017 Mar 14];70:871–7. Available from: https://www.ncbi.nlm.nih.gov/pmc/articles/PMC2398001/pdf/postmedj00048-0016.pdf

96. Alving AS, Carson PE, Flanagan CL, Ickes CE. Enzymatic deficiency in primaquine-sensitive erythrocytes. Science [Internet]. 1956 Sep 14 [cited 2017 Mar 14];124(3220):484–5. Available from: http://www.ncbi.nlm.nih.gov/pubmed/13360274

97. Patra KC, Hay N. The pentose phosphate pathway and cancer. Trends Biochem Sci [Internet]. 2014 Aug [cited 2017 Mar 14];39(8):347–54. Available from: http://www.ncbi.nlm.nih.gov/pubmed/25037503

98. Szabo P, Purrello M, Rocchi M, Archidiacono N, Alhadeff B, Filippi G, et al. Cytological mapping of the human glucose-6-phosphate dehydrogenase gene distal to the fragile-X site suggests a high rate of meiotic recombination across this site. Proc Natl Acad Sci U S A [Internet]. 1984 Dec [cited 2017 Mar 16];81(24):7855–9. Available from: http://www.ncbi.nlm.nih.gov/pubmed/6595664

99. Trask BJ, Massa H, Kenwrick S, Gitschier J. Mapping of human chromosome Xq28 by two-color fluorescence in situ hybridization of DNA sequences to interphase cell nuclei. Am J Hum Genet [Internet]. 1991 Jan [cited 2017 Mar 16];48(1):1–15. Available from: http://www.ncbi.nlm.nih.gov/pubmed/1985451

100. Cappellini MD, Fiorelli G. Glucose-6-phosphate dehydrogenase deficiency. Lancet (London, England) [Internet]. 2008 Jan 5 [cited 2017 Mar 16];371(9606):64–74. Available from: http://linkinghub.elsevier.com/retrieve/pii/S0140673608600732

101. Howes RE, Piel FB, Patil AP, Nyangiri OA, Gething PW, Dewi M, et al. G6PD Deficiency Prevalence and Estimates of Affected Populations in Malaria Endemic Countries: A Geostatistical Model-Based Map. von Seidlein L, editor. PLoS Med [Internet]. 2012 Nov 13 [cited 2017 Mar 19];9(11):e1001339. Available from: http://www.ncbi.nlm.nih.gov/pubmed/23152723

102. Vulliamy T, Luzzatto L, Hirono A, Beutler E. Hematologically important mutations: glucose-6-phosphate dehydrogenase. Blood Cells Mol Dis [Internet]. 1997 Aug [cited 2017 Mar 16];23(2):302–13. Available from: http://www.ncbi.nlm.nih.gov/pubmed/9410474

103. Arese P, Gallo V, Pantaleo A, Turrini F. Life and Death of Glucose-6-Phosphate Dehydrogenase (G6PD) Deficient Erythrocytes - Role of Redox Stress and Band 3 Modifications. Transfus Med Hemother [Internet]. 2012 Oct [cited 2017 Mar 16];39(5):328–34. Available from: http://www.ncbi.nlm.nih.gov/pubmed/23801924

104. Elyassi AR, Rowshan HH. Perioperative management of the glucose-6-

phosphate dehydrogenase deficient patient: a review of literature. Anesth Prog [Internet]. 2009 [cited 2017 Mar 16];56(3):86–91. Available from: http://www.ncbi.nlm.nih.gov/pubmed/19769422

105. Gilles HM, Fletcher KA, Hendrickse RG, Lindner R, Reddy S, Allan N. Glucose-6-phosphate-dehydrogenase deficiency, sickling, and malaria in African children in South Western Nigeria. Lancet (London, England) [Internet]. 1967 Jan 21 [cited 2017 Mar 16];1(7482):138–40. Available from: http://www.ncbi.nlm.nih.gov/pubmed/4163314

106. Ruwende C, Khoo SC, Snow RW, Yates SN, Kwiatkowski D, Gupta S, et al. Natural selection of hemi- and heterozygotes for G6PD deficiency in Africa by resistance to severe malaria. Nature [Internet]. 1995 Jul 20 [cited 2017 Mar 16];376(6537):246–9. Available from: http://www.nature.com/doifinder/10.1038/376246a0

107. Leslie T, Briceño M, Mayan I, Mohammed N, Klinkenberg E, Sibley CH, et al. The impact of phenotypic and genotypic G6PD deficiency on risk of plasmodium vivax infection: a case-control study amongst Afghan refugees in Pakistan. Rogerson SJ, editor. PLoS Med [Internet]. 2010 May 25 [cited 2017 Mar 16];7(5):e1000283. Available from: http://dx.plos.org/10.1371/journal.pmed.1000283

108. Louicharoen C, Patin E, Paul R, Nuchprayoon I, Witoonpanich B, Peerapittayamongkol C, et al. Positively selected G6PD-Mahidol mutation reduces Plasmodium vivax density in Southeast Asians. Science [Internet]. 2009 Dec 11 [cited 2017 Mar 16];326(5959):1546–9. Available from: http://www.sciencemag.org/cgi/doi/10.1126/science.1178849

109. Ayi K, Turrini F, Piga A, Arese P. Enhanced phagocytosis of ring-parasitized mutant erythrocytes: a common mechanism that may explain protection against falciparum malaria in sickle trait and beta-thalassemia trait. Blood [Internet]. 2004 Nov 15 [cited 2017 Mar 16];104(10):3364–71. Available from: http://www.bloodjournal.org/cgi/doi/10.1182/blood-2003-11-3820

110. Arese P, Turrini F, Schwarzer E. Band 3/complement-mediated recognition and removal of normally senescent and pathological human erythrocytes. Cell Physiol Biochem [Internet]. 2005 Nov 15 [cited 2017 Mar 16];16(4–6):133–46. Available from: http://www.karger.com/?doi=10.1159/000089839

111. Cappadoro M, Giribaldi G, O'Brien E, Turrini F, Mannu F, Ulliers D, et al. Early phagocytosis of glucose-6-phosphate dehydrogenase (G6PD)-deficient erythrocytes parasitized by Plasmodium falciparum may explain malaria protection in G6PD deficiency. Blood [Internet]. 1998 Oct 1 [cited 2017 Mar 16];92(7):2527–34. Available from: http://www.ncbi.nlm.nih.gov/pubmed/9746794

112. Courtin D, Milet J, Bertin G, Vafa M, Sarr JB, Watier L, et al. G6PD A-variant influences the antibody responses to Plasmodium falciparum MSP2. Infect Genet Evol [Internet]. 2011 Aug [cited 2017 Mar 16];11(6):1287–92. Available from: http://linkinghub.elsevier.com/retrieve/pii/S1567134811001225

113. Luzzatto L. G6PD deficiency: a polymorphism balanced by heterozygote advantage against malaria. Lancet Haematol [Internet]. 2015 Oct [cited 2017 Mar 16];2(10):e400–1. Available from: http://www.ncbi.nlm.nih.gov/pubmed/26686037

114. Uyoga S, Ndila CM, Macharia AW, Nyutu G, Shah S, Peshu N, et al. Glucose-6-phosphate dehydrogenase deficiency and the risk of malaria and other diseases in children in Kenya: a case-control and a cohort study. Lancet Haematol [Internet]. 2015 Oct [cited 2017 Mar 16];2(10):e437–44. Available from: http://www.ncbi.nlm.nih.gov/pubmed/26686045

115. Bienzle U, Ayeni O, Lucas AO, Luzzatto L. Glucose-6-phosphate dehydrogenase and malaria. Greater resistance of females heterozygous for enzyme deficiency and of males with non-deficient variant. Lancet (London, England) [Internet]. 1972 Jan 15 [cited 2017 Mar 16];1(7742):107–10. Available from: http://www.ncbi.nlm.nih.gov/pubmed/4108978

116. Guindo A, Fairhurst RM, Doumbo OK, Wellems TE, Diallo DA. X-Linked G6PD Deficiency Protects Hemizygous Males but Not Heterozygous Females against Severe Malaria. Krishna S, editor. PLoS Med [Internet]. 2007 Mar 13 [cited 2017 Mar 16];4(3):e66. Available from: http://www.ncbi.nlm.nih.gov/pubmed/17355169

117. Sirugo G, Predazzi IM, Bartlett J, Tacconelli A, Walther M, Williams SM. G6PD A- deficiency and severe malaria in The Gambia: heterozygote advantage and possible homozygote disadvantage. Am J Trop Med Hyg [Internet]. 2014 May [cited 2017 Mar 16];90(5):856–9. Available from: http://www.ncbi.nlm.nih.gov/pubmed/24615128

118. Rhee SG. Redox signaling: hydrogen peroxide as intracellular messenger. Exp Mol Med [Internet]. 1999 Jun 30 [cited 2017 Apr 5];31(2):53–9. Available from: http://www.ncbi.nlm.nih.gov/pubmed/10410302

119. Bedard K, Krause K-H. The NOX Family of ROS-Generating NADPH Oxidases: Physiology and Pathophysiology. Physiol Rev [Internet]. 2007 Jan 1 [cited 2017 Apr 5];87(1):245–313. Available from: http://www.ncbi.nlm.nih.gov/pubmed/17237347

120. Circu ML, Aw TY. Reactive oxygen species, cellular redox systems, and apoptosis. Free Radic Biol Med [Internet]. 2010 Mar 15 [cited 2017 Apr 5];48(6):749–62. Available from: http://www.ncbi.nlm.nih.gov/pubmed/20045723

121. Reiter RJ, Melchiorri D, Sewerynek E, Poeggeler B, Barlow-Walden L, Chuang J, et al. A review of the evidence supporting melatonin’s role as an antioxidant. J Pineal Res [Internet]. 1995 Jan [cited 2017 Apr 5];18(1):1–11. Available from: http://www.ncbi.nlm.nih.gov/pubmed/7776173

122. Sadrzadeh SM, Graf E, Panter SS, Hallaway PE, Eaton JW. Hemoglobin. A biologic fenton reagent. J Biol Chem [Internet]. 1984 Dec 10 [cited 2017 Apr 5];259(23):14354–6. Available from: http://www.ncbi.nlm.nih.gov/pubmed/6094553

123. Hrycay EG, Bandiera SM. Involvement of Cytochrome P450 in Reactive Oxygen Species Formation and Cancer. In: Advances in pharmacology (San Diego, Calif) [Internet]. 2015 [cited 2017 Apr 4]. p. 35–84. Available from: http://www.ncbi.nlm.nih.gov/pubmed/26233903

124. Hrycay EG, Bandiera SM. The monooxygenase, peroxidase, and peroxygenase properties of cytochrome P450. Arch Biochem Biophys [Internet]. 2012 Jun 15 [cited 2017 Apr 5];522(2):71–89. Available from: http://linkinghub.elsevier.com/retrieve/pii/S0003986112000057

125. Lewis DF V. Molecular modeling of human cytochrome P450–substrate interactions. Drug Metab Rev [Internet]. 2002 Jan 15 [cited 2017 Apr 5];34(1–2):55–67. Available from: http://www.ncbi.nlm.nih.gov/pubmed/11996012

126. del Río LA, López-Huertas E. ROS Generation in Peroxisomes and its Role in Cell Signaling. Plant Cell Physiol [Internet]. 2016 Apr 14 [cited 2017 Apr 5];57(7):pcw076. Available from: http://www.ncbi.nlm.nih.gov/pubmed/27081099

127. del Rio LA. Peroxisomes. Preface. Subcell Biochem [Internet]. 2013 [cited 2017 Apr 5];69:vii–x. Available from: http://www.ncbi.nlm.nih.gov/pubmed/25039096

128. Foyer CH. Plant Peroxisomes: Biochemistry, Cell biology and Biotechnological Applications: Edited by Alison Baker, Ian A. Graham, Kluwer Academic Publishers, Dordrecht, The Netherlands, 2002. 505 pp., ISBN 1402005873, €180. Plant Sci [Internet]. 2003 Nov [cited 2017 Apr 5];165(5):1171–2. Available from: http://linkinghub.elsevier.com/retrieve/pii/S0168945203003248

129. Žárský V, Tachezy J. Evolutionary loss of peroxisomes--not limited to parasites. Biol Direct [Internet]. 2015 Dec 23 [cited 2017 Apr 5];10:74. Available from: http://www.ncbi.nlm.nih.gov/pubmed/26700421

130. Kumerova A, Lece A, Skesters A, Silova A, Petuhovs V. Anaemia and antioxidant defence of the red blood cells. Mater Med Pol [Internet]. [cited 2017 Apr 5];30(1–2):12–5. Available from: http://www.ncbi.nlm.nih.gov/pubmed/10214469

131. George A, Pushkaran S, Konstantinidis DG, Koochaki S, Malik P, Mohandas N, et al. Erythrocyte NADPH oxidase activity modulated by Rac GTPases, PKC, and plasma cytokines contributes to oxidative stress in sickle cell disease. Blood [Internet]. 2013 Mar 14 [cited 2017 Apr 5];121(11):2099–107. Available from: http://www.ncbi.nlm.nih.gov/pubmed/23349388

132. Mohanty JG, Nagababu E, Rifkind JM. Red blood cell oxidative stress impairs oxygen delivery and induces red blood cell aging. Front Physiol [Internet]. 2014 [cited 2017 Apr 5];5:84. Available from: http://www.ncbi.nlm.nih.gov/pubmed/24616707

133. Gonzales R, Auclair C, Voisin E, Gautero H, Dhermy D, Boivin P. Superoxide dismutase, catalase, and glutathione peroxidase in red blood cells from patients with malignant diseases. Cancer Res [Internet]. 1984 Sep [cited 2017 Apr 5];44(9):4137–9. Available from:

http://www.ncbi.nlm.nih.gov/pubmed/6589047

134. Nagababu E, Chrest FJ, Rifkind JM. Hydrogen-peroxide-induced heme degradation in red blood cells: the protective roles of catalase and glutathione peroxidase. Biochim Biophys Acta [Internet]. 2003 Mar 17 [cited 2017 Apr 5];1620(1–3):211–7. Available from: http://www.ncbi.nlm.nih.gov/pubmed/12595091

135. Lee T-H, Kim S-U, Yu S-L, Kim SH, Park DS, Moon H-B, et al. Peroxiredoxin II is essential for sustaining life span of erythrocytes in mice. Blood [Internet]. 2003 Feb 27 [cited 2017 Apr 5];101(>12):5033–8. Available from: http://www.ncbi.nlm.nih.gov/pubmed/12586629

136. Nagababu E, Mohanty JG, Friedman JS, Rifkind JM. Role of peroxiredoxin-2 in protecting RBCs from hydrogen peroxide-induced oxidative stress. Free Radic Res [Internet]. 2013 Mar 9 [cited 2017 Apr 5];47(3):164–71. Available from: http://www.ncbi.nlm.nih.gov/pubmed/23215741

137. McDonagh EM, Bautista JM, Youngster I, Altman RB, Klein TE. PharmGKB summary: methylene blue pathway. Pharmacogenet Genomics [Internet]. 2013 Sep [cited 2017 Apr 9];23(9):498–508. Available from: http://www.ncbi.nlm.nih.gov/pubmed/23913015

138. Francis SE, Sullivan DJ, Goldberg and DE. Hemoglobin metabolism in the malaria parasite Plasmodium falciparum. Annu Rev Microbiol [Internet]. 1997 Oct [cited 2017 Apr 5];51(1):97–123. Available from: http://www.ncbi.nlm.nih.gov/pubmed/9343345

139. Egan TJ, Combrinck JM, Egan J, Hearne GR, Marques HM, Ntenteni S, et al. Fate of haem iron in the malaria parasite Plasmodium falciparum. Biochem J [Internet]. 2002 Jul 15 [cited 2017 Apr 5];365(Pt 2):343–7. Available from: http://www.ncbi.nlm.nih.gov/pubmed/12033986

140. Foth BJ, Zhang N, Chaal BK, Sze SK, Preiser PR, Bozdech Z. Quantitative Time-course Profiling of Parasite and Host Cell Proteins in the Human Malaria Parasite Plasmodium falciparum. Mol Cell Proteomics [Internet]. 2011 Aug 1 [cited 2017 Apr 5];10(8):M110.006411-M110.006411. Available from: http://www.ncbi.nlm.nih.gov/pubmed/21558492

141. Sztajer H, Gamain B, Aumann K-D, Slomianny C, Becker K, Brigelius-Flohe R, et al. The Putative Glutathione Peroxidase Gene of Plasmodium falciparum Codes for a Thioredoxin Peroxidase. J Biol Chem [Internet]. 2001 Mar 9 [cited 2017 Apr 5];276(10):7397–403. Available from: http://www.ncbi.nlm.nih.gov/pubmed/11087748

142. Clarebout G, Slomianny C, Delcourt P, Leu B, Masset A, Camus D, et al. Status of Plasmodium falciparum towards catalase. Br J Haematol [Internet]. 1998 Oct [cited 2017 Apr 5];103(1):52–9. Available from: http://www.ncbi.nlm.nih.gov/pubmed/9792289

143. Müller S, Gilberger TW, Krnajski Z, Lüersen K, Meierjohann S, Walter RD. Thioredoxin and glutathione system of malaria parasite Plasmodium falciparum. Protoplasma [Internet]. 2001 [cited 2017 Apr 5];217(1–3):43–9.

Available from: http://www.ncbi.nlm.nih.gov/pubmed/11732337

144. Wrenger C, Schettert I, Liebau E. Oxidative stress in human infectious diseases – present and current knowledge about its druggability.

145. Müller S. Role and Regulation of Glutathione Metabolism in Plasmodium falciparum. Molecules [Internet]. 2015 Jun 8 [cited 2017 Mar 14];20(6):10511–34. Available from: http://www.ncbi.nlm.nih.gov/pubmed/26060916

146. Urscher M, Alisch R, Deponte M. The glyoxalase system of malaria parasites—Implications for cell biology and general glyoxalase research. Semin Cell Dev Biol [Internet]. 2011 May [cited 2017 Apr 5];22(3):262–70. Available from: http://www.ncbi.nlm.nih.gov/pubmed/21310259

147. Jortzik E, Becker K. Thioredoxin and glutathione systems in Plasmodium falciparum. Int J Med Microbiol [Internet]. 2012 Oct [cited 2017 Apr 5];302(4–5):187–94. Available from: http://www.ncbi.nlm.nih.gov/pubmed/22939033

148. Knöckel J, Müller IB, Butzloff S, Bergmann B, Walter RD, Wrenger C. The antioxidative effect of de novo generated vitamin B6 in Plasmodium falciparum validated by protein interference. Biochem J [Internet]. 2012 Apr 15 [cited 2017 Mar 14];443(2):397–405. Available from: http://biochemj.org/lookup/doi/10.1042/BJ20111542

149. Butzloff S, Groves MR, Wrenger C, Müller IB. Cytometric quantification of singlet oxygen in the human malaria parasite Plasmodium falciparum. Cytom Part A [Internet]. 2012 Aug [cited 2017 Apr 5];81A(8):698–703. Available from: http://www.ncbi.nlm.nih.gov/pubmed/22736452

150. Ménard R. Malaria : methods and protocols. Humana Press; 2013. 626 p.

151. Sambrook J, Russell DW (David W. Molecular cloning : a laboratory manual. Cold Spring Harbor Laboratory Press; 2001.

152. Crabb BS, Rug M, Gilberger T-W, Thompson JK, Triglia T, Maier AG, et al. Transfection of the Human Malaria Parasite <I>Plasmodium falciparum<I> In: Parasite Genomics Protocols [Internet]. New Jersey: Humana Press; 2004 [cited 2017 Mar 14]. p. 263–76. Available from: http://www.ncbi.nlm.nih.gov/pubmed/15153633

153. Wrenger C, Müller S. The human malaria parasite Plasmodium falciparum has distinct organelle-specific lipoylation pathways. Mol Microbiol. 2004;

154. Müller IB, Knöckel J, Eschbach M-L, Bergmann B, Walter RD, Wrenger C. Secretion of an acid phosphatase provides a possible mechanism to acquire host nutrients by *Plasmodium falciparum*. Cell Microbiol [Internet]. 2010 May 1 [cited 2017 Mar 14];12(5):677–91. Available from: http://www.ncbi.nlm.nih.gov/pubmed/20070315

155. Trager W, Jensen JB. In vitro cultivation of malaria parasites - Cultivation of erythrocytic stages*. Bull World Health Organ [Internet]. 1977 [cited 2017 Mar 14];55(3):363–5. Available from: https://www.ncbi.nlm.nih.gov/pmc/articles/PMC2366733/pdf/bullwho00446-

0223.pdf

156. Das Gupta R, Krause-Ihle T, Bergmann B, Müller IB, Khomutov AR, Müller S, et al. 3-Aminooxy-1-aminopropane and derivatives have an antiproliferative effect on cultured Plasmodium falciparum by decreasing intracellular polyamine concentrations. Antimicrob Agents Chemother [Internet]. 2005 Jul [cited 2017 Mar 14];49(7):2857–64. Available from: http://www.ncbi.nlm.nih.gov/pubmed/15980361

157. Wu Y, Sifri CD, Lei HH, Su XZ, Wellems TE. Transfection of Plasmodium falciparum within human red blood cells. Proc Natl Acad Sci U S A [Internet]. 1995 Feb 14 [cited 2017 Mar 14];92(4):973–7. Available from: http://www.ncbi.nlm.nih.gov/pubmed/7862676

158. Romano RL, Liria CW, Machini MT, Colepicolo P, Zambotti-Villela L. Cadmium decreases the levels of glutathione and enhances the phytochelatin concentration in the marine dinoflagellate Lingulodinium polyedrum. J Appl Phycol [Internet]. 2016 Aug 20 [cited 2017 Mar 16];1–10. Available from: http://link.springer.com/10.1007/s10811-016-0927-z

159. Hiller N, Fritz-Wolf K, Deponte M, Wende W, Zimmermann H, Becker K. Plasmodium falciparum glutathione S-transferase--structural and mechanistic studies on ligand binding and enzyme inhibition. Protein Sci [Internet]. 2006 Feb [cited 2017 Mar 14];15(2):281–9. Available from: http://doi.wiley.com/10.1110/ps.051891106

160. Müller IB, Knöckel J, Groves MR, Jordanova R, Ealick SE, Walter RD, et al. The Assembly of the Plasmodial PLP Synthase Complex Follows a Defined Course. Song H, editor. PLoS One [Internet]. 2008 Mar 19 [cited 2017 Mar 16];3(3):e1815. Available from: http://www.ncbi.nlm.nih.gov/pubmed/18350152

161. Ertl P, Rohde B, Selzer P. Fast calculation of molecular polar surface area as a sum of fragment-based contributions and its application to the prediction of drug transport properties. J Med Chem. 2000 Oct;43(20):3714–7.

162. Brenk R, Schipani A, James D, Krasowski A, Gilbert IH, Frearson J, et al. Lessons learnt from assembling screening libraries for drug discovery for neglected diseases. ChemMedChem. 2008 Mar;3(3):435–44.

163. Hawkins PCD, Skillman AG, Warren GL, Ellingson BA, Stahl MT. Conformer generation with OMEGA: algorithm and validation using high quality structures from the Protein Databank and Cambridge Structural Database. J Chem Inf Model. 2010 Apr;50(4):572–84.

164. Hawkins PCD, Skillman AG, Nicholls A. Comparison of shape-matching and docking as virtual screening tools. J Med Chem. 2007 Jan;50(1):74–82.

165. Tobergte D, Curtis S. Molecular Operating Environment (MOE). J Chem Inf Model. 2013;53(9):1689–99.

166. Smilkstein M, Sriwilaijaroen N, Kelly JX, Wilairat P, Riscoe M. Simple and inexpensive fluorescence-based technique for high-throughput antimalarial drug screening. Antimicrob Agents Chemother [Internet]. 2004 May [cited 2017

Mar 14];48(5):1803–6. Available from: http://www.ncbi.nlm.nih.gov/pubmed/15105138

167. Croom E. Metabolism of Xenobiotics of Human Environments. In: Progress in molecular biology and translational science [Internet]. 2012 [cited 2017 Mar 14]. p. 31–88. Available from: http://www.ncbi.nlm.nih.gov/pubmed/22974737

168. Saha D, Tamrakar A. www.asianpharmaonline.org Xenobiotics, Oxidative Stress, Free Radicals Vs. Antioxidants: Dance Of Death to Heaven's Life. Asian J Res Pharm Sci. 2011;1(2):36–8.

169. Perbandt M, Eberle R, Fischer-Riepe L, Cang H, Liebau E, Betzel C. High resolution structures of Plasmodium falciparum GST complexes provide novel insights into the dimer–tetramer transition and a novel ligand-binding site. J Struct Biol [Internet]. 2015 Sep [cited 2017 Mar 14];191(3):365–75. Available from: http://linkinghub.elsevier.com/retrieve/pii/S1047847715300125

170. Meissner KA, Lunev S, Wang Y-Z, Linzke M, Batista FA, Wrenger C, et al. Drug target validation methods in malaria - Protein interference assay (PIA) as a tool for highly specific drug target validation. Curr Drug Targets. 2016;17(16).

171. Atamna H, Ginsburg H. Origin of reactive oxygen species in erythrocytes infected with Plasmodium falciparum. Mol Biochem Parasitol [Internet]. 1993 Oct [cited 2017 Apr 6];61(2):231–41. Available from: http://www.ncbi.nlm.nih.gov/pubmed/8264727

172. Omodeo-Salè F, Motti A, Basilico N, Parapini S, Olliaro P, Taramelli D. Accelerated senescence of human erythrocytes cultured with Plasmodium falciparum. [cited 2017 Apr 7]; Available from: http://www.bloodjournal.org/content/bloodjournal/102/2/705.full.pdf?sso-checked=true

173. Gazzinelli RT, Kalantari P, Fitzgerald KA, Golenbock DT. Innate sensing of malaria parasites. Nat Rev Immunol [Internet]. 2014 Oct 17 [cited 2017 Apr 9];14(11):744–57. Available from: http://www.ncbi.nlm.nih.gov/pubmed/25324127

174. Pandey A V, Bisht H, Babbarwal VK, Srivastava J, Pandey KC, Chauhan VS. Mechanism of malarial haem detoxification inhibition by chloroquine. Biochem J [Internet]. 2001 Apr 15 [cited 2017 Apr 7];355(Pt 2):333–8. Available from: http://www.ncbi.nlm.nih.gov/pubmed/11284719

175. Bolchoz LJC, Gelasco AK, Jollow DJ, McMillan DC. Primaquine-induced hemolytic anemia: formation of free radicals in rat erythrocytes exposed to 6-methoxy-8-hydroxylaminoquinoline. J Pharmacol Exp Ther [Internet]. 2002 Dec 1 [cited 2017 Apr 7];303(3):1121–9. Available from: http://jpet.aspetjournals.org/cgi/doi/10.1124/jpet.102.041459

176. Haynes RK, Krishna S. Artemisinins: activities and actions. Microbes Infect [Internet]. 2004 Nov [cited 2017 Apr 7];6(14):1339–46. Available from: http://linkinghub.elsevier.com/retrieve/pii/S1286457904002734

177. Roth EF, Raventos-Suarez C, Rinaldi A, Nagel RL, Nagel RL. Glucose-6-

phosphate dehydrogenase deficiency inhibits in vitro growth of Plasmodium falciparum. Proc Natl Acad Sci U S A [Internet]. 1983 Jan [cited 2017 Apr 6];80(1):298–9. Available from: http://www.ncbi.nlm.nih.gov/pubmed/6337374

178. Liebau E, Bergmann B, Campbell AM, Teesdale-Spittle P, Brophy PM, Lüersen K, et al. The glutathione S-transferase from Plasmodium falciparum. Mol Biochem Parasitol [Internet]. [cited 2017 Apr 7];124(1–2):85–90. Available from: http://www.ncbi.nlm.nih.gov/pubmed/12387854

179. Hubatsch I, Ridderström M, Mannervik B. Human glutathione transferase A4-4: an alpha class enzyme with high catalytic efficiency in the conjugation of 4-hydroxynonenal and other genotoxic products of lipid peroxidation. Biochem J [Internet]. 1998 Feb 15 [cited 2017 Apr 7];175–9. Available from: http://www.ncbi.nlm.nih.gov/pubmed/9461507

180. Danielson UH, Esterbauer H, Mannervik B. Structure-activity relationships of 4-hydroxyalkenals in the conjugation catalysed by mammalian glutathione transferases. Biochem J [Internet]. 1987 Nov 1 [cited 2017 Apr 7];247(3):707–13. Available from: http://www.ncbi.nlm.nih.gov/pubmed/3426557

181. Srivastava P, Puri SK, Kamboj KK, Pandey VC. Glutathione-S-transferase activity in malarial parasites. Trop Med Int Health [Internet]. 1999 Apr [cited 2017 Apr 7];4(4):251–4. Available from: http://www.ncbi.nlm.nih.gov/pubmed/10320651

182. Harwaldt P, Rahlfs S, Becker K. Glutathione S-Transferase of the Malarial Parasite Plasmodium falciparum: Characterization of a Potential Drug Target. Biol Chem [Internet]. 2002 Jan 15 [cited 2017 Apr 7];383(5):821–30. Available from: http://www.ncbi.nlm.nih.gov/pubmed/12108547

183. Fritz-Wolf K, Becker A, Rahlfs S, Harwaldt P, Schirmer RH, Kabsch W, et al. X-ray structure of glutathione S-transferase from the malarial parasite Plasmodium falciparum. Proc Natl Acad Sci [Internet]. 2003 Nov 25 [cited 2017 Apr 7];100(24):13821–6. Available from: http://www.ncbi.nlm.nih.gov/pubmed/14623980

184. Deponte M, Becker K. Glutathione S-transferase from Malarial Parasites: Structural and Functional Aspects. In: Methods in enzymology [Internet]. 2005 [cited 2017 Apr 7]. p. 241–53. Available from: http://www.ncbi.nlm.nih.gov/pubmed/16399390

185. Ahmad R, Srivastava AK, Tripathi RP, Batra S, Walter RD. Synthesis and biological evaluation of potential modulators of malarial glutathione-S-transferase(s). J Enzyme Inhib Med Chem [Internet]. 2007 Jan 4 [cited 2017 Apr 7];22(3):327–42. Available from: http://www.ncbi.nlm.nih.gov/pubmed/17674815

186. Sturm N, Hu Y, Zimmermann H, Fritz-Wolf K, Wittlin S, Rahlfs S, et al. Compounds structurally related to ellagic acid show improved antiplasmodial activity. Antimicrob Agents Chemother [Internet]. 2009 Feb 1 [cited 2017 Apr 7];53(2):622–30. Available from: http://aac.asm.org/cgi/doi/10.1128/AAC.00544-08

187. Beutler E, Duparc S, G6PD Deficiency Working Group. Glucose-6-phosphate dehydrogenase deficiency and antimalarial drug development. Am J Trop Med Hyg [Internet]. 2007 Oct [cited 2017 Apr 9];77(4):779–89. Available from: http://www.ncbi.nlm.nih.gov/pubmed/17978087

188. Fletcher KA, Barton PF, Kelly JA. Studies on the mechanisms of oxidation in the erythrocyte by metabolites of primaquine. Biochem Pharmacol [Internet]. 1988 Jul 1 [cited 2017 Apr 9];37(13):2683–90. Available from: http://www.ncbi.nlm.nih.gov/pubmed/2839199